CELL WALL LYTIC ENZYMES IN STREPTOMYCES COELICOLOR

AN INVESTIGATION OF CELL WALL LYTIC ENZYMES IN STREPTOMYCES COELICOLOR

By

HENRY JOSEPH HAISER, B.Sc.

A Thesis

Submitted to the School of Graduate Studies

in Partial Fulfillment of the Requirements

for the Degree

Doctor of Philosophy

McMaster University

DOCTOR OF PHILOSOPHY (2011) **McMaster University**

(Biology) **Hamilton, Ontario**

TITLE: **An investigation of cell wall lytic enzymes in *Streptomyces coelicolor***

AUTHOR: **Henry Joseph Haiser, B.Sc. (University of Waterloo)**

SUPERVISOR: **Dr. Marie A. Elliot**

NUMBER OF PAGES: xiv, 157

ABSTRACT

An increasing appreciation for the role of small RNA regulators prompted us to investigate the scope of RNA regulation in the bacterium, *Streptomyces coelicolor*. Our search revealed an antisense RNA that corresponds to the upstream region of four genes encoding cell wall cleavage enzymes (cell wall hydrolases), and a previously uncharacterized population of transfer RNA (tRNA) cleavage products. Further characterization of the tRNAs led to the discovery that *S. coelicolor* tRNAs are cleaved into 'tRNA halves' in a developmentally-regulated fashion. All tRNAs seem to be susceptible to tRNA cleavage, although a bias was detected for tRNAs specifying highly used codons. To date, our work is the sole description of 'tRNA half' production in a bacterium, and recent studies suggest that it is a widespread phenomenon among eukaryotic organisms.

In a separate line of investigation, we noticed that a previous study had predicted that the genes associated with the antisense RNA are under the control of a riboswitch – a regulatory RNA element that directly controls gene expression in response to specific conditions. Our multifaceted characterization of this system began with the construction and phenotypic analyses of deletion mutant strains for several of the cell wall hydrolase-encoding genes. We demonstrate that *S. coelicolor* cell wall hydrolases are involved in germination, vegetative growth, and sporulation. Finally, we studied the potential for riboswitch regulation of one of the cell wall hydrolase-encoding genes, *rpfA*. RpfA is a resuscitation-promoting factor protein that is important for the revival of dormant bacteria, including the human pathogen and *S. coelicolor* relative – *Mycobacterium tuberculosis*. Our investigation uncovered evidence suggesting that the riboswitch region is involved in the regulation of *rpfA*, and we identified specific conditions under which it is repressed. This work represents a novel paradigm in the regulation of cell wall hydrolase expression.

ACKNOWLEDGEMENTS

This thesis would not have been possible without the guidance and steadfast support of my supervisor – Dr. Marie Elliot; her tireless work is truly inspiring. I would like to thank Dr. Elliot for taking a chance on me when she was starting up her lab, providing me with many incredible opportunities along the way, and teaching me how to do meaningful science. Her advice and careful editing have also greatly improved the quality of this thesis document.

I would like to thank the members of my supervisory committee – Drs. Turlough Finan, Yingfu Li, and Justin Nodwell. Their input over the years, through all of the twists and turns of my research, kept me on track and helped me to think about my work from multiple angles. Also – thank you for all of the reference letters!

Throughout the years I have had the pleasure of working with some great people in the Elliot lab. I would like to thank all members of the Elliot lab (past and present), especially: Dave Capstick (for being a pop culture 'guru'), Andrew Duong (for his mind-blowing one-liners), Michael Hewak (for having so many Michael Hewak-like qualities), Matt Moody (for his dulcet tones and fancy footwork), and Julia Swiercz (for listening to all of my stories); and also, Dr. Mary Yousef, Lauren Brady, and Nolan D'Souza for assisting with experiments presented in this thesis.

I would like to thank my friends from McMaster, especially: Mai Almardini, Maja Cvetkovic, Kevin Kelly, Megan McKerlie, and Kyster Nanan; my friends from the Waterloo days, including: James Hull, Akhil "Shaq" Katarya, Christine St-Denis, Matt Strauss, Jeremy Weber, and Jamie "Wheels" Wheeler – you have all contributed to making my time away from the lab most memorable. Also, the early encouragement and advice I received from Kristin Pouw helped me in more ways than she will ever know.

Throughout the duration of this thesis I was privileged to spend time with two of the best friends a person could ask for. A special thank you goes out to Jon Midwood and Hung Vo for being there for me unconditionally – I vow to remain life-long friends with you both.

I would like to thank my brother – Eric Haiser, for keeping up with the perpetual dialogue between us. I hope it never stops. Eric: I bet you didn't think

you'd ever see the words "Baba Booey" in a thesis – but look, Boff, there they are!

I would like to thank all members of the Haiser and Zeller families for their continual support. A special thank you goes out to Tante Ellie, Tanta Suzy – for giving me the academic bug (Fig. 1.1 is for you!), Onkel Nicky – for sharing stories during the many rides back to Hamilton, and Oma, and Opa Zeller – for their love and generosity.

Finally, I would like to thank my parents – Christine and Henry Haiser. I cannot imagine more supportive and loving role models. They taught me how to work hard, and provided an environment that allowed me to find and pursue my passion. None of this could have happened without my parents – to them I dedicate this thesis.

TABLE OF CONTENTS

LIST OF FIGURES

LIST OF TABLES

LIST OF ABBREVIATIONS AND SYMBOLS

A number of abbreviations and symbols are used in this document, many of which are defined when introduced. Those standard abbreviations that are not defined, include:

-OH	Hydroxyl group
^{32}P	Phosphorus-32 isotope
A	Adenine
Ala	Alanine
AMP	Adenosine monophosphate
Asn	Asparagine
ATP	Adenosine triphosphate
bp	Base pair
BSA	Bovine serum albumin
C	Cytosine *or*
C	Carbon
cDNA	Complementary DNA
cm	Centimeter
CTP	Cytosine triphosphate
dH_2O	Distilled water
DNA	Deoxyribonucleic acid
Dpm	Diaminopimelic acid
DTT	Dithiothreitol
EDTA	Ethylenediaminetetraacetic acid
G	Guanine
g	Gram
GC buffer	PCR reaction buffer for high G+C DNA
Glu	Glutamic acid
Gly	Glycine
GMP	Guanosine monophosphate
GTP	Guanine triphosphate
HF buffer	High fidelity PCR reaction buffer
His	Histidine
KCl_2	Potassium chloride
kDa	Kilo Daltons
KOH	Potassium hydroxide
Leu	Leucine
M	Molar
Mbp	Mega bp
Met	Methionine
$MgSO_4$	Magnesium sulfate
ml	Milliliter
mM	Millimolar
mRNA	Messenger RNA
nt	Nucleotide
pCp	Cytidine-3',5'-bis-phosphate

PCR	Polymerase chain reaction
ppGpp	Guanosine pentaphosphate
Pro	Proline
PVDF	Polyvinylidene fluoride
RACE	Rapid amplification of cDNA ends
RNA	Ribonucleic acid
rRNA	Ribosomal RNA
Ser	Serine
T	Thymine
Taq	DNA polymerase from *Thermus aquaticus*
TES buffer	N-Tris(hydroxymethyl)methyl-2-aminoethanesulfonic acid
Thr	Threonine
Tris	Tris(hydroxymethyl)aminomethane
tRNA	Transfer RNA
U	Uracil *or*
U	Enzyme unit
UDP	Uridine diphosphate
UTP	Uridine triphosphate
UV	Ultra-violet
V	Volts
µg	Microgram
µl	Microliter

CHAPTER 1:
GENERAL INTRODUCTION

1.1 ACTINOMYCETES AND THE GENUS *STREPTOMYCES*

1.1.1 The Actinobacteria

The term 'Actinobacteria' refers to a group of Gram-positive microorganisms belonging to the bacterial order *Actinomycetales*. The first published image of an actinomycete bacterium likely appeared in a paper by the German scientist Ferdinand J. Cohn in 1875 (Fig. 1.1; (Waksman, 1967, Cohn, 1875)). Shortly after the initial discovery of these organisms, scientists began systematically classifying them, originally believing them to be intermediates between fungi and bacteria (Hopwood, 1999). Interest in this group intensified following Selman Waksman's 1940 discovery of 'actinomycin' – the first antibiotic isolated from an actinomycete, and subsequently, 'streptomycin' – the first antibiotic treatment for tuberculosis (TB) (Waksman & Woodruff, 1940). In 1952 Waksman was awarded the Nobel Prize in medicine for these discoveries. At approximately the same time, Sir David A. Hopwood began the first genetic studies of an actinomycete named *Streptomyces* (*reviewed in:* Hopwood, 1999). Through his electron microscopy work, Hopwood would show that *Streptomyces* was a bacterium and was not a member of the fungi, as it lacked a nuclear envelope and displayed a cell wall characteristic of Gram-positive bacteria (Hopwood, 2007). Over the next 50 years or so, the field of *Streptomyces* genetics continued to grow, with the emergence of new genetic techniques and technological advancements (Chater, 1999).

Actinomycetes can be found in both fresh and marine water environments, as well as in the soil, where their saprophytic lifestyle makes an important contribution to the recycling of organic material (Chater *et al.*, 2010). Furthermore, there are examples of actinomycetes that live on plant and animal hosts, and are ubiquitous members of the human skin and gut microbiota (Turnbaugh *et al.*, 2009). Actinomycetes of relevance to human disease include members of the genera *Mycobacterium* (including *M. tuberculosis* – the causative agent of TB, and *M. leprae* – the causative agent of leprosy), *Corynebacterium* (including *C. diphtheriae* – the causative agent of diphtheria) (Brun & Shimkets, 2000). Among the most well studied actinomycetes, however, are members of the genus *Streptomyces*. Comparisons between the genome sequences of *C. diphtheria*, *M. tuberculosis*, and *S. coelicolor* led to the discovery of a conserved 'core' chromosomal region, further supporting their evolutionary relatedness (Bentley *et al.*, 2002).

1.1.2 The genus *Streptomyces* – some unique features

One of the defining features of the streptomycetes is the diversity of their secondary metabolism. Secondary metabolites are compounds not directly used

for growth and reproduction, but that confer some competitive advantage in a particular environment. Therefore, it is thought that secondary metabolism enhances species survival in their natural environment, although this idea remains to be tested experimentally. The genus *Streptomyces* is arguably the most important microbial genus when it comes to the production of clinically useful antibiotics and other therapeutic drugs. Two-thirds of all antibiotics produced by microorganisms come from the actinomycetes, and of these, nearly 80% are produced by the streptomycetes (Kieser *et al.*, 2000). One staggering estimate predicts that they are capable of producing >100,000 antimicrobial compounds, yet only ~3% of these have been discovered (Watve *et al.*, 2001). An examination of the genome sequences from representative streptomycetes has uncovered previously unidentified gene clusters, resembling those that often encode secondary metabolite biosynthetic pathways. The discovery of these so-called 'cryptic' clusters suggests the genetic potential to produce many more antibiotics than previously realized. Activating these clusters represents a major, but potentially rewarding challenge for geneticists (Challis & Hopwood, 2003).

In addition to the chemical diversity exhibited by the streptomycetes, some interesting characteristics distinguish them from other bacteria. In contrast to many prokaryotes which possess circular chromosomes, *S. coelicolor* (and likely most streptomycetes) possesses a single linear chromosome with a G+C content of ~72% (Bentley *et al.*, 2002, Kieser *et al.*, 2000). Many of the essential genes are located in the 'core' region of the chromosome, while many of the genes for non-essential function (including secondary metabolism) are located in the chromosomal 'arm' regions. The *S. coelicolor* genome is 8.6 Mbp in size – this is considered to be a large genome among the prokaryotes, especially in comparison to the genomes of *M. tuberculosis*, *Bacillus subtilis*, and *Escherichia coli* which all fit into the 4.0 – 4.6 Mbp range (Bentley *et al.*, 2002). The genome encodes ~7,800 proteins which is about double the ~4,000 proteins encoded by *M. tuberculosis, B. subtilis*, and *E. coli*. Approximately 10% of the proteins in *S. coelicolor* are secreted, and many of these serve to hydrolyze the multitude of organic materials encountered by a soil bacterium (Chater *et al.*, 2010). Finally, the *S. coelicolor* genome dedicates a large portion (~12%) of its protein-coding genes to regulatory function (Bentley *et al.*, 2002). Both the secreted proteins and those dedicated to regulatory function are likely to be important components of the complex life cycles exhibited by *S. coelicolor*.

1.2 GROWTH AND DEVELOPMENT IN *STREPTOMYCES*

1.2.1 'Prokaryotic development' – the *S. coelicolor* life cycle

For many biologists, the term 'development' likely conjures up thoughts and images of the complexities of mammalian embryonic development, or differentiated groups of cells coming together to form tissues and eventually organs. And although it is true that many prokaryotes divide by the relatively simple process of binary fission (the splitting of a cell into two nearly identical

daughter cells), others display complex developmental programs, reminiscent of those exhibited by higher eukaryotic organisms. This is perhaps best exemplified by the formation of reproductive 'fruiting bodies' by *Myxococcus xanthus* in response to nutrient deprivation (Kaiser, 2004). This behavior highlights an interesting distinction – while development in higher eukaryotes often proceeds independently of changes in the natural environment, prokaryotic development is often initiated as a direct response to environmental changes (e.g. nutrient limitation) (Brun & Shimkets, 2000). Indeed, this seems to be the case for development in *S. coelicolor* as well. The *Streptomyces* life cycle provides it with a way to both reproduce, and spread into different niches.

As *S. coelicolor* is a sporulating bacterium, this description assumes that 'life' commences with the germination of a dormant exospore. Germination is most likely initiated as a direct response to conditions that are conducive to growth. In *S. coelicolor*, germination is physically manifested by the emergence of one or two germ tube(s). As the germ tubes elongate, long, filamentous cells are formed. These filamentous cells exhibit extensive branching, and eventually form what is known as the substrate, or 'vegetative mycelia'. This term refers to the tangled mat of mycelia that extends below the surface of the soil (during growth in natural conditions), or the agar-containing growth medium (during growth in laboratory conditions). After a period of time, presumably following a shift to nutrient-limiting conditions, structures called 'aerial hyphae' emerge from the vegetative mycelia, a non-branching filamentous type of cell that grows away from the substrate mycelia into the air. The aerial hyphae eventually undergo septation to form unigenomic 'prespore' compartments, which mature into chains of exospores (cell types are illustrated in Fig. 1.2) (Elliot *et al.*, 2008). It should be highlighted that the initiation of aerial development coincides temporally with secondary metabolism. Moreover, these two processes share many of the same genetic regulators (Champness, 1988).

1.2.1.1 Germination

Of all the major events in the *S. coelicolor* life cycle, germination is perhaps the least well studied. In the endospore-forming *B. subtilis*, the triggers that initiate germination (germinants), and the proteins involved in sensing and responding (germinant receptors) to these cues are fairly well defined (Setlow, 2003). Germinant receptors are localized to the inner membrane of dormant spores, and bind specific germinants, including combinations of specific amino acids, sugars, and potassium ions (Paidhungat & Setlow, 2001). Germinant binding initiates a cascade of events that includes the hydrolysis of spore cell wall material, the shedding of the outer layer of the spore (spore coat), the release of dipicolonic acid (DPA) and calcium, and an influx of water, that ultimately leads to a return to vegetative growth (Ghosh & Setlow, 2009). This process of spore germination is not one that is wholly shared by the streptomycetes. For one, *S. coelicolor* spores do not contain DPA, and while *Streptomyces* spores germinate in response to specific amino acids (in particular, L-valine), germinant receptors

have yet to be identified (Ensign, 1978). Genetic studies have revealed a few *Streptomyces*-specific proteins that contribute to germination. Deletion of both the adenylate cyclase gene (*cya*) (Susstrunk *et al.*, 1998), and the cyclic AMP receptor protein (CRP) (Derouaux *et al.*, 2004), produces spores that germinate infrequently; while deletion of the *nepA* gene, the product of which is an uncharacterized small secreted protein, results in spores that germinate more rapidly (de Jong *et al.*, 2009). Two additional proteins, DivIVA and SsgA (see below) have been shown to mark the sites of emerging germ tubes (Flärdh, 2003a, Traag & van Wezel, 2008).

1.2.1.2 Vegetative growth

One of the most fascinating aspects of *Streptomyces* biology is its branching hyphal growth. In most rod-shaped bacteria, growth is directed by the helical framework provided by the cytoskeletal protein, MreB (Carballido-Lopez & Errington, 2003). In these systems, new cell wall material is deposited along the lateral wall. In contrast, vegetative growth in *S. coelicolor* depends on the essential coiled-coil protein, DivIVA (Flärdh, 2003b, Flärdh, 2003a). DivIVA directs the deposition of new cell wall material at the cell pole; a completely unique form of bacterial growth (Flärdh, 2003b, Daniel & Errington, 2003). As the filamentous cells extend, cell division is infrequent, but occasional 'cross-walls' are laid down, which divide the cell into two compartments. The frequent branching experienced during vegetative growth depends on DivIVA, as it determines the sites of new cell poles, and likely recruits the enzymes necessary for cell wall hydrolysis and biosynthesis to these sites (Hempel *et al.*, 2008). This growth by 'apical tip extension' occurs not only during vegetative growth and branching, but continues during the aerial stage of growth as well.

1.2.1.3 Aerial development

Researchers have identified many genes required for aerial hyphae formation in *S. coelicolor*. Historically, these genes have been designated the '*bld*' (bald) genes, indicating the absence of a 'fuzzy' colony surface typically seen during aerial hyphae formation (Fig. 1.3). Many of the *bld* genes are important not only during morphogenesis, but also for secondary metabolism (Chater, 1993). An example of this is the *bldA* gene; while most of the *bld* genes encode regulatory proteins, *bldA* encodes a tRNA required for translating the UUA leucine codon (Leskiw *et al.*, 1991). The high G+C content of the *S. coelicolor* genome makes the UUA codon very rare in open reading frames, and *bldA* is the only tRNA that specifies this codon. *bldA* deletion mutants fail to raise aerial hyphae, but also do not produce any of the four antibiotics that the laboratory strain is capable of making (Lawlor *et al.*, 1987).

While many of the classical *bld* genes encode regulatory proteins, more recent studies have begun to reveal some of the structural elements that contribute to the specific characteristics of the aerial hyphae. The growth of these hyphae out of the aqueous soil environment (or growth medium under laboratory conditions)

and into the air is accompanied by cell surface changes. This includes the production of surface-active molecules that aid in lowering the water surface tension to permit aerial growth (SapB and the 'chaplins'), and proteins that decorate the aerial surfaces (the 'chaplins' and the 'rodlins') (Willey *et al.*, 1991, Elliot & Talbot, 2004, Claessen *et al.*, 2006, Elliot *et al.*, 2003). It has been proposed that both SapB and the chaplins are crucial for aerial hyphae formation on rich medium, while the chaplins alone are sufficient for this process on minimal medium (Capstick *et al.*, 2007). Despite the advances in understanding the role of cell surface-associated proteins in promoting aerial growth, there is still much that is unknown about development, particularly with regard to any growth phase-specific changes in cell wall composition that take place.

1.2.1.4 Sporulation

For a filamentous exospore-forming bacterium such as *S. coelicolor*, the process of sporulation requires the coordination of critical cellular events. These include chromosome replication, condensation, and segregation, and also hyphal septation/division, and spore maturation. A collection of proteins encoded by the '*whi*' (white) genes, named for the white colony appearance exhibited by strains lacking these genes (Fig. 1.3), have been implicated in various aspects of the sporulation process (Flärdh & Buttner, 2009). As classical regulators of sporulation, many of the *whi* genes encode transcription factors. In more recent advances, proteins of structural and enzymatic function have also been implicated in the sporulation process.

Cell division is not required for vegetative or aerial growth to proceed in *S. coelicolor*, however it is essential for sporulation. Universally within the bacteria, the tubulin-like FtsZ protein polymerizes to form a ring structure at future division sites (Lowe *et al.*, 2004). Recently, it was shown that two members of a group of proteins named the 'SALP' proteins (SsgA-like proteins) mediate FtsZ recruitment. The first protein to arrive at future division sites is SsgA. This protein is followed by SsgB, which then recruits FtsZ and promotes assembly of the Z-ring structure (Willemse *et al.*, 2011). Highlighting an additional role for SsgA is the fact that it remains associated with sporulation septa, and it is involved in the later stages of spore maturation (Traag & van Wezel, 2008). A possible role for additional SALP proteins during the later sporulation stages is in controlling the development of the thickened spore wall, and the division of spore chains into individual spores, based on the phenotypic characteristics of the different SALP mutant strains (Noens *et al.*, 2005). Both of these activities would involve the coordination of cell wall biosynthetic and cell wall hydrolytic enzymes.

Another key player in spore wall development is the MreB protein. Indeed, *mreB* deletion strains produce defective spores with abnormally thin walls and irregular morphologies (Mazza *et al.*, 2006). These spores are also heat sensitive, and thus have a reduced capacity to survive harsh conditions during dormancy. A recent study has shown that MreB, and other proteins encoded

within the *mre* cluster, interact with cell wall biosynthetic proteins, and a protein named RodZ (Kleinschnitz *et al.*, 2011). RodZ was recently shown to be a structural link between cell wall biosynthetic machinery and the cytoskeletal framework in *E. coli* (van den Ent *et al.*, 2010). These observations, combined with the role of MreB in coordinating vegetative cell wall biosynthesis in other bacteria (Cabeen & Jacobs-Wagner, 2005), establish the *S. coelicolor* MreB protein as a key player in recruiting and coordinating the activities of proteins in spore wall biosynthesis. Like the cell walls of aerial hyphae, little is known about the composition of the cell walls in dormant *Streptomyces* spores.

1.2.2 Bacterial dormancy

Sporulation provides *Streptomyces* with a way of surviving harsh environmental insults that would not be tolerated during vegetative growth. The metabolically inactive spores suspend growth indefinitely, until they encounter favorable conditions. This is exemplified by the discovery of viable 70-year old *Streptomyces* exospores, although endospores as old as 9,000 years have been isolated (Renberg & Nilsson, 1992). Nutrient limitation likely initiates the developmental program that results in *S. coelicolor* spore formation, and many microorganisms adopt analogous states of dormancy in response to similar conditions. Growing bacteria can sense that their surroundings are not ideal to support growth through a variety of environmental cues. These include nutrient depletion, temperature shifts, and the presence of toxic chemicals, including in some cases, those derived from host immune responses (Oliver, 2005, Gilbert *et al.*, 1990). The microbial response to these conditions varies significantly. Adaptations involving the formation of endo- or exospores represent major morphological transformations. Not all responses involve such physical changes, but most result in the reduction or virtual cessation of metabolism (Dworkin & Shah, 2010). Many human pathogens can exist in dormant states, including *B. anthracis* (the causative agent of anthrax), and *Clostridium difficile* (an increasingly common nosocomially-acquired pathogen) – both of these endospore-formers rely on dormancy for their dissemination (Oliver, 2010). Furthermore, the actinomycete *M. tuberculosis* enters a state of latency that aids in its indefinite survival within human hosts (Barry *et al.*, 2009). Although it is unlikely that *M. tuberculosis* forms spores (Traag *et al.*, 2010), morphological changes during the transition to reduced metabolic activity includes the thickening of cell walls (Cunningham & Spreadbury, 1998).

1.3 THE BACTERIAL CELL EVELOPE

For bacteria, the first line of defense from the harsh external stresses of the extracellular environment is the cell envelope. The bacterial cell envelope protects cells against lysis, by resisting turgor pressure, and also serves as the primary determinant of cell shape (*reviewed in:* Cabeen & Jacobs-Wagner, 2007). Additionally, the cell envelope plays an important role in the

transport/transmission of chemicals, nutrients, and signals that enable the cell to interact with its environment. This important structure is in a constant state of flux, as it changes to meet the requirements dictated by a given set of growth conditions. The 'Gram stain' divides most bacteria into one of two groups: Gram-positive or Gram-negative (Gram, 1884, Beveridge, 1990). A cytoplasmic membrane, a thin layer of peptidoglycan (PG), and an outer membrane, separate the cytoplasm from the external environment in Gram-negative bacteria. In contrast, Gram-positive bacteria lack an outer membrane, but have a much thicker PG layer (Fig. 1.4). The essential nature of PG is perhaps best shown by the fact that antimicrobial compounds target all major steps in PG biosynthesis (*reviewed in:* Walsh, 2003).

1.3.1 Peptidoglycan structure

As much as 90% of the total mass of the Gram-positive cell wall is the macromolecule, PG (Fig. 1.5) (Seltmann & Holst, 2001), made up long sugar strands joined together in parallel by short peptides. While the basic sugar strand composition is relatively conserved across all bacterial species, the residues making up the peptide side chains vary considerably from species-to-species (Schleifer & Kandler, 1972).

1.3.1.1 The glycan strand

The sugar – or glycan – strand is composed of alternating residues of *N*-acetylglucosamine (Glc*N*Ac) and *N*-acetylmuramic acid (Mur*N*Ac), linked by β-1,4-glycosidic bonds (*reviewed in:* Shockman & Holtje, 1994). The length of the glycan strand can vary from ~3 to over 200 disaccharide units, depending on the species and growth conditions (Scheffers & Pinho, 2005).

Both the Glc*N*Ac and Mur*N*Ac residues can be chemically modified. One such example is *N*-deacetylation, which is catalyzed by PG deacetylases to yield Glc*N* and Mur*N* residues (Vollmer, 2008). *N*-Deacetylation reduces the susceptibility of the glycan strand to cleavage by lysozymes (enzymes that hydrolyze the bond between Mur*N*Ac and Glc*N*Ac) (Araki *et al.*, 1971). As lysozymes are key players in mammalian innate immune responses, *N*-deacetylation of the PG by many pathogenic bacteria is likely used to evade host immune factors (Vollmer, 2008). Another modification that interestingly, appears to be actinomycete-specific is the *N*-glycolylation modification – the substitution of the muramic acid acetate residue with a glycolyl residue (Amano *et al.*, 1977). Although the biological significance of this modification remains unknown, it is primarily confined to mycolic acid-containing bacteria (e.g. *Mycobacterium* sp.), and other closely related actinobacteria; however, it does not appear to be present in *Streptomyces* (Uchida & Aida, 1979). A final example of glycan strand modification is the *O*-acetylation of Mur*N*Ac residues. This is a variation found in Gram-positive and Gram-negative bacteria, many of which are of pathogenic significance (Clarke & Dupont, 1992). *O*-Acetylation involves the addition of an acetyl group to the C6-OH of Mur*N*Ac residues, creating 2,6-*N*,*O*-diacetyl

muramic acid (Weadge & Clarke, 2006). Much like *N*-deacetylation, *O*-acetylation increases resistance to cell wall lytic enzymes and plays a role during pathogenesis. Moreover, this type of substrate modification may serve as a means of regulating the activity of endogenous cell wall lytic enzymes during bacterial growth (Weadge & Clarke, 2007, Weadge & Clarke, 2006, Weadge *et al.*, 2005).

1.3.1.2 The peptide side chains

Tetrapeptide side chains, bound at their N-terminus to the carboxyl group of Mur*N*Ac residues, connect parallel glycan strands together (Vollmer & Bertsche, 2008). Although their composition varies across all bacteria, side chains generally consist of L- and D-amino acids, with a dibasic amino acid usually found in the third position. This third residue is most variable, and may form a cross-link via an 'interpeptide bridge' between peptide chains from parallel glycan strands (Fig. 1.5) (Scheffers & Pinho, 2005), or may be linked directly to a second side chain, without the addition of a peptide bridge (e.g. *E. coli* and *B. subtilis*) (Hladny *et al.*, 1972). Side chains in *S. coelicolor* consist of L-Ala – D-Glu – LL-Dpm – D-Ala residues (N- to C-terminal), with a single glycine residue forming the interpeptide bridge between a LL-Dpm residue, and the terminal D-Ala residue of the adjacent side chain (Fig. 1.5) (Schleifer & Kandler, 1972). Cross-linking of the peptide chains is thought to provide the rigidity required for maintaining cell shape. The extent of cross-linking varies between organisms, and the environments they are faced with. For example, while about 50% of stem peptides are cross-linked in *E. coli* and *B. subtilis* during vegetative growth, this is increased to around 90% in *Staphylococcus aureus* (Scheffers & Pinho, 2005). In *S. coelicolor,* there is evidence suggesting that PG cross-linking frequency is ~50% under laboratory conditions (Paget *et al.*, 1999a). Through close examination of *B. subtilis* spore wall composition, it was discovered that while side chain cross-linking remains unchanged in the outermost layers, it is reduced to as little as ~2% in the inner layers. This cross-linking gradient has been proposed to aid in the establishment of a dehydrated spore core (Popham *et al.*, 1999).

1.3.1.3 Peptidoglycan modifications associated with bacterial dormancy

Several cell wall-related modifications have been associated with bacteria during sporulation, and other dormant states. For example, in *B. subtilis* spores, in addition to the changes in cross-linking, about half of the Mur*N*Ac residues exhibit a modified delta-lactam structure (Atrih & Foster, 1999). This modification is specifically recognized by enzymes involved in cell wall cleavage during germination (Heffron *et al.*, 2009). Similarly, in dormant *Enterococcus faecalis* cells, there is an increase in the amount of *O*-acetylated PG (Pfeffer *et al.*, 2006). Finally, dormant *E. coli* cells completely alter their morphology (from rod- to cocci-shaped), drastically reducing the length of glycan strands, and increasing the frequency of cross-linking (Signoretto *et al.*, 2002). To date, the chemical composition of *S. coelicolor* spore walls remains unexplored. In most cases the

biological significance of the modifications during sporulation/dormancy is not known, however the widespread modification of the cell wall during dormancy highlights the need for additional studies in this area.

1.3.1.4 Brief overview of peptidoglycan biosynthesis

PG biosynthesis is a highly complex process that involves enzymatic reactions in the cytoplasm, and on both sides of the cytoplasmic membrane (Uehara & Park, 2008). The cytoplasmic reactions direct the synthesis of the nucleotide precursors of the sugar monomers (UDP-Mur*N*Ac and UDP-Glc*N*Ac), as well as the synthesis and assembly of stem peptides, including the generation of D-amino acids (Barreteau *et al.*, 2008). Interestingly, the 'D' isomer of amino acids is found almost exclusively in the bacterial cell wall, with enzymes known as 'racemases' interconverting L- and D-enantiomers of specific amino acids for their incorporation into stem peptides (Lam *et al.*, 2009). The cytoplasmic steps culminate with the formation of the soluble intermediate, UDP-Mur*N*Ac-pentapeptide, which is then transferred to undecaprenol-phosphate to form 'lipid 1' (Uehara & Park, 2008). UDP-Glc*N*Ac is then added to form 'lipid 2', which is transported to the outside of the cytoplasmic membrane where it is incorporated into the existing PG through the action of penicillin binding proteins (PBPs) (Bouhss *et al.*, 2008). The PBPs carry out the two major PG polymerization reactions: transglycosylation (polymerization of the glycan strand) and transpeptidation (cross-linking of the stem peptides) (Sauvage *et al.*, 2008). Bacteria possess differing numbers of PBPs, and it is thought that these share some degree of functional redundancy between them. For example, *B. subtilis* and *M. tuberculosis* each encode 16 PBPs, while *S. coelicolor* is predicted to encode 21 (Sauvage *et al.*, 2008). PBPs have diverse architectures, and are often modular proteins that frequently possess cell wall hydrolytic domains – this highlights the need for coordination between these two opposing (degradation/biosynthesis) activities.

1.4 CELL WALL HYDROLASES

While providing rigid structural support, the bacterial cell wall is also remarkably dynamic, undergoing significant remodeling to accommodate changes in cell size and shape during growth and differentiation. An essential part of this process is the breaking of the bonds that hold the PG structure together. This task is carried out by a diverse group of cell wall (or PG) hydrolases that target both glycan strands and amino acid side chains. For every bond in PG, there exists a cognate hydrolase that can cleave it (Fig. 1.5). While cell wall hydrolases are important during normal vegetative growth, they can also have specialized functions. These can include: facilitating the assembly of secretion systems, flagella, and pili across Gram negative cell walls (Hoppner *et al.*, 2005, Scheurwater & Burrows, 2011); hydrolyzing spore PG during spore germination (Heffron *et al.*, 2009); and resuscitating dormant cell populations (discussed below). There is also significant

variation in the number of cell wall hydrolases encoded by a given organism. For example *E. coli* and *B. subtilis* are predicted to encode 30 and 35 cell wall hydrolases respectively, while we predict that *S. coelicolor* encodes ~58 (Haiser *et al.*, 2009). This drastic difference is likely explained by the differences in lifestyle between these organisms. Conceivably, all stages of the *S. coelicolor* life cycle including germination, highly branched vegetative growth, aerial development, and sporulation would require significant cell wall remodeling.

1.4.1 Cell wall cleavage enzyme specificities

PG cleavage enzymes are typically classified based on their substrate specificities. The *N*-acetylglucosaminidases, lysozymes, and lytic transglycosylases target the glycosidic bonds of the glycan strand; *N*-acetylmuramyl-L-alanine amidases (hereinafter referred to as amidases) target the bond between Mur*N*Ac and the first residue of the peptide stem (L-Ala), and a group of carboxy- and endopeptidases cleave the various LD-, DL-, and DD-bonds within the peptide stems (Fig. 1.5) (Vollmer *et al.*, 2008b). Lysozymes are ubiquitous in nature, and are produced by organisms as diverse as bacteria, phage, invertebrates and vertebrates. Proteins possessing a 'lysozyme-like' fold can be further divided into nine categories, all of which cleave the β-1,4-glycosidic bond between Mur*N*Ac and Glc*N*Ac, resulting in a terminal reducing Mur*N*Ac residue (Pei & Grishin, 2005). The lytic transglycosylases cleave the same bond as the lysozymes, however the product of their activity includes a 1,6-anhydro ring on Mur*N*Ac residues, and thus they are technically not 'hydrolases' (*reviewed in:* Scheurwater *et al.*, 2008). The activity of both enzyme types, however, can be affected by glycan strand modifications like *O*-acetylation (see above).

Recent studies have identified a group of specialized cell wall cleavage enzymes with a role in exiting dormant states: the resuscitation-promoting factors (Rpfs). The observation that dormant *Micrococcus luteus* could be 'resuscitated' through the addition of supernatant from exponentially growing cultures, led to the discovery of the Rpf proteins (Mukamolova *et al.*, 1998). Rpf proteins are usually secreted, and are structurally and functionally similar to lysozymes (Cohen-Gonsaud *et al.*, 2005, Mukamolova *et al.*, 2006). The mechanism by which the Rpf proteins promote growth re-activation is currently unknown, however their role in the biology of *S. coelicolor* will be discussed in subsequent sections (Chapters 3 and 4).

Amidase activity effectively separates the stem peptide from the glycan strand. In *E. coli*, enzymes belonging to this class play a crucial role in the separation of daughter cells during cell division (Bernhardt & de Boer, 2003). Additionally, amidases are involved in the recycling of PG (discussed further in Chapter 4), as they cleave the peptide stems off muro-tri- and tetra-peptide fragments (Jacobs *et al.*, 1995). Carboxypeptidases cleave the C-terminal amino acids from stem peptides, and they often work in concert with the PG biosynthetic enzymes (Vollmer *et al.*, 2008b). Finally, a myriad of endopeptidases cleave the

amide bonds internal to the amino acid side chains, and those shared by the side chains and interpeptide bridges.

1.4.2 Control of cell wall hydrolase activity

Given the inherently destructive nature of PG hydrolases, and the importance of maintaining the integrity of the PG, it is clear that these enzymes must be under strict control. PG hydrolase regulation occurs at all levels including post-translational processing, control by substrate modification and localization, and transcriptional control.

In cases where transcriptional control has been studied, the master regulators that control specific cellular processes often control the PG hydrolases involved in these processes. For example, regulatory proteins controlling sporulation in *B. subtilis* also activate transcription of the cell wall hydrolases needed for spore wall synthesis/development (Smith *et al.*, 2000). Although transcriptional control is an important aspect of cell wall hydrolase regulation, there are far more examples of post-translational control.

In addition to the hydrolase-controlling substrate modifications that have already been discussed, the presence and chemical nature of cell wall accessory polymers also plays a role in modulating hydrolase activity. The cell walls of Gram-positive bacteria are often decorated with polymers of glycerol (or ribitol) phosphate, which are either covalently linked to Mur*N*Ac residues (teichoic acids) or membrane lipids (lipoteichoic acids) (D'Elia *et al.*, 2006, Rahman *et al.*, 2009). Through their interaction with cations and proteins, teichoic acids influence the electro- and physiochemical properties of the cell envelope. Proton binding to teichoic acid lowers the local cell wall pH and a consequence of this is often the inhibition of PG hydrolase activity (Fischer *et al.*, 1981, Calamita & Doyle, 2002).

Another example of post-translational control is the modulation of PG hydrolases through differential binding to the cell wall via their cell-wall-binding domains. Cell wall hydrolase proteins are often modular in nature. They commonly possess catalytic domains specifying a cleavage activity, fused with a substrate-binding domain that enhances this activity (Vollmer *et al.*, 2008b). There are at least seven known PG-binding domains, two of which specify binding to teichoic acids (the 'GW' and 'choline-binding' domains) (Vollmer *et al.*, 2008b). However, one of the most widespread binding domains in the 'LysM' domain, which facilitates direct binding to PG (Buist *et al.*, 2008). LysM domains consist of a 40 amino acid motif that is typically present at one end of the protein, and can be found individually, or repeated up to six times (Steen *et al.*, 2003). Importantly, these domains are found in many bacterial proteins involved in pathogenicity, including numerous Rpf proteins (Ravagnani *et al.*, 2005). Substrate modulation, as introduced for the spore walls of *B. subtilis*, represents another method of control. The delta lactam modification to the Mur*N*Ac residues in the spore wall are substrates for only the germination-specific hydrolases, and not those active during vegetative growth (Heffron *et al.*, 2009). Additionally,

researchers studying sporulation in *B. subtilis* have shown that during this process, a lytic transglycosylase will only cleave its substrate after the stem peptides have been removed by another PG hydrolase (Morlot *et al.*, 2010). And in a final example, a recent study has shown that two amidases important for cell division in *E. coli* require activation by protein factors belonging to the cell division machinery (Uehara *et al.*, 2010). These examples highlight some of the diverse modes of spatial and temporal activation that ensure the proper coordination of cell wall remodeling during specific cellular processes.

1.5 GENE REGULATION IN BACTERIA

In order to conserve energy, organisms regulate most of their genes at the transcriptional level. The RNA polymerase core enzyme (RNAP) directs transciption. RNAP is a multi-subunit complex that has the ability to synthesize RNA using DNA as a template. An essential component of bacterial transcription is the activity of a dissociable protein called a 'sigma factor', which interacts with RNAP, directing it to specific promoters (Helmann, 2002). Most bacteria encode several sigma factors that direct the transcription of genes under specific conditions. While *B. subtilis* encodes ~10 sigma factors, *S. coelicolor* encodes 65 (Bentley *et al.*, 2002). DNA-binding protein can also modulate gene expression by acting as either repressors or activators of transcription. In general, transcriptional activator proteins bind regions upstream, or just overlapping promoter regions and enhance RNAP binding (Barnard *et al.*, 2004).

1.5.1 RNA-based regulation

While the best-characterized transcriptional activators/repressors are protein factors, RNA molecules can also influence gene regulation. Small RNA regulators in bacteria (sRNAs) can be encoded in *cis* or in *trans* relative to their targets. *Trans*-encoded sRNAs are the best understood RNA regulators in bacteria, and they typically associate with their cognate messenger RNA (mRNA) via imperfect base pairing. Pairing can result in changes in mRNA transcript stability, or can affect translation, by blocking the ribosome-binding site (RBS) (translational repression) or alleviating an inhibitory secondary structure that had sequestered the RBS of its cognate mRNA (translational activation) (Majdalani *et al.*, 2005). sRNA regulation often involves the RNA-binding protein Hfq, which facilitates pairing and stabilizing sRNA–mRNA interactions. This tripartite complex is also associated with mRNA degradation, through the recruitment of the single stranded ribonuclease, RNase E (Morita & Aiba, 2011).

While a role for RNAs in regulating plasmid copy number has long been established, the extent of sRNA regulation in bacteria was not fully appreciated until recently (Waters & Storz, 2009). In 2001, the bacterial sRNA field began a rapid expansion when several groups initiated genome-wide computational searches for sRNAs in *Escherichia coli* (Wassarman *et al.*, 2001, Argaman *et al.*, 2001, Rivas & Eddy, 2001), and successfully identified ~50 novel sRNAs. These

screens relied on predicated sRNA attributes, including their location in intergenic (IG) regions >200 nt in size, the association with rho-independent terminators, and high levels of IG sequence conservation between closely related species (Fig. 1.6). A complementary method to identifying sRNAs is the direct cloning of size-fractionated RNA (Lau *et al.*, 2001). Applying this technique to identify *E. coli* sRNAs revealed very little overlap between the two methods, suggesting that the saturation point for sRNA identification had not yet been reached (Kawano *et al.*, 2005). Today, whole genome transcriptomic studies have made it possible to identify RNAs (both coding and non-coding) on an even larger scale, providing an unbiased means of cataloging RNA populations (Sharma *et al.*, 2010). The advent of multiplex DNA sequencing technology, and its application to whole genome transcriptomic studies, will undoubtedly aid investigators in the identification of sRNAs in the future.

Perhaps the most intriguing type of regulatory RNA is the *cis*-encoded riboswitch. Around the same time that the small RNA regulators were being identified and characterized in *E. coli*, members of Dr. Ronald R. Breaker's research group published the first example of a metabolite-sensing regulatory RNA called a 'riboswitch' (Nahvi *et al.*, 2002). In this report, the authors showed that coenzyme B_{12} bound directly to the 5' untranslated region (UTR) of the mRNA encoding the cobalamin transporter, BtuB. The unique observation here was that regulation occurred in the absence of all protein factors: metabolite (B_{12}) binding induced a structural rearrangement in the mRNA that resulted in sequestration of the RBS, thus shutting down BtuB expression (Nahvi *et al.*, 2002). Conceptually, coupling metabolite sensing to the expression of a product that is only required when that metabolite is present, is analogous to feedback loops present in many protein based regulatory systems. However, the fact that BtuB regulation does not require protein factors sets it apart as a completely new regulatory mechanism.

Riboswitches are often located in 5' UTRs of bacterial mRNAs, and consist of two functional domains. Typically, a 70-200 nt 'aptamer domain' located at the extreme 5' end of the riboswitch is responsible for binding a metabolite with high specificity. Metabolite binding causes a structural change in the adjacent 'expression platform' that then leads to expression changes in the downstream gene(s) (Fig. 1.7) (Winkler & Breaker, 2005). The state of the aptamer (bound or unbound) modulates the switching between transcriptional terminators/ribosome-occluding structures, and alternative non-inhibitory structures (Roth & Breaker, 2009). Although riboswitches typically act as negative regulators, there are examples of riboswitches that positively control downstream expression (Dambach & Winkler, 2009). Generally, metabolites are sensed by aptamers controlling the expression of proteins involved in the synthesis, metabolism, or transport of that specific metabolite. Thus, riboswitches represent a means of elegantly coupling gene expression to the physiological and chemical needs of the cell.

1.6 AIMS AND OUTLINE OF THESIS

Fuelled by the recent increase in bacterial sRNA work, our research group set out to identify regulatory RNAs in *S. coelicolor*. Broadly, our strategy included a combination of computational (comparative genomics), and experimental (direct cloning) approaches. In 2008, we published a summary of our findings from this work, relating to sRNAs in *S. coelicolor* (Swiercz *et al.*, 2008). The significance of this publication will be discussed further in Chapter 5. However, the direct cloning experiment revealed some interesting findings that were subjected to separate characterization, and have laid the foundation for the work presented in this thesis.

During a preliminary direct cloning experiment, we examined size-fractioned total RNA extracted from wild-type *S. coelicolor*, grown on different media types, for stable small RNA species. This revealed a population of RNAs ~30-35 nt in size, unique to samples grown on minimal medium. After cloning and sequencing this population, we identified several interesting transcripts including a population of 'tRNA halves', and a 27 nt antisense RNA that is complementary to regions upstream of three genes in *S. coelicolor* – each predicted to encode a cell wall hydrolase protein (Fig. 1.8). Computational analysis revealed that all three of these hydrolase-encoding genes contained predicted leader regions belonging to the '*ydaO*' class of orphaned/uncharacterized riboswitches (Barrick *et al.*, 2004).

Chapter 2 is dedicated to describing the characterization of the population of 'tRNA halves'. Our discovery of this unique RNA species during the cloning experiment prompted us to further characterize the occurrence of tRNA cleavage in *S. coelicolor*. Relying primarily on northern blots we probed for various tRNA halves both in wild-type, and developmental mutant backgrounds. We also attempted to find conditions that induce tRNA cleavage, as this event had recently been shown to be a direct response to amino starvation in another organism (Lee & Collins, 2005). Although we were unable to identify conditions that prompted tRNA cleavage, our findings indicated that the production of tRNA halves was a global phenomenon in *S. coelicolor*. We published these observations in the journal Nucleic Acids Research (Haiser *et al.*, 2008).

In Chapter 3, I describe our characterization of the biological role for the cell wall hydrolases encoded downstream of the predicted '*ydaO*' riboswitch. After confirming that these proteins could cleave the *S. coelicolor* cell wall, we constructed a series of cell wall hydrolase deletion mutants and analyzed their phenotypes. We demonstrated that these cell wall hydrolases likely play a role in all of the major stages of the *S. coelicolor* life cycle – germination, vegetative growth, and sporulation. These finding were published in the Journal of Bacteriology (Haiser *et al.*, 2009).

Having established the importance of the riboswitch-associated cell wall hydrolases for *Streptomyces* biology, we focused our attention on the regulation of the genes encoding these proteins. Chapter 4 provides a summary of our

progress to date in testing the hypothesis that the hydrolases characterized in Chapter 3 are riboswitch-controlled. Our findings suggest that a factor that accumulates in conditioned growth medium represses the expression of at least one of the cell wall hydrolases, RpfA. Moreover, we show that regions of the UTR are important for mediating this repression. Chapter 4 represents unpublished work.

1.7 FIGURES AND TABLES

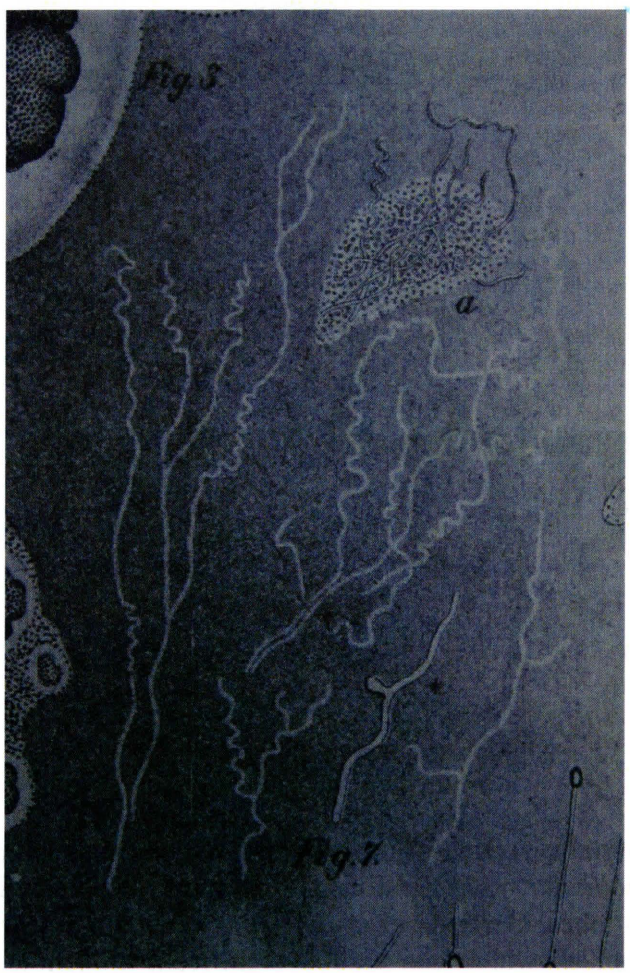

Figure 1.1. The first published photograph of an actinomycete bacterium. This is likely the first published image of an actinomycete. The photo was taken by Ferdinand Cohn (1875) (labeled '*Fig. 7.*' in image). The filamentous organism was isolated from a human tear duct, and Cohn named the organism "*Streptothrix foersteri*". Image modified from: (Waksman, 1967).

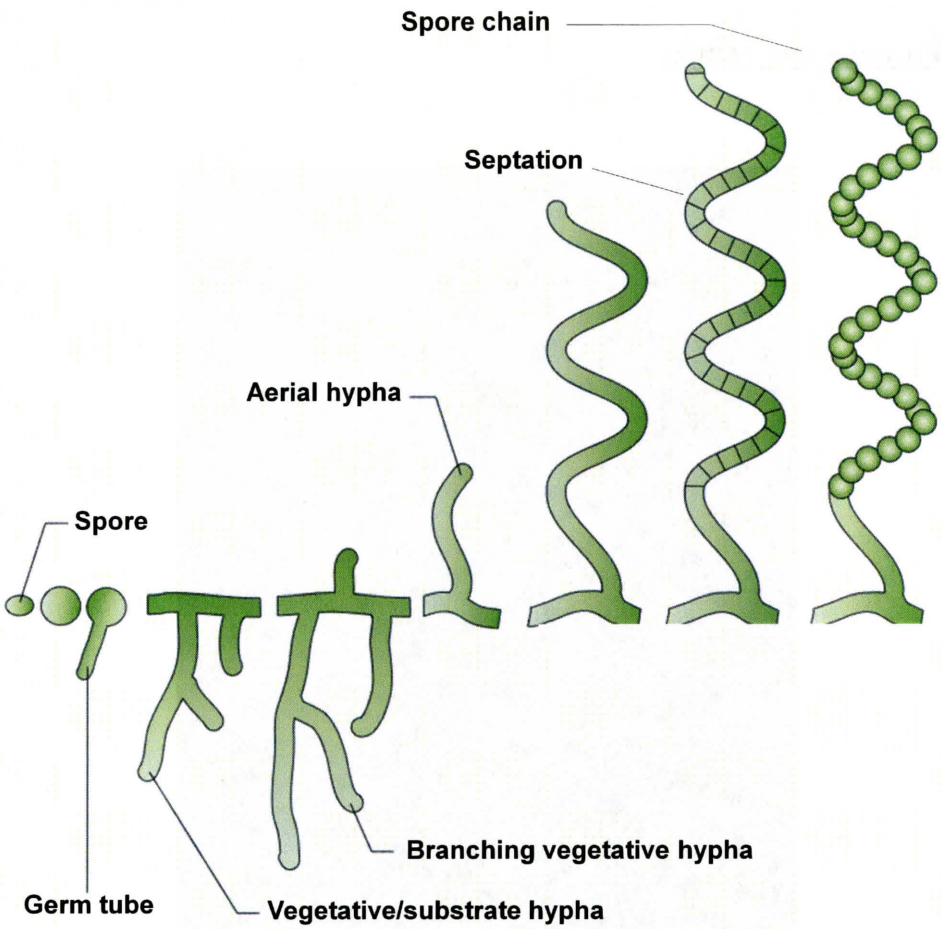

Figure 1.2. Schematic representations of the different cell types exhibited by *Streptomyces coelicolor*. Germination of free spores involves the emergence of one or two germ tubes. Germ tubes grow by tip extension to form the vegetative (or substrate) hyphae, which can exhibit significant branching. Presumably, in response to nutrient depletion, aided by the chaplins and SapB (section 1.2.1.3), the non-branching aerial hyphae grow up into the air. This event coincides with the onset of secondary metabolism (e.g. antibiotic production). The aerial hyphae eventually undergo septation and mature into chains of exospores. Image modified from: (Flärdh and Buttner, 2010).

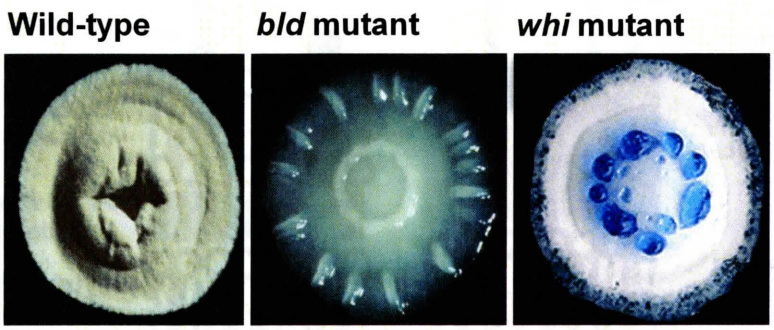

Figure 1.3. Colony appearance of wild-type *Streptomyces coelicolor* vs. *bld* and *whi* mutants. When sporulating, the wild-type *S. coelicolor* colony surface has a grey appearance (left panel). Developmental mutants with the '*bld*' designation lack the 'fuzzy' colony surface seen in the wild-type, as they are unable to raise aerial hyphae (center panel). Mutants with the '*whi*' designation can raise aerial hyphae, but are unable to sporulate (right panel). The white colony surface is characteristic of aerial hyphae formation. The blue droplets on the surface contain the antibiotic actinorhodin – one of the four antibiotics produced by the laboratory strain *S. coelicolor* A3(2). (Photo credit: Brenda Leskiw [left and middle panels], unknown [right panel]; Image modified from: *http://spider.science.strath.ac.uk/sipbs/staff/Paul_Hoskisson.htm*)

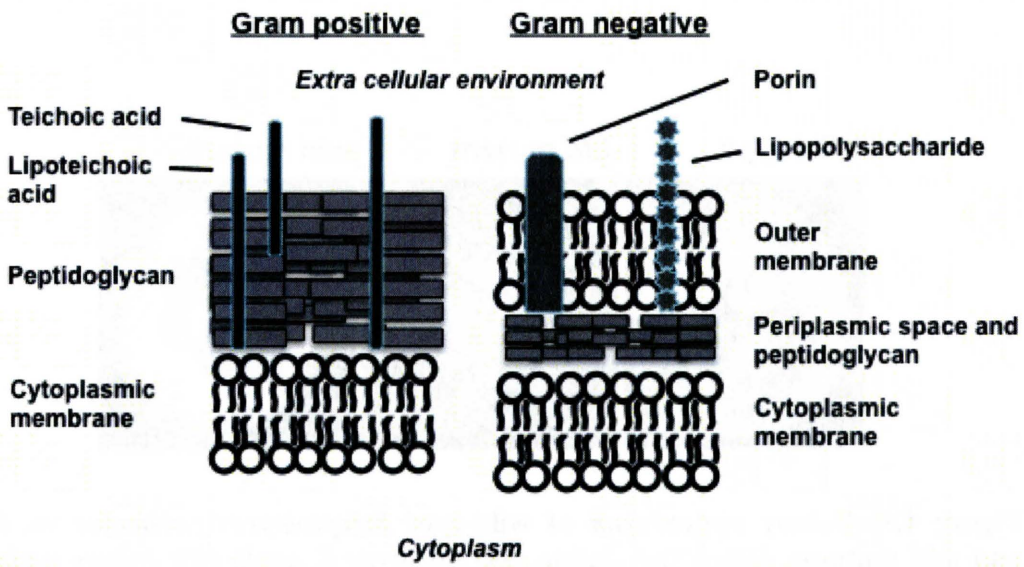

Figure 1.4. General structures of Gram positive and Gram negative cell envelope. Separating the cytoplasm from the extracellular milieu in Gram positive bacteria is the cytoplasmic membrane, and a thick layer of peptidoglycan. Gram positive cell walls are alse decorated teichoic acids which can influence the activity of cell wall lytic enzymes (left panel). Gram negative bacteria have a much thinner layer of peptidoglycan, and an additional 'outer membrane', which includes porins and lipopolysaccharides. (This diagram is not drawn to scale)

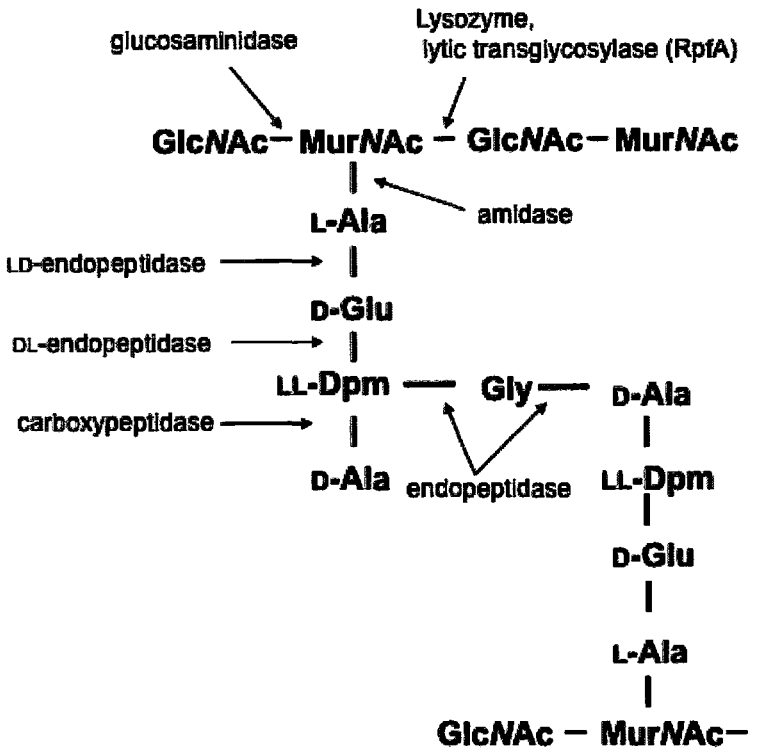

Figure 1.5. The peptidoglycan structure of *S. coelicolor* with potential cell wall hydrolase cleavage sites indicated. Shown is a schematic representation of two parallel glycan strands, linked together by stem peptides connected by an interpeptide bridge (Gly). Also indicated are the cleavage sites of the major groups of cell wall hydrolases, including the site for cleavage by RpfA. (Glc*N*Ac = *N*-acetylglucosamine; Mur*N*Ac = *N*-acetylmuramic acid; LL-Dpm = diaminopimelic acid)

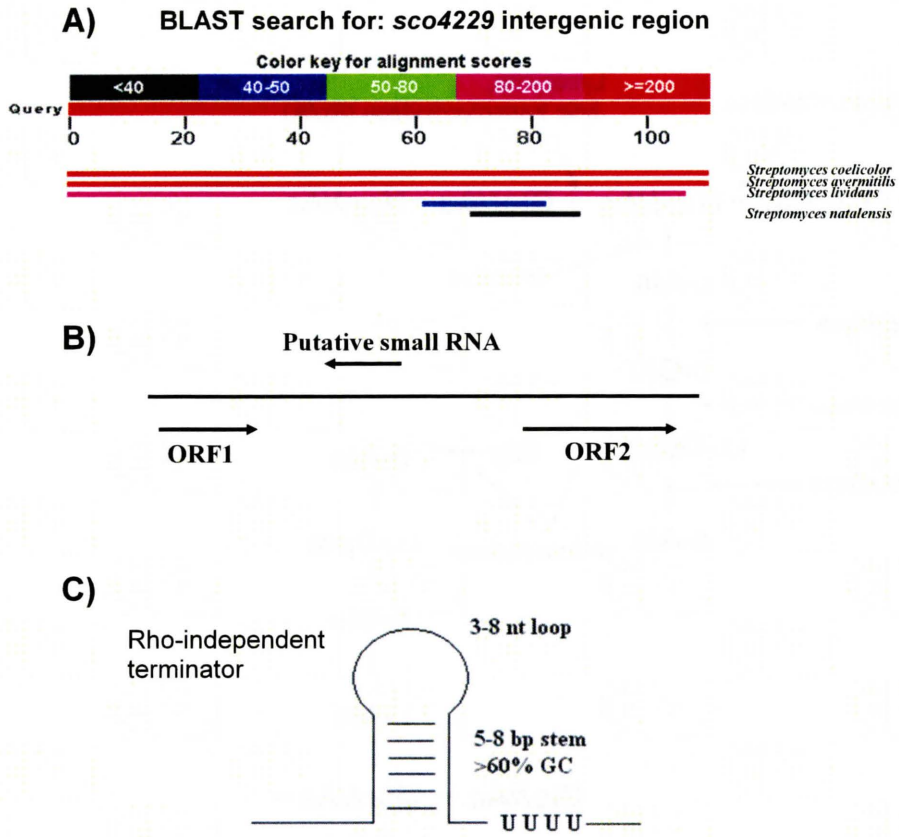

Figure 1.6. Methodology behind computational approach to finding small RNAs. Some considerations for computational screens for small RNAs include conservation of intergenic (IG) sequences between closely related species, putative small RNA gene orientation with respect to local open reading frames, and the presence of rho-independent terminator structures. A) Shown is the BLASTn (Altschul *et al.*, 1990) search result of a 100 nt portion of the 215 nt IG region on the 5' side of the gene annotated as *sco4229*. In this case there appears to be a high level of sequence conservation of the IG region in closely related *Streptomyces* genomes. B) Examining genomic orientation can eliminate false positive small RNA candidates that are often conserved mRNA leaders or trailers. C) The presence of an 'orphaned' Rho-independent terminator (depicted as RNA: G+C rich stem-loop, followed by at least four uridine residues) in an IG region is one of the hallmarks of a small RNA.

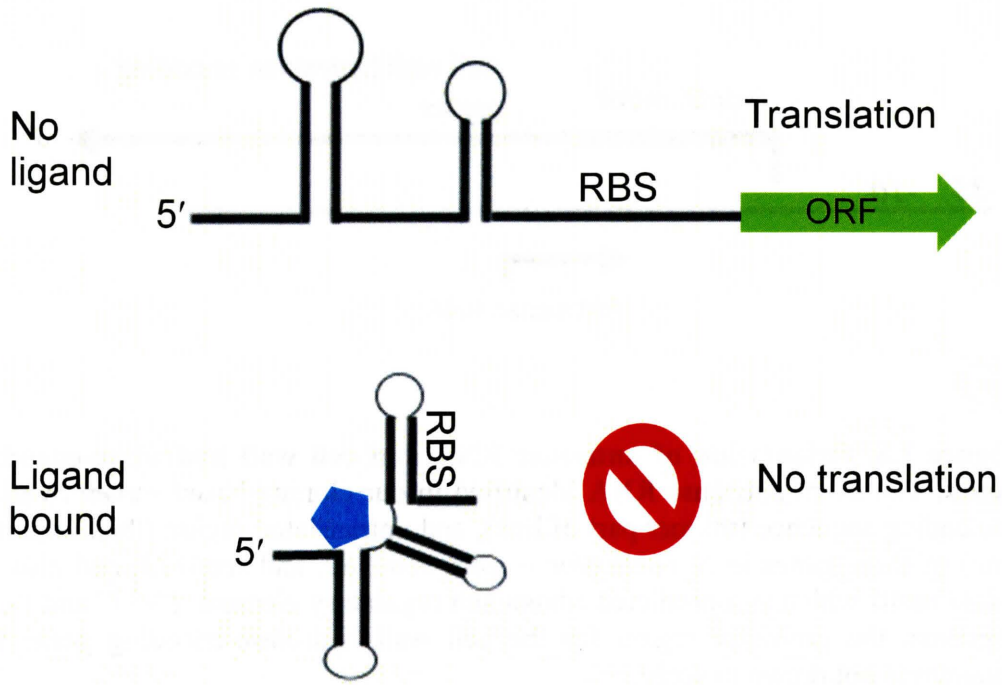

Figure 1.7. Riboswitch regulation. Riboswitches are structured regulatory elements contained within the 5' untranslated region of mRNAs. In the top panel, the structured leader region is in its metabolite- (or ligand) unbound form, and the downstream open reading frame (ORF) is free to be translated into its protein product. However, in the bottom panel a metabolite (represented by the pentagon) binds to the riboswitch 'aptamer domain', causing a structural change that results in the occlusion of the ribosome binding site (RBS), thus preventing ribosome binding, and translation of the downstream ORF. Typically, the function of the protein encoded by the ORF is related to the metabolism or transport of the metabolite. Riboswitches can also impart transcriptional regulation (not depicted here). This involves the 'switching' between transcriptional terminator and anti-terminator structures in the presence/absence of the metabolite.

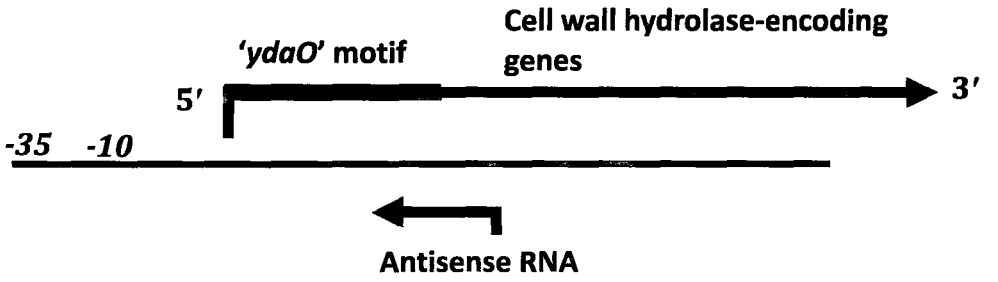

Figure 1.8. Orientation of antisense RNA and cell wall hydrolase-encoding genes. The 27 nt antisense RNA identified in our cloning-based screen overlaps the coding sequence (thinner part of line), and untranslated region (thicker part of line) of three genes in *S. coelicolor* – *rpfA*, *sco4582*, and *sco6773*, and also the *ydaO* motif which is a predicted riboswitch regulatory element. ("*-35*" and "*-10*" represent the promoter region for the cell wall hydrolase-encoding gene; this diagram is not drawn to scale)

CHAPTER 2:

DEVELOPMENTALLY REGULATED CLEAVAGE OF tRNAS IN THE BACTERIUM *STREPTOMYCES COELICOLOR*

Haiser, H. J., F. V. Karginov, G. J. Hannon, and M. A. Elliot.

Preface:
This chapter was published in the journal *Nucleic Acids Research* (Haiser *et al.*, 2008). In collaboration with F.V.K., I carried out the RNA cloning experiments that laid the foundation for this work. I performed all of the additional experiments, and in collaboration with M.A.E., interpreted all of the data. The initial draft of the manuscript was written by M.A.E., while I prepared all of the figures, wrote the methods section, and was involved in editing of the various drafts. This chapter is based on the original manuscript but has been largely rewritten to provide for a more cohesive thesis document, and to include more recent findings in the field. All figures and tables included in this chapter (with the exception of Fig. 2.6) are reproductions from the original manuscript. *Nucleic Acids Research* is an open access journal that grants copyright permissions to the authors.

2.1 CHAPTER SUMMARY

The ability to sense and respond to environmental and physiological signals is critical for the survival of the soil-dwelling Gram-positive bacterium *Streptomyces coelicolor*. Nutrient deprivation triggers the onset of a complex morphological differentiation process that involves raising aerial hyphae and forming spore chains, and coincides with the production of a diverse array of clinically relevant antibiotics and other secondary metabolites. These processes are tightly regulated; however, the genes and signals involved have not been fully elucidated. Here, we report a novel tRNA cleavage event that is growth medium dependent, and follows the same temporal regulation as morphological and physiological differentiation. All tRNAs appear to be susceptible to cleavage; however, there appears to be a bias towards increased cleavage of those tRNAs that specify highly utilized codons. In contrast to what has been observed in other organisms, accumulation of tRNA halves in *S. coelicolor* is not significantly affected by amino acid starvation, and is also not affected by induction of the stringent response or inhibition of ribosome function. Mutants defective in aerial development and antibiotic production exhibit altered tRNA cleavage profiles relative to wild-type strains.

2.2 INTRODUCTION

One of the defining features of the soil-dwelling *Streptomyces* bacteria is their developmental life cycle. During vegetative growth *Streptomyces* grows filamentously, forming a tangled web of mycelia. Nutrient starvation ultimately prompts the growth of reproductive structures called 'aerial hyphae', and this cycle culminates with the formation of dormant exospore chains (Elliot *et al.*, 2008). These developmental changes are associated with major metabolic shifts, including the initiation of secondary metabolism – a process that has provided several clinically relevant antibiotics (Hopwood, 2007). Genetic studies into *Streptomyces* morphological development have revealed a number of key regulators, including the *'bld'* (for 'bald') genes whose products are primarily regulatory proteins that control the raising of aerial hyphae (Elliot *et al.*, 2008).

Interestingly, several *bld* mutants have lost the ability to discriminate between preferred and poorly utilized carbon sources (Pope *et al.*, 1996). These same strains exhibit mutant phenotypes that are conditionally-dependant on the available carbon source (Kelemen & Buttner, 1998). The connection between nutritional status and development is further highlighted by the observation that nitrate limitation affects both aerial hyphae formation, and antibiotic production (Chakraburtty & Bibb, 1997).

The bacterial response to amino acid starvation is often associated with a phenomenon known as the stringent response. In this process, the ratio of uncharged to aminoacylated transfer RNAs (tRNAs) is sensed by the ribosome and can shut down protein synthesis. Excess uncharged tRNAs stimulates the

expression of the protein RelA, which subsequently produces the small molecule, ppGpp. Major metabolic changes occur when ppGpp directly binds RNA polymerase, causing a down regulation of ribosomal proteins and RNA expression, and an up regulation of only the nucleic and amino acids required for survival (Chatterji & Ojha, 2001, Magnusson *et al.*, 2005). Interestingly, in *Streptomyces,* the stringent response is also associated with development and secondary metabolism (Hesketh *et al.*, 2007).

In addition to its role in signaling starvation, tRNAs are perhaps best known because they play an essential role in the transmission of information in all living organisms. The 3' end of mature tRNAs serves as the site for the covalent attachment of amino acids, a reaction catalyzed by aminoacyl tRNA synthetases. Mature tRNAs also contain a single stranded anticodon region that can base pair with a corresponding mRNA codon. As key components of the translational machinery, tRNAs 'transfer' amino acids to growing polypeptide chains in the ribosome. Therefore, tRNAs represent a physical link between mRNA and protein. In the well-studied bacteria *B. subtilis* and *E. coli*, tRNAs are often transcribed together with 5S, 16S, and 23S rRNA genes (Sonenshein *et al.*, 2002, Fournier & Ozeki, 1985). In *S. coelicolor,* however, this does not seem to be the case, as its 63 tRNAs are often encoded alone, or adjacent to other tRNAs (Bentley *et al.*, 2002). To attain their functional form, tRNA transcripts must be processed by ribonucleases. In a well-conserved process, RNase P cleaves off the leader sequence in 'pre-tRNA' molecules, generating the mature 5' end (Condon, 2007). Processing of the 3' end is less well understood, and in *S. coelicolor,* it likely involves several ribonucleases, including the endonucleases RNase E and RNase Z, and exonucleases RNase PH and PNPase (Condon & Putzer, 2002, Phizicky & Hopper, 2010). Because of their complex structures, and their close association with the translational machinery, tRNAs and rRNAs are considered to be more stable than mRNAs. Quality control pathways for improperly processed or modified tRNAs have been well studied in *E. coli* (Deutscher, 2003, Li *et al.*, 2002). Additionally, since stable RNAs represent ~95% of the cellular RNA store, they are often targeted for recycling during stressful conditions (Deutscher, 2006). In *E. coli*, tRNAs are also susceptible to cleavage by the anticodon nuclease PrrC, which cleaves tRNAs as a protective mechanism during T4 bacteriophage infection (Levitz *et al.*, 1990). Moreover, the *E. coli*-encoded 'tRNases' (colicin E5, and D) are functionally analogous to PrrC, although they exhibit exquisite specificity with respect to the substrate tRNAs on which they will act (Masaki & Ogawa, 2002).

In this study, we present evidence for a unique tRNA cleavage event that coincides with the initiation of aerial development in *S. coelicolor*. Our study followed the observation of a similar phenomenon in the ciliated protozoan *Tetrahymena thermophila* (Lee & Collins, 2005). Since the publication of our work, additional reports suggest that tRNA cleavage is a widespread response to stress.

2.3 Materials and Methods

2.3.1 Bacterial strains and culture conditions

Wild-type *S. coelicolor* strain M145 and developmental mutants *bldA* (Piret & Chater, 1985), *bldB* (Merrick, 1976), *bldC* (Hunt *et al.*, 2005), *bldH* (Chater *et al.*, 1982), *whiG* (Flärdh *et al.*, 1999), and *whiB* (Flärdh *et al.*, 1999) were grown on R2YE or MS (mannitol soy flour) agar media, or minimal agar medium supplemented with 0.5% w/v mannitol, or minimal agar medium supplemented with components of R2YE, for 12-72 hours (as indicated). Liquid minimal medium (MM) was supplemented with 0.5% w/v mannitol. All *Streptomyces* cultures were grown at 30°C. OneShot® TOP10 competent *E. coli* cells (Invitrogen) were used for the cloning of cDNA-containing plasmids. *E. coli* was grown at 37°C in Luria-Bertani (LB) liquid or on LB solid medium. *Streptomyces* strains used in this study are summarized in Table 2.1.

2.3.2 RNA isolation and detection

RNA was isolated as described previously (Hopwood DA, 1985); however, plate grown cultures were harvested by directly scraping cells from agar overlaid with cellophane discs, into modified Kirby's mixture [1% w/v N-lauroylsarcosine sodium salt, 6% w/v sodium 4-amino salycilate, 6% v/v phenol mixture (pH 7.9) made in 50 mM Tris (pH 8.3)]. Total RNA samples were quantified by UV spectroscopy using the Ultrospec 3100 pro (Biochrom), and RNA quality was assessed using agarose gel electrophoresis. Total RNA was detected using either SYBR Gold (Molecular Probes) staining or 3' pCp end-labeling with T4 RNA Ligase (Roche). Samples were run on 12% denaturing polyacrylamide gels, and were visualized using either UV light or autoradiography, respectively.

2.3.4 Oligonucleotides

The sequences of all DNA oligonucleotides used in this study, as well as the hybrid RNA/DNA adaptors used for RNA cloning, are summarized in Table 2.2.

2.3.5 RNA cloning

Total RNA (~100 µg) was separated on a denaturing 12% polyacrylamide gel and the region corresponding to abundant 30-35 nt RNA species was excised. RNA was eluted from the gel slice overnight at 4°C in 20 mM Tris (pH 8.0), 0.5% SDS, 1 mM EDTA, and 0.4 M sodium acetate. Cloning of the excised RNA species was carried out using a previously described method (Lau *et al.*, 2001), with minor modifications. Briefly, RNA was recovered from the elutate by ethanol precipitation with 20 µg of glycogen, and samples were re-suspended in 30 µl dH_2O. Ligation of the 3' adapter (Modban; Table 2.2) was carried out for one hour at 37°C in a 20 µl reaction volume consisting of 13 µl purified RNA, 10 µM 3' DNA adapter oligonucleotide (IDT DNA Technologies), 50 mM Tris-HCl (pH 7.5), 10 mM $MgCl_2$, 10 mM DTT, 60 µg/ml BSA, 10% DMSO, 40 U T4 RNA Ligase (Amersham Biosciences). The ligation mixture was ethanol precipitated,

and separated on a 12% denaturing polyacrylamide gel followed by purification of the ligated products as described above, except that the RNA was resuspended in 20 μL dH_2O. The 3'-adapter-ligated RNA was then ligated to the DNA/RNA 5'-adapter (Nelson's linker; IDT DNA Technologies; Table 2.2) as described above, with the inclusion of 1 mM ATP. The ligation mixture was again ethanol precipitated and separated on a 12% denaturing polyacrylamide gel prior to purification. The RNA was then used as a template for reverse transcription (RT) using 200 U SuperScript II reverse transcriptase (Invitrogen) and the BanOne oligonucleotide (Table 2.2), whose sequence corresponded to the inverse complement of the 3'-adapter. The RT reaction was carried out at 42°C for one hour. The resulting cDNA was used as a template for PCR amplification with *Taq* DNA polymerase (Invitrogen) using oligonucleotides BanOne and BanTwo (Table 2.2). Products ~80 bp in size were recovered from a 2% agarose gel using a gel extraction kit (Qiagen) and were directly cloned into the pCR®2.1 – TOPO® vector (Invitrogen). Plasmid DNA was isolated from positive clones, and was sequenced using M13 forward and M13 reverse oligonucleotides (Table 2.2). The resulting sequences were then analyzed using BLAST (Altschul *et al.*, 1990).

2.3.6 Northern blot analysis

Total RNA samples were separated on 12% denaturing polyacrylamide gels and transferred to Zeta-Probe nylon membranes (Bio-Rad) using a Trans-Blot semi-dry transfer cell (Bio-Rad) (25 V for 30 minutes). Membranes were cross-linked using an XL-1000 UV crosslinker (Spectronics). 5' end-labeled oligonucleotides, complementary to either the 5′ or 3′ half of the tRNA of interest, were hybridized with the membranes overnight at 42°C in ULTRAhyb-oligo hybridization buffer (Ambion). Membranes were washed twice with 2 × SSC, 0.1% SDS for 30 minutes, followed by a single wash with 0.2 × SSC, 0.1% SDS for 10 minutes. Detection and quantification of signals were achieved using a Storm 820 phosphorimager (Molecular Dynamics) and ImageQuant v 5.2 (Molecular Dynamics) software. Where applicable, the change in the ratio of full-length tRNA: tRNA half was determined using intensity values obtained from the 'Volume Report' function of this software. To correct for background signals, we subtracted the intensities of equally sized areas on the blot adjacent to the bands, from all data points before using the resultant values for determining the ratio.

2.3.7 Translational inhibition and stringent response assay

Wild-type *S. coelicolor* strain M145 was grown in 20 ml liquid minimal medium (MM) supplemented with 0.5% w/v mannitol for 41 h at 30°C. Cultures were then homogenized using a glass homogenizer before adding the indicated antibiotic or chemical (spectinomycin [200 mg/ml], hygromycin [50 mg/ml], thiostrepton [50 mg/ml], serine hydroxamate [25 mM]). Cultures were then incubated for 30, 60, or 90 minutes, after which RNA was isolated as described above.

2.4 RESULTS

2.4.1 Detection of medium-dependant 30-35 nt RNAs

We were interested in taking a direct cloning approach to discovering novel regulatory RNA species in *S. coelicolor* (Kawano *et al.*, 2005). Examining total RNA stained with either ethidium bromide or the more sensitive SYBR Gold following separation on a high percentage polyacrylamide gel typically reveals bands corresponding to 23S rRNA, 16S rRNA, 5S rRNA, and tRNA. However, smaller (<80 nt) RNAs are typically missed with these procedures. To increase the sensitivity of our RNA survey, we chose to 3' end-label total RNA samples using [^{32}P] pCp and RNA ligase, prior to separation on a polyacrylamide gel. Additionally, since there have been many examples of small regulatory RNAs expressed in response to specific conditions including nutrient stress (Gottesman *et al.*, 2006), we reasoned that a comparison of RNA expression between nutrient rich (R2YE) and nutrient limiting (MS) conditions might reveal such different RNA populations in *Streptomyces*. To broaden the coverage of possible expressed RNAs, we also examined RNAs isolated at two time points in our initial analysis: after 24 and 48 hours of growth. Our analysis revealed an abundant population of 30-35 nt RNAs present in RNA samples harvested from minimal growth medium, but absent from samples originating from rich growth medium (Fig. 2.1A). Notably, this RNA population appeared more than twice as abundant in the 24-hour sample when compared to the 48-hour sample. Following up on this observation, we examined a full RNA time course encompassing all major cell types in *S. coelicolor* and found that the 30-35 nt RNA species peaks in abundance after ~24 hours of growth and then tapers off, but remains detectable as the cells approach the sporulation phase of growth (Fig. 2.1B). The 30-35 nt RNA species is not detectable at any stage of development in RNA samples harvested from cells grown in rich medium conditions (data not shown).

2.4.2 The 30-35 nt RNA species is dominated by tRNA halves

We employed a direct cloning approach to obtain sequence information corresponding to the 30-35 nt RNA species. Briefly, RNA isolated from cultures grown on MS medium for 24-hours was size-fractionated and the region on the gel corresponding to the 30-35 nt RNA species was excised and the RNA was extracted and purified. To facilitate identification of the RNAs present, nucleic acid linkers were ligated onto the ends of the RNA molecules. The linker-ligated RNAs were then reverse transcribed, creating of a cDNA library that was then cloned and sequenced.

The vast majority of cloned sequences corresponded to intergenic regions (IG). Of the intergenic sequences cloned, 72% corresponded to tRNA genes, and 25% matched either rRNA or signal recognition particle (SRP) fragments (see Appendix, Table 6.1). Further analysis of the tRNA sequence subset revealed an interesting trend - all sequences corresponded to either the 5' or 3' half of the tRNA molecule, suggesting that they were the result of a cleavage event in, or

near the tRNA anticodon loop. In total, sequences from 17 of the 63 *S. coelicolor* tRNAs were obtained, although there were significant differences in the relative proportion of clones represented (Table 2.3). We did not detect an overall bias towards either the 5' or 3' tRNA half, as approximately equal proportions of both halves were obtained. In *S. coelicolor*, some tRNAs are encoded by as many as five genes (e.g. Met/CAU), while others are encoded by a single gene (e.g. His/GUG). Additional analyses revealed that there did not seem to be a correlation between the number of genes encoding a given tRNA and number of 'tRNA half' clones obtained. However, there did appear to be a codon-usage bias, as we identified at least 7-fold more 'frequently used' tRNAs when compared to those used 'less frequently' (*S. coelicolor* codon-usage statistics from TIGR). Importantly, we noticed that those tRNA halves cloned multiple times exhibited heterogeneity at both ends. This suggests that tRNA cleavage was unlikely to be dependent upon site specificity. Finally, the 3' halves that were cloned typically included the terminal 'CCA' sequence (or some portion of it) (see Appendix, Table 6.1). The CCA sequence is added post-transcriptionally for almost all *Streptomyces* tRNAs (Sedlmeier *et al.*, 1994), in contrast to *E. coli,* where the CCA sequences is encoded as part of all tRNA genes (Fournier & Ozeki, 1985). This indicates that the substrate for this tRNA cleavage event is likely to be mature tRNA, as opposed to a partially processed tRNA precursor.

2.4.3 Cleavage of tRNAs in the anticodon loop generates a stable population of 30-35 nt RNAs

To validate our findings from the cloning experiment, we set out to see if we could detect 'tRNA half' species via northern blotting. To accomplish this, we separated RNA isolated from several time points throughout the *S. coelicolor* life cycle on denaturing polyacrylamide gels, transferred these RNAs to a nylon membrane, and probed for specific tRNA halves using end-labeled DNA oligonucleotides. The His/GUG tRNA was the most-represented tRNA in our cloning experiment (both 5' and 3' halves were cloned). Therefore, in our initial experiments we probed for both halves of this tRNA. Indeed, we were able to detect both 5' and 3' halves for the tRNA His/GUG via northern blotting. Moreover, the expression pattern correlated with that of the 30-35 nt RNA species detected in end-labeled total RNA samples (Fig. 2.2). Next, we asked whether these findings could be extended to include tRNA fragments not identified in our original cloning experiment. To address this, we carried out northern blot analysis for the following tRNA fragments: 5' and 3' Met (5' halves were cloned but 3' halves were not), 5' and 3' Leu/UUA (the least frequently used codon in *S. coelicolor*, whose tRNA is encoded by the *bldA* gene; neither half was cloned), 3' Ser (5' halves were cloned but 3' halves were not), and 5' Asn (3' halves were cloned but 5' halves were not). In all cases just described, we could detect the 5' tRNA halves (Fig. 2.3). Interestingly, however, despite having detected 5' halves for Met, Leu, and Ser, we were unable to detect the corresponding 3' halves. It should be emphasized that this was not the case for all 3' halves, as we detected 3'

halves via cloning and northern blotting for several tRNAs (Fig. 2.2; data not shown). Taken together, these data suggest that under the conditions tested, the 3' halves for some tRNAs are less stable than their corresponding 5' half.

2.4.4 tRNAs cleavage proceeds differently in developmental mutants compared to wild-type strains

After growing *S. coelicolor* on MS medium for ~24 h, developmental changes begin to occur, as reproductive structures called aerial hyphae are produced. Aerial hyphae formation coincides with the production of secondary metabolites. We noticed that the appearance of the 30-35 nt RNA species, which we have shown includes an abundance of 'tRNA half' fragments, is temporally correlated with these developmental changes. Given the established genetic links between development and secondary metabolism, we wondered whether tRNA half production was dependant upon any of the genes that play important roles during this developmental stage. Since the *bld* genes control aerial hyphae formation, we sought to monitor tRNA half production in genetic backgrounds lacking different *bld* genes. For these experiments we chose to examine the presence of 5' His and 5' Met tRNA halves, as we had previously identified each of these in our cloning experiment and also detected each via northern blotting of RNA from the wild-type strain. Four *bld* mutant strains were chosen - *bldA* (encodes the rare leucine UUA tRNA) (Piret & Chater, 1985), *bldB* (encodes a small actinomycete-specific protein of unknown function) (Merrick, 1976), and *bldC* and *H* (both encode DNA-binding transcription factors) (Hunt *et al.*, 2005). Our northern blot analyses indicated that for all *bld* strains tested, the 5' His tRNA halves did not appear until 48 h of growth, reached maximal intensity after 72 h, and were mostly absent by 96 h in the *bldA* and *C* backgrounds, although they were still detectable in the *bldB* and *H* backgrounds (Fig. 2.4). Interestingly, the 5' Met tRNA half had a very different expression pattern. It was only detected in the *bldB* background, where it was present (albeit at low levels) by 48 h of growth, reached maximal expression after 72 h of growth, and was still visible after 96 h (Fig. 2.4). It should be noted that the delays in the appearance of tRNA halves in the *bld* mutants might be explained by the fact that these strains grow more slowly than the wild-type strain under the conditions used.

The second major group of developmentally relevant genes in *S. coelicolor*, the *whi* genes, are essential for sporulation, and we therefore wanted to test if mutants lacking these genes also produced tRNA halves. We found that both of the *whi* strains tested (*whiB* and *G*) generated 5' His and 5' Met tRNA halves like the wild-type strain (Fig. 2.5). These results suggest that although the tRNA half profiles in some of the developmental mutants tested differs from those of the wild-type strain, tRNA half production does not depend on aerial hyphae production, antibiotic production, or sporulation.

2.4.5 tRNA cleavage is not dependant upon nutrient stress

At the time this study was carried out, there was recent evidence to suggest that amino acid starvation caused a similar tRNA cleavage phenomenon in the protozoan *T. thermophila* (Lee & Collins, 2005). In our study, we successfully identified both conditions under which tRNA cleavage occurred, and those under which it did not; however, the exact nature of the signal or event that triggered tRNA cleavage remained unknown. As a first step toward narrowing down the nature of a potential tRNA cleavage 'cue', we examined the components of the growth media used in our studies. We detected tRNA cleavage only when cultures were grown on MS medium – a medium containing soya flour, and with mannitol as the primary (sub-optimal) carbon source (Kieser *et al.*, 2000). However, when we grew cultures on a defined minimal medium (MM) (Kieser *et al.*, 2000) supplemented with asparagine as the sole amino acid, we found that tRNA halves accumulated in a manner similar to that seen on MS medium (Fig. 2.6). With defined growth conditions that are conducive to tRNA cleavage we then began adding individual components of the rich growth medium (R2YE) on which tRNA halves are not produced, to the MM, in an effort to identify factors that could inhibit tRNA cleavage.

We first supplemented MM with yeast extract and proline (individually and together). These are the major amino acid sources of R2YE; however, we found that tRNA cleavage proceeded as had been previously observed on MS medium (Fig. 2.6). We also tested whether the carbon source affected tRNA cleavage by replacing mannitol (a poorly utilized carbon source) with glucose (the primary carbon source of R2YE). Notably, growth did not seem to be affected by carbon source (data not shown), and after testing RNA isolated from cells grown under these two conditions, we found no decrease or delay in tRNA cleavage (Fig. 2.6), suggesting that carbon source is not a major factor in this phenomenon. Additionally, we tested the effect of an osmotic growth medium (by including sucrose to 10.3% - as is found in R2YE), and buffering the growth medium (by adding TES buffer – another component of R2YE). Neither of these manipulations resulted in any change in tRNA half cleavage when compared to the low-osmolarity and unbuffered medium control experiments, respectively (Fig. 2.6).

2.4.6 tRNA cleavage is not dependent upon the stringent response, or ribosome inhibition

Studies have linked ppGpp and the initiation of the stringent response with antibiotic production and morphological development in *Streptomyces* sp. (Ochi, 1986, Ochi, 1987). Given the established connection between amino acid starvation and tRNA cleavage (Lee & Collins, 2005), we reasoned that inducing the stringent response might induce tRNA cleavage in *S. coelicolor*. The stringent response can be induced in multiple ways including amino acid starvation, and growth in the presence of amino acid analogues. The bacteriostatic compound L-serine hydroxamate (SHX) is a serine analogue that inhibits protein synthesis by competitively binding to seryl tRNA synthetases (Tosa & Pizer, 1971). Thus, we

added SHX to cultures that had been growing in liquid culture for ~40 h, allowed them to grow for an additional 1.5 h during which three RNA samples were harvested for subsequent analysis of tRNA cleavage in response to this induced starvation. Comparing 5' His, Met, and Ser tRNA half accumulation to that of untreated control samples did not reveal any significant changes in tRNA cleavage under the induced stress (Fig. 2.7).

Finally, we wondered if tRNA cleavage could be a response to translational stress. One way of inducing this is through the use of ribosome-targeting antibiotics. Spectinomycin, hygromycin, and thiostrepton are antibiotics that interact with either 16S rRNA or ribosomal proteins to effectively shut down protein synthesis (Bilgin *et al.*, 1990, Jonker *et al.*, 2007, Pfister *et al.*, 2003). Of these three treatments, hygromycin was the only one to show any significant change as it decreased the overall amount of tRNA halves present; treatment with spectinomycin and thiostrepton had no significant effect (Fig. 2.7).

These results suggest that neither induction of the stringent response nor the stalling of protein synthesis is sufficient to significantly stimulate tRNA cleavage in *S. coelicolor*.

2.5 Discussion

In this work we describe a unique tRNA cleavage event that correlates temporally with the initiation of the well-studied developmental program of *S. coelicolor*. This discovery was made fortuitously during a direct cloning screen for sRNAs.

Preceding the work described here, Lee and Collins (2005) identified a tRNA cleavage phenomenon that occurred in response to amino acid starvation in the protozoan *T. thermophila*. The work presented here was the second example of what has turned out to be a widespread phenomenon. Indeed, oxidative stress causes tRNA half accumulation in *Saccharomyces cerevisiae*, plants, and human cells (Thompson *et al.*, 2008, Yamasaki *et al.*, 2009), and tRNA halves also accumulate in the protozoan *Giardia lamblia* following starvation-induced morphogenesis (Li *et al.*, 2008). Additionally, several transcriptomic studies have identified tRNA halves in a multitude of organisms including the fungus *Aspergillus* (Jochl *et al.*, 2008), human liver cell carcinoma lines (Kawaji *et al.*, 2008), pumpkin phloem sap (Zhang *et al.*, 2009), and the fruit fly *Drosophila* (Aravin *et al.*, 2003). The widespread nature of this tRNA cleavage event suggests the potential for a conserved yet still poorly understood biological process.

Several aspects of the tRNA cleavage phenomena are of significant interest and warrant further study. Perhaps most interesting, are the nature of the signals that induce tRNA cleavage, the identity of the ribonucleases that carry out the cleavage, and the biological significance of cleaving tRNAs to produce tRNA halves.

With respect to the cues that induce tRNA cleavage - stress is a commonality between most examples described so far. Lee and Collins (2005)

indicate that the routine propagation of *Tetrahymena* requires supplementation with 11 amino acids, and removing just one of these is sufficient to promote tRNA cleavage. In another study where oxidative stress was implicated in inducing tRNA cleavage, glucose starvation, and UV irradiation could not induce similar effects, suggesting that tRNA cleavage is not a general stress response, but rather results from specific stresses (Thompson *et al.*, 2008). One of the key findings of this work is that in *S. coelicolor*, tRNA cleavage is growth medium-dependent. More specifically, tRNA halves are detectable only when cultures have been propagated on minimal (MS/MM) growth medium, and not rich medium (R2YE) (Fig. 2.1A). We were unable to determine a specific component of rich medium that prevented tRNA cleavage from proceeding. Moreover, amino acid starvation is not likely to be involved, as *Streptomyces* is capable of producing all of the amino acids it requires. Given that cleavage coincides with aerial hyphae formation, a process initiated in response to nutrient limitation, we infer a potential link to stress/starvation. However, an alternative explanation for this medium-dependence is that tRNAs are actually cleaved with equal frequency when grown on rich and minimal medium, but are more rapidly degraded on rich medium and thus not detected.

Recently, some exciting studies have shed light on the nature of the ribonucleases responsible for tRNA cleavage. In *S. cerevisiae*, Rny1, an RNase T2 family member has been implicated in tRNA cleavage (Thompson & Parker, 2009b). Interestingly, mammalian cells contain an Rny1 homolog but it does not appear to cleave tRNAs; instead, mammalian cells utilize angiogenin, a member of the RNase A family, to produce tRNA halves (Fu *et al.*, 2009, Yamasaki *et al.*, 2009). In contrast to PrrC and the colicins of *E. coli*, both of these ribonucleases act non-specifically, and exhibit cleavage activity against other RNAs, including rRNAs (Thompson & Parker, 2009b, Yamasaki *et al.*, 2009, Thompson & Parker, 2009a). Another feature common to both RNases is that each requires some form of activation. This is accomplished either through the elimination of an inhibitory protein, or secretion/subcellular localization to the cytosol. *S. coelicolor* lacks obvious homologs of both these ribonucleases (data not shown), nevertheless we are tempted to speculate on the nature of the cleavage enzyme in this organism. Given that tRNA halves seem to result from cleavage within the anticodon loop, a single stranded region of RNA, an attractive candidate would be the single-stranded ribonuclease RNase E (Cohen & McDowall, 1997). An interesting feature of the *S. coelicolor* RNase E enzyme is that its activity increases with development (Hagège & Cohen, 1997), a feature shared with the tRNA cleavage phenomenon we have described. However, upregulation of RNase E activity is absent from the *bldA* strain and is not affected by *bldC* mutations (Hagège & Cohen, 1997). As we did not detect any significant differences in tRNA cleavage between *bldA* and *bldC* (Fig. 2.4), it is unlikely that RNase E contributes significantly to tRNA half production in *S. coelicolor*.

Full length tRNAs are generally stable molecules, with half lives exceeding two days in some eukaryotes (Nwagwu & Nana, 1980), and it is

thought that extensive tertiary structure, and association with aminoacyl tRNA synthetases and ribosomes, likely protects tRNAs from degradation. Interestingly, the rate of turnover for 5′ and 3′ tRNA halves differs, as we were unable to detect 3′ halves for a number of tRNAs despite observing 5′ halves (Fig. 2.3). This suggests that the 3′ halves are either more susceptible to degradation, or are being preferentially degraded relative to the 5′ halves. A possible mechanism to explain this discrepancy would be through the activity of a 5′ → 3′ exonuclease such as RNase J1 (Mathy *et al.*, 2007), which has a role in the maturation of 16S rRNA. The substrate preferences for RNase J1 include monophosphorylated or hydroxylated single stranded 5′ ends (which typically result from endonucleolytic cleavage and spontaneous 'in-line' cleavage, respectively) but not the 5′ triphosphorylated ends of unprocessed transcripts (Mathy *et al.*, 2007, Deana *et al.*, 2008). Thus, endonucleolytic cleavage in the anticodon loop would render 3′ tRNA halves susceptible to RNase J1 degradation. There is an RNase J1 homologue in *S. coelicolor* (SCO5745), and it is predicted to have ~40% amino acid identity (60% similarity) to the *B. subtilis* RNase J1 protein, suggesting that it likely shares a similar function. Thus, it is of significant interest to test whether RNase J1 plays a role in tRNA cleavage in *S. coelicolor*.

Perhaps the most elusive aspect of the tRNA cleavage phenomenon has been pinpointing its biological consequences. Typically, tRNAs and rRNAs are highly transcribed molecules, with one study demonstrating that yeast cells produce an average of ~3 million tRNAs per generation, compared to ~60 thousand mRNAs (Waldron & Lacroute, 1975). Considering the magnitude of energy invested in producing tRNAs, it is tempting to suggest that under nutrient limiting conditions, cells might seek to cleave tRNAs to simultaneously arrest translation (and therefore protein synthesis), and recover a portion of the energy invested in tRNA through a degradation/recycling pathway. There is a problem, however, with this argument: if the goal of tRNA cleavage is to slow down protein synthesis, one would expect full length tRNAs to become significantly depleted once tRNA cleavage pathways have been initiated. Our results and the results of others suggest that this is not the case (Fig. 2.1; 2.3) (Thompson *et al.*, 2008, Yamasaki *et al.*, 2009).

One exciting study has shown that tRNA half fragments were part of an RNA mixture capable of inhibiting the translation of mRNAs *in vitro* (Zhang *et al.*, 2009), while another demonstrated that when transfected into human cell lines, 5' (and not 3') tRNA halves are capable of inhibiting protein synthesis (Yamasaki *et al.*, 2009). The latter observation is exciting in light of the fact that at least in *S. coelicolor*, 5' halves are more stable than 3' halves, and would thus be better suited to act as a signaling molecule. Furthermore, another study using HeLa cells showed that tRNAs bind to cytochrome c, preventing it from binding to the caspase activator protein, which inhibits programmed cell death. Interestingly, tRNA cleavage relives this block and causes apoptosis (Mei *et al.*, 2010). Some have proposed that upon the initiation of aerial growth in *S. coelicolor*, the substrate hyphae undergo programmed cell death (Manteca *et al.*,

2006). The appearance of tRNA halves coincides with aerial growth; moreover, *S. coelicolor* encodes several caspase-related proteins (data not shown). It would be interesting if future studies focused on directly testing whether tRNA halves function similarly in *S. coelicolor*, or are perhaps even able to act as a cue for the initiation of developmental programs in this organism.

Acknowledgements from original manuscript:

This work was funded by the Natural Sciences and Engineering Council of Canada (NSERC) Discovery Grant (No. 312495). We would like to thank Mary Yousef, Christian Baron and Mark Buttner for helpful discussions and/or comments on the manuscript, and Debrah Thompson and Roy Parker for their willingness to share unpublished data. F.V.K. is supported by a post-doctoral fellowship (# PF-07-058-01-GMC) from the American Cancer Society. Funding to pay the Open Access publication charges for this article was provided by McMaster University

2.6 FIGURES AND TABLES

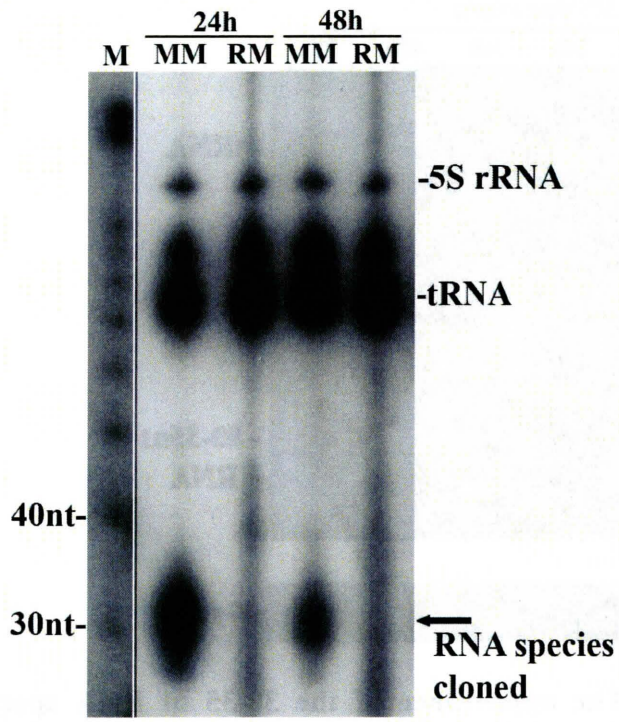

Figure 2.1A. Accumulation of a 30-35 nt RNA species in *S. coelicolor* grown on minimal medium. Total RNA harvested from minimal and rich media after 24 or 48 h was end-labeled with pCp. Samples were separated on a 12% denaturing acrylamide gel and exposed to X-ray film. Distinct 30-35 nt RNA species were detected only in samples harvested from minimal medium. (M=Decade marker [Applied Biosystems]; MM=Minimal medium; RM=Rich medium)

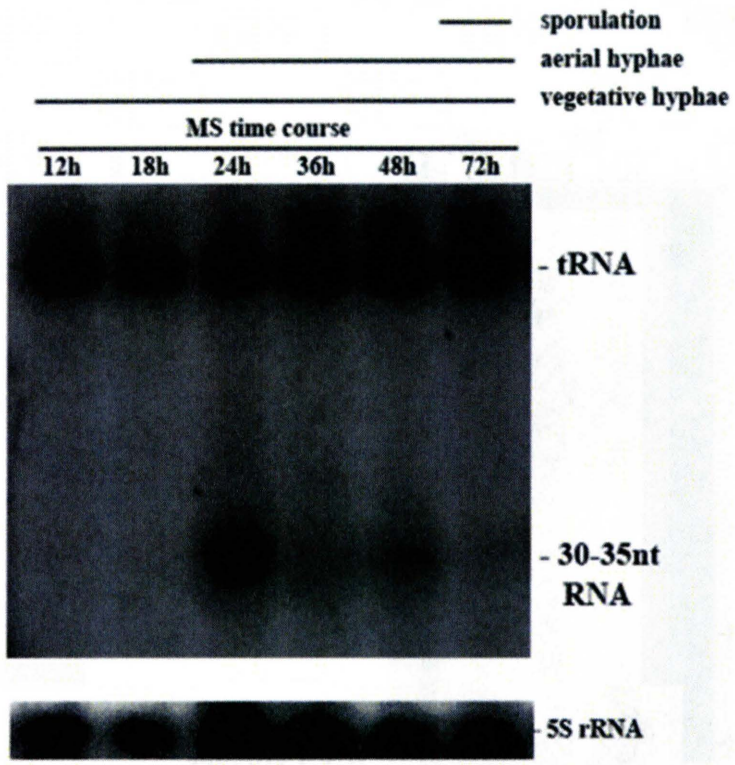

Figure 2.1B. The appearance of the 30-35 nt RNA species is temporally correlated with aerial development. The appearance of the 30-35 nt RNA species is temporally correlated with aerial development. A time course of 3' end-labeled RNA harvested from minimal medium was separated on an acrylamide gel. Shown is the 30-35 nt region of the acrylamide gel, and below that is shown the 5S RNA region of the gel (control for RNA loading and RNA integrity).

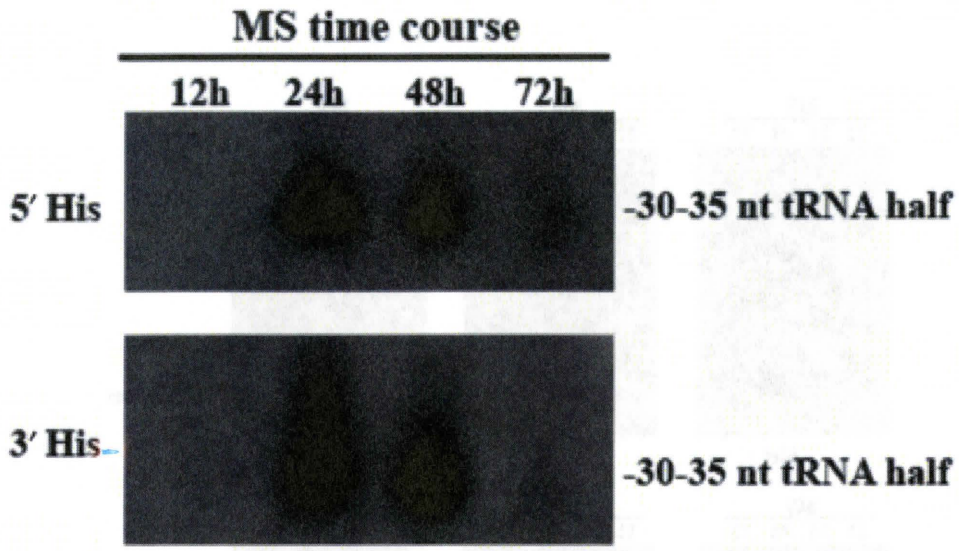

Figure 2.2. Northern blot analysis for the 5′ and 3′ halves of histidine tRNA in a wild-type background. Total RNA samples harvested from MS medium were separated on 12% polyacrylamide gels and were subjected to northern blotting using probes complementary to the 5′ and 3′ halves of the histidine tRNA. Blots were exposed to a phosphorimager.

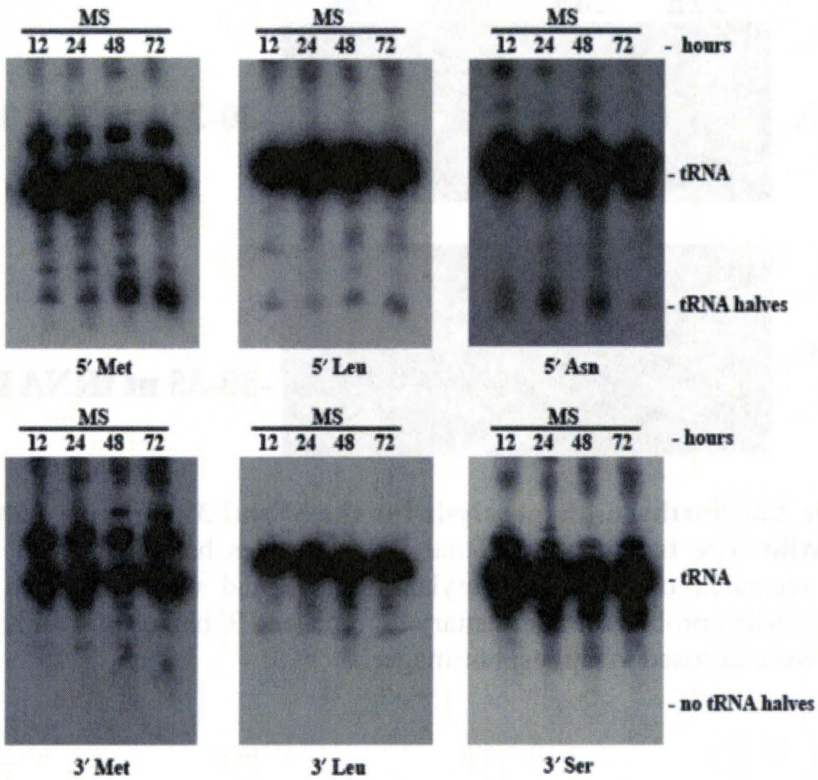

Figure 2.3. Northern blot analysis of tRNAs isolated from MS medium grown cultures. Total RNA was isolated from MS medium-grown cultures after 12, 24, 48 and 72 h of growth. The RNA was separated on 12% polyacrylamide gels and was subjected to northern blotting using probes that were complementary to the indicated tRNA half before being exposed to X-ray film.

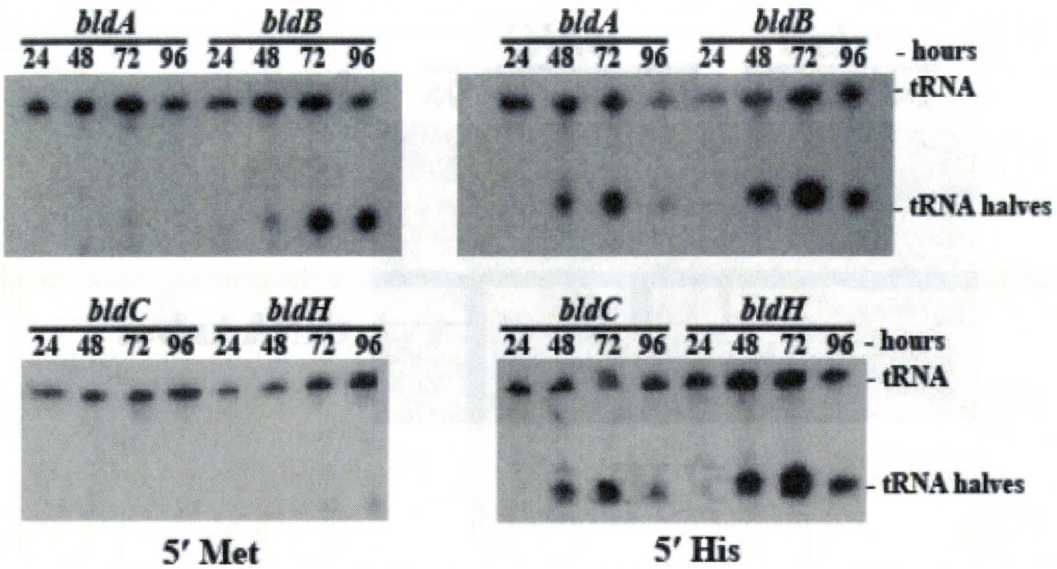

Figure 2.4. Northern blot analysis of tRNAs isolated from *bld* mutants. Total RNA from *bldA*, *bldB*, *bldC*, and *bldH* mutant strains was isolated from MS-grown cultures after 24, 48, 72 and 96 h of growth, as indicated. The RNA was separated on 12% polyacrylamide gels, and was subjected to northern blotting using probes complementary to the 5′ half of Met (left panels) or His (right panels) tRNA.

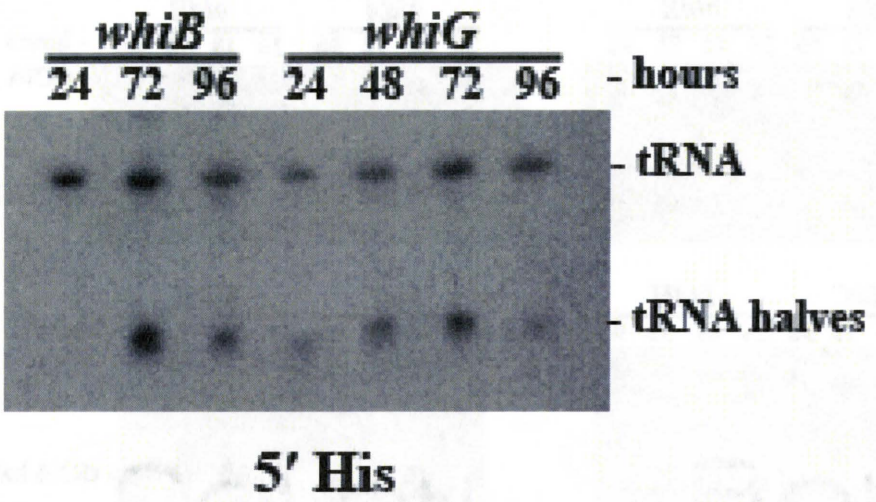

Figure 2.5. Northern blot analysis of tRNAs isolated from *whi* mutants. Total RNA from *whiB*, and *whiG* mutant strains was isolated from MS-grown cultures after 24, 48, 72 and 96 h of growth, as indicated. The RNA was separated on 12% polyacrylamide gels, and was subjected to northern blotting using probes complementary to the 5′ half of the His tRNA.

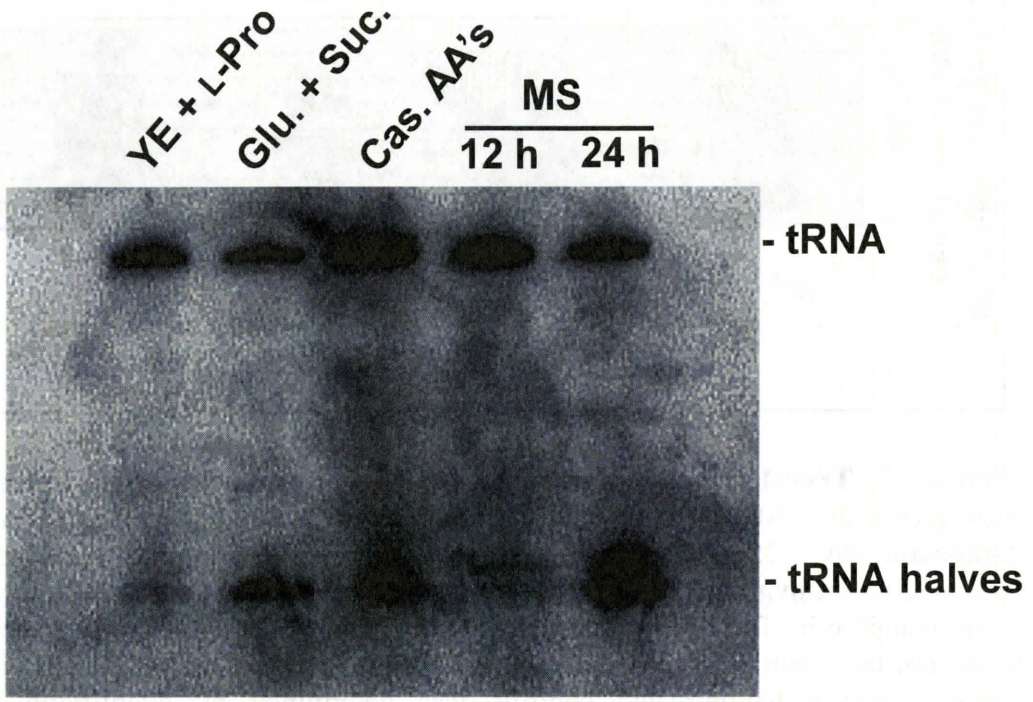

Figure 2.6. Northern blot analysis of tRNAs isolated MS-grown cultures supplemented with components of rich growth medium. Total RNA from wild-type *S. coelicolor* was isolated from MS-grown cultures after 12 and 24 h of growth (as indicated), and after 24 h of growth for supplemented MS-grown cultures. An amount equal to that which is normally present in rich R2YE growth medium (section 2.3.1) was used for supplementation with yeast extract (YE), L-proline, glucose (Glu.), sucrose (Suc.), and casamino acids (Cas. AA's). The RNA was separated on 12% polyacrylamide gels, and was subjected to northern blotting using probes complementary to the 5′ half of the His tRNA.

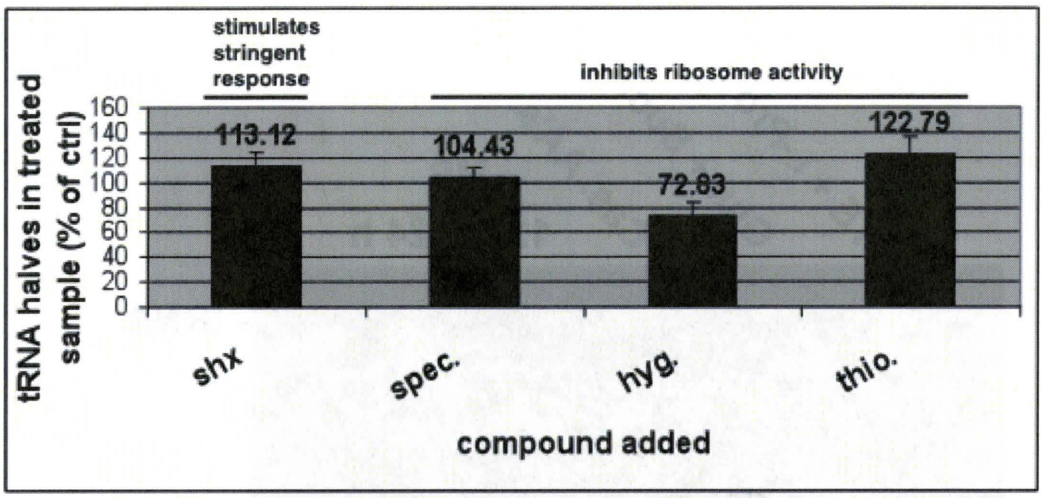

Figure 2.7. Translational inhibition and stringent response assay. Cultures were grown for ~40 h in liquid MM at 30°C before the addition of the indicated compound (shx = 25 mM serine hydroxamate; spec = 200 μg/ml spectinomycin; hyg = 50 μg/ml hygromycin; thio = 50 μg/ml thiostrepton) and incubation for an additional 60 min. Total RNA was then harvested and tRNA halves were detected using northern blot hybridization. The change in the ratio of tRNA halves in treated samples to untreated controls was determined by quantifying the appropriate bands after normalizing for background signal. The data shown are the average of results from three independent experiments. Error bars indicate one standard deviation from the mean.

Table 2.1. *S. coelicolor* strains used in this study.

S. coelicolor strain	Genotype	Reference
M145	SCP1– SCP2–	(Kieser *et al.*, 2000)
J1501	*hisA1 uraA1 strA1 pgl- SCP1- SCP2-*	(Chater *et al.*, 1982)
C109	J1501 *bldH*	(Champness, 1988)
J660	*bldC18 mthB2 cysD18 agaA1* $SCP1^{NF}$ SCP2*	(Merrick, 1976)
J669	*bldB43 mthB2 cysD18 agaA1* $SCP1^{NF}$ SCP2*	(Merrick, 1976)
J1700	J1501 *bld*A39	(Piret & Chater, 1985)
J2400	M145 *whiG::hyg*	(Flärdh *et al.*, 1999)
J2402	M145 *whiB::hyg*	(Flärdh *et al.*, 1999)

Table 2.2. Oligonucleotide sequences used in this study.

Linker/oligo name	Sequence (5' to 3')	Function
BanOne	ATTGATGGTGCCTACAG	Primer for reverse transcription and PCR amplification of cDNA
BanTwo	ATCGTAGGCACCTGAAA	Primer for PCR amplification of cDNA
ModBan	AMP-5'p-5'p/CTGTAGGCACCATCAATdi-deoxyC-3'	3' adaptor for RNA cloning
Nelson's linker	5'-ATCGTaggcaccugaaa-3'*	5' adaptor for RNA cloning
M13 forward	GTAAAACGACGGCCAG	Sequencing of cDNA clones
M13 reverse	CAGGAAACAGCTATGAC	Sequencing of cDNA clones
5' Ala	GCTCTACCAACTGAGCTATAGCCCC	Northern blot analysis
3' Ala	GAATTGAACTCCTGACCTCCTGCATGCCATGC	Northern blot analysis
5' Asn	GCCGGCTGCTCTGCCAATTGAGCTACCG	Northern blot analysis
5' His	AACCAGGTGCTCTACCAGCTGAGCTACACCCAC	Northern blot analysis
3' His	GTGAGTGACGGGACTTGAACCCGCGGCATCCTG	Northern blot analysis
5' Leu	CGCCGTGTCTGCATTCCACCATCCGGG	Northern blot analysis
3' Leu	GGACTTGAACCGGCACGCCCTCGAAGGGGCAGC	Northern blot analysis
5' Met	CCCAGCGAGCTACCGAGCTGCTCCACCCC	Northern blot analysis
3' Met	CGGGGACAGGATTTGAATCTGCGACCTCTG	Northern blot analysis
5' Ser	AGTGCGGCGCCATAGACCGGACTAGGCGACGCCTCC	Northern blot analysis
3' Ser	GATTTGAACCCACGGTGACTTGCGCCACGAC	Northern blot analysis
3' Trp	CTTGAACCCCCAACCGCTGGTTTTGG	Northern blot analysis

* The sequence written in lower case represents RNA

Table 2.3. Summary of cloned tRNA halves.

tRNA half	Amino Acid	Anticodon	# cloned	% of tRNAs cloned
3'	Arg	CCT	8	4.7%
3'	Asn	GTT	23	13.5%
5'	Gln	CTG	9	5.3%
3'	Glu	CTC	3	1.8%
3'	Glu	TTC	2	1.2%
5'	Gly	GCC	1	0.6%
5'	His	GTG	13	7.6%
3'	His	GTG	36	21.2%
5'	Leu	GAG	6	3.5%
5'	Leu	CAG	1	0.6%
5'	Leu	TAG	1	0.6%
3'	Lys	CTT	1	0.6%
5'	Met	CAT	34	20.0%
5'	Phe	GAA	1	0.6%
5'	Pro	CGG	6	3.5%
5'	Ser	TGA	21	12.4%
3'	Thr	GGT	2	1.2%
3'	Val	CAC	2	1.2%
			170	

CHAPTER 3:

CELL WALL HYDROLASES AFFECT GERMINATION, VEGETATIVE GROWTH, AND SPORULATION IN *STREPTOMYCES COELICOLOR*

Haiser, H.J., Yousef, M.R., and Elliot, M.A.

Preface:
This chapter was published in the *Journal of Bacteriology* (Haiser *et al.*, 2009). The small RNA cloning project introduced in Chapter 2 led to the discovery of an antisense RNA encoded immediately upstream, and on the opposite strand of several cell wall hydrolase-encoding genes in *S. coelicolor*. Our interest in this antisense RNA lead to the characterization of the proteins encoded immediately downstream. I performed the majority of the experiments presented in this work. M.R.Y. performed the fluorescence microscopy experiments, and assisted with various other aspects. Marcia Reid prepared all samples for scanning and transmission electron microscopy in Faculty of Health Sciences Electron Microscopy Facility, McMaster University. All of the authors analyzed the data, and I prepared all of the figures and tables. This chapter is largely based on the published manuscript (with a modified introduction and discussion) that I wrote in collaboration with M.A.E. All figures and tables included in this chapter are reproductions from the original manuscript, used with permission from the American Society for Microbiology.

3.1 CHAPTER SUMMARY

Peptidoglycan is a major cell wall constituent of Gram-positive bacteria. It is a dynamic macromolecule that is actively remodeled to enable cell growth and differentiation through a tightly choreographed interplay of lytic and biosynthetic enzyme activities. The filamentous bacterium *S. coelicolor* has a complex life cycle that is likely to require considerable cell wall remodeling. In silico analysis of the *S. coelicolor* genome enabled identification of 58 genes encoding candidate lytic enzymes. We found that seven of these genes share a highly conserved 5' untranslated region and are expressed during both vegetative growth and sporulation; the products of four of these genes were selected for more extensive biochemical and biological characterization. The proteins encoded by these genes, termed RpfA, SwlA, SwlB, and SwlC, were confirmed to be lytic enzymes, as they could cleave *S. coelicolor* cell walls. Phenotypic analyses revealed that these enzymes are important throughout development; deletion of each gene resulted in a mutant strain that was heat sensitive, defective in spore formation, and either altered in vegetative growth or delayed in spore germination. Our results indicated that these enzymes play key roles at multiple stages in the growth and development of *S. coelicolor*, highlighting both the lack of redundancy in lytic activity and the importance of cell wall remodeling in the *S. coelicolor* life cycle.

3.2 INTRODUCTION

Peptidoglycan (PG) is a dynamic macromolecule that effectively opposes the osmotic pressure from within the bacterial cytoplasm to prevent cell lysis. PG provides the framework for anchoring cell surface proteins and is also a main contributor to the maintenance of bacterial morphology (Cabeen & Jacobs-Wagner, 2005). Physically, PG is a mesh-like polymer consisting of parallel glycan strands that are linked together by short amino acid side chains protruding perpendicularly from the gylcan strands. In all bacteria containing PG, the glycan strands consist of alternating *N*-acetylglucosamine (Glc*N*Ac) and *N*-acetylmuramic (Mur*N*Ac) acid residues, which can be subjected to chemical modifications (see Chapter 1). The peptide chains differ in composition from species-to-species, especially in the interpeptide bridges that link the amino acid side chains together (Fig. 1.5) (Schleifer & Kandler, 1972). PG synthesis is a complex and tightly choreographed process that begins with the production of muropeptide precursors in the cytoplasm. This is followed by the synthesis of lipid-linked intermediates on the inner side of the cytoplasmic membrane, and culminates with the polymerization and incorporation of new cell wall material outside of the cytoplasmic membrane (Bouhss *et al.*, 2008, Vollmer & Bertsche, 2008, Barreteau *et al.*, 2008). The two major activities required for effective PG polymerization are transglycosylation, which involves the β-1,4-glycosidic linkage of disaccharide precursors to existing glycan strands, and

transpeptidation, which is the covalent linkage of pentapeptide side chains to the lactyl group of Mur*N*Ac residues; each of these activities can be carried out by the well-studied penicillin binding proteins (PBPs) (section 1.3.1.4) (Scheffers & Pinho, 2005).

During growth and development, the bacterial exoskeleton is remodeled to accommodate the physical changes required for cell growth and division. To accomplish this, the activities of cell wall synthetic and lytic enzymes must be coordinated. The term 'cell wall hydrolase' (or PG hydrolase) describes a highly diverse group of proteins that can be subdivided into several categories largely based on substrate specificity. Those enzymes that cleave the glycan strand include the *N*-acetylmuramidases (lysozymes and lytic transglycosylases) (Vollmer *et al.*, 2008b, Holtje *et al.*, 1975) and the *N*-acetylglucosaminidases, which hydrolyze the same bond between Glc*N*Ac and Mur*N*Ac residues. Cell wall hydrolases that cleave the peptide side chains include the amidases (cleave between Mur*N*Ac and the first residue [L-Ala] of the peptide chain), the LD/DL-endopeptidases (cleave between middle residues of the peptide chain, and also between the side chains and interpeptide bridges), and the carboxypeptidases (cleave the terminal residue [D-Ala] in the peptide chain) (see Fig. 1.5) (Vollmer *et al.*, 2008b). Cell wall lytic enzymes are essential for the routine turnover of PG during growth, but they also impact specialized processes including spore germination, daughter cell separation during cell division, and the resuscitation of cells from dormant states (Mukamolova *et al.*, 1998).

Dormancy is a metabolically inactive state adopted by many different bacteria in order to survive unfavorable growth conditions (Dworkin & Shah, 2010). The molecular mechanisms controlling the exit from dormancy remained largely elusive until a breakthrough report showed that exogenously adding a protein to dormant *Micrococcus luteus* cell populations restored growth (Mukamolova *et al.*, 1998). Further investigation revealed that this protein, named the resuscitation-promoting factor (Rpf), is structurally and functionally similar to lysozyme (Cohen-Gonsaud *et al.*, 2004, Cohen-Gonsaud *et al.*, 2005). Genes encoding the conserved 'Rpf domain' are confined to the Actinomycetes, although a cognate gene family exists in the Firmicutes (Ravagnani *et al.*, 2005). Importantly, Rpf proteins are found in number of pathogenic bacteria, including *Corynebacterium*, and *Mycobacterium* (where it is crucial for the reactivation of TB infection in a mouse model) (Kana *et al.*, 2008, Russell-Goldman *et al.*, 2008). *S. coelicolor* is predicted to encode seven Rpf proteins, although two of these show only weak amino acid sequence similarity to the Rpf domain (Ravagnani *et al.*, 2005).

Like all Gram-positive bacteria a thick layer of PG surrounds *S. coelicolor* cells. Growth for *S. coelicolor* initiates with the germination of dormant exospores, a process that likely depends upon the activity of cell wall hydrolases. The extensive lateral branching characteristics of vegetative cells would also require significant cell wall remodeling, as would all of the subsequent stages of growth, namely the raising of aerial hyphae and the septation and separation of

hyphal compartments during spore chain formation (Fig. 1.2). Surprisingly little is known about the cell wall hydrolases in *S. coelicolor*, and as such, we set out to investigate their role in the biology of this developmentally complex organism.

In this work, we describe the first investigation of cell wall hydrolase activity and function in *Streptomyces*. We identify a subset of hydrolases whose genes share a conserved 5' untranslated region (UTR), demonstrate enzymatic activity for four of these proteins, and reveal that these enzymes function at multiple stages in the *S. coelicolor* life cycle.

3.3 MATERIALS AND METHODS

3.3.1 Bioinformatic search for cell wall hydrolase enzymes

Amino acid sequences corresponding to characterized cell wall hydrolases from both Gram-positive and Gram-negative bacteria and representing each of the functional categories listed in Table 3.1 were used to identify candidate cell wall hydrolases in *S. coelicolor*. The following query sequences were obtained from the ExPASy database (http://ca.expasy.org/sprot/): Slt70 from *Escherichia coli* (Engel *et al.*, 1991) and the Rpf domain from *M. luteus* (Ravagnani *et al.*, 2005) for the *N*-acetylmuramidases; DacB from *E. coli* (Korat *et al.*, 1991) for the carboxypeptidases; LytE from *Bacillus subtilis* (Margot *et al.*, 1998) and multiple protein sequences housing the NlpC/P60-like domain as described by Anantharaman and Aravind (Anantharaman & Aravind, 2003) for the endopeptidases; and CwlA from *B. subtilis* (Kuroda & Sekiguchi, 1990) for the amidases. The sequences were subjected to BLASTp analysis (Altschul *et al.*, 1990) against the sequenced genome of *S. coelicolor* A3(2) (Bentley *et al.*, 2002). The *Streptomyces* annotation server (http://streptomyces.org.uk/) was also used to identify cell wall hydrolase candidates, which were further validated by the conserved domain function of BLASTp. Potential candidates with an E value of $<10^{-4}$ and possessing >25% identity over 100 amino acids were included. Signal peptides were predicted using SignalP 3.0 (Bendtsen *et al.*, 2004).

3.3.2 Bacterial strains and culture conditions

S. coelicolor A3(2) wild-type strain M145 and mutant derivatives (Table 3.2) were grown on R2YE or R5 (rich) and MS (mannitol-soy flour; minimal) agar media or in liquid tryptic soy broth supplemented with antibiotics to maintain selection when appropriate. The growth medium composition and standard culture techniques used have been described previously (Kieser *et al.*, 2000). *E. coli* strains used for cloning and protein overexpression are indicated in Table 3.2. Standard *E. coli* growth conditions for DNA manipulation and protein purification were used (Sambrook & Russell, 2001).

3.3.3 RNA isolation

Cultures were grown on agar plates overlaid with cellophane disks, and once desired stages of growth were reached, mycelia were scraped off and total RNA

was harvested as described in Chapter 2. All RNA samples were quantified by UV spectroscopy using an Ultrospec 3100 pro (Biochrom), and RNA quality was assessed by agarose gel electrophoresis.

3.3.4 Transcript end mapping

S1 nuclease mapping was performed as described previously (Elliot *et al.*, 2003). Reaction products were separated on 6% denaturing polyacrylamide sequencing gels. Sizes were estimated by running an end-labeled 100-bp ladder (Invitrogen) beside the samples. 5′ rapid amplification of cDNA ends (RACE) was carried out using an RNA ligase-mediated (RLM) RACE kit (Applied Biosystems) according to the manufacturer's instructions with minor modifications, as described previously (Swiercz *et al.*, 2008).

3.3.5 RT-PCR

Total RNA samples were subjected to reverse transcription (RT) using SuperScript III reverse transcriptase (Invitrogen). The annealing reaction mixtures consisted of 2 pmol of gene-specific primer (see Table 3.3), 1 μg total RNA, and 2 μl of a 5 mM deoxynucleoside triphosphate mixture. The annealing reaction mixture was incubated at 65°C for 5 min, followed by a 1 min incubation on ice and subsequent addition of 4 μl 5×First-Strand buffer, 1 μl 0.1 M DTT, 40 U RNaseOUT (Invitrogen), and 200 U SuperScript. The RT reaction mixture and subsequent additions were mixed and then incubated at 55°C for 1 h, followed by 15 min of incubation at 70°C to inactivate the enzyme. Following RT, PCR mixtures were prepared using 2 μl cDNA (from the RT reaction), 0.5 μl each 50 μM gene-specific primer (Table 3.3), 1 μl 5 mM deoxynucleoside triphosphate mixture, 2.5 μl 10× PCR buffer, 2.5 μl 20 mM $MgSO_4$, 2.5 μl 50% dimethyl sulfoxide, 1.25 U *Taq* DNA polymerase (UBI), and enough distilled H_2O (dH_2O) to obtain a final volume of 25 μl. The PCR mixtures were heated at 95°C for 5 min; optimal annealing temperatures were determined empirically and varied between 58 and 64°C for 45 s; the extension time was 45 s for all reactions; and the number of cycles varied between 15 and 28 cycles for the template-primer pairs to ensure that products were generated during the exponential phase of the reaction (within the linear range of amplification). Ten microliters of each PCR mixture was separated on 2% agarose gels and visualized by ethidium bromide staining. The controls for RT-PCR included 16S rRNA as a positive control for RNA integrity and equal RNA loading and a 'no-RT' sample as a negative control for each template-primer combination to ensure that reaction mixtures were not contaminated with DNA.

3.3.6 Protein overexpression and purification

DNA fragments encompassing the predicted binding and catalytic domains of each protein of interest were PCR amplified using the iProof polymerase system (Bio-Rad) by following the manufacturer's recommendations (see Table 3.3 for oligonucleotide sequences). In each case, the region encompassing the SignalP-

predicted signal peptide was not included in the DNA to be cloned. PCR products were purified using a PCR purification kit (Qiagen). Purified DNA fragments were sequentially digested with the *Bam*HI and *Nde*I restriction endonucleases. The resulting fragments were ligated into the expression vector pET15b (Novagen), which had been similarly digested with *Bam*HI and *Nde*I, before they were dephosphorylated with alkaline phosphatase (Roche). Plasmid DNA was isolated and positive clones were confirmed by PCR and restriction endonuclease digestion. Inserts were confirmed by sequencing with T7 promoter and terminator primers (see Table 3.3). Constructs were then transformed into either *E. coli* Rosetta2 or *E. coli* BL21(DE3)/pLysS (Novagen) (Table 3.4). Overexpression trials with small-volume cultures were carried out by sub-culturing the plasmid-containing strains to the exponential growth phase, inducing them with isopropyl-β-d-thiogalactopyranoside (IPTG) (Table 3.4), and monitoring the growth for various periods of time and at different temperatures to empirically determine the best conditions for overexpression of soluble protein (see Table 3.4). Proteins were then purified by incubating lysates from overexpressing cells with Ni-nitrilotriacetic acid agarose resin (Qiagen) and passing the resulting slurry through PolyPrep chromatography columns (Bio-Rad). Three washes were performed using increasing concentrations of imidazole (20 mM to 200 mM), before purified protein was eluted with either 250 mM (RpfA and SwlB) or 500 mM (SwlA and SwlC) imidazole. Purified protein was examined by separating aliquots of each elutate on 12% or 15% sodium dodecyl sulfate (SDS)-polyacrylamide gels. Proteins were quantified by the Bradford assay (Bradford, 1976), using bovine serum albumin and lysozyme as standards.

3.3.7 *S. coelicolor* cell wall harvest

Cultures were grown in liquid tryptic soy broth for ~48 h, after which cells were collected by centrifugation. The cell pellet was resuspended in a 1% SDS solution and boiled for 30 min, followed by centrifugation at 13,793 × *g* for 30 min. This procedure was repeated once before a series of washes in 60°C dH_2O were carried out. After the final wash in dH_2O, the pellet was resuspended in acetone, and the cell wall preparation was spun down one final time before it was air-dried. The dry weight of the cell wall preparation was then determined, and the resulting cell wall material was used in zymogram assays (see below).

3.3.8 Cell wall hydrolase activity assay

Zymograms were used to assay the putative cell wall hydrolases for cleavage activity (Leclerc & Asselin, 1989). Cell wall material was incorporated into SDS-polyacrylamide (0.1%, w/v) gels, within which purified proteins were separated. Following electrophoresis, gels were incubated in renaturation buffer (see Table 3.4) overnight at 30°C. Gels containing renatured proteins were then stained with 0.1% methylene blue, 0.01% KOH for 2 h, followed by destaining using several washes with dH_2O. Zones of clearing indicated cell wall solubilisation by the purified proteins. The controls for the zymogram assays included purified

lysozyme (BioShop) as a positive control and a purified His_6-tagged transcription factor (Crp) from *S. coelicolor* (not expected to possess cell wall cleavage activity) as a negative control. Zymograms were run in parallel with Coomassie blue-stained gels to confirm that the proteins migrated at the expected sizes compared to the size markers.

3.3.9 Hydrolase mutant strain construction

Single null mutations of the coding regions for the cell wall hydrolases were created using a standard PCR-targeted gene replacement technique (Gust *et al.*, 2003). The *aac(3)IV* (apramycin) resistance cassette from pIJ773 (Gust *et al.*, 2003) was used to create all single mutations. An *rpfA swlB* double-mutant strain was created by replacing the *swlB* gene in the *rpfA::aac(3)IV* strain with a *vph* (viomycin) resistance cassette from pIJ780 (Gust *et al.*, 2003). An *rpfA swlB swlC* triple-mutant strain was constructed by removing the viomycin cassette that had replaced *swlB* in the *rpfA swlB* double-mutant strain via FLP recombinase-mediated excision as described previously (Elliot *et al.*, 2003, Gust *et al.*, 2003) and then replacing the *swlC* coding region with the viomycin resistance cassette. Mutant cosmids used in the disruption procedure were confirmed by digestion and PCR amplification performed with several combinations of primers upstream, inside, and downstream of the disrupted gene. *S. coelicolor* mutant strains were confirmed by PCR as per the cosmid mutants (data not shown).

3.3.10 Construction of complementation vectors

Mutant strains were complemented by cloning DNA corresponding to the coding region (in the case of *rpfA*, this included SCO3098), along with extended upstream and downstream sequences in order to include all regulatory elements, into the integrating *Streptomyces* vector pIJ82 (see Tables 3.2; 3.3). Constructs were introduced into mutant strains via conjugation between the complementation plasmid-containing *E. coli* strain ET12567/pUZ8002 (which mobilizes the *oriT*-containing plasmid pIJ82 for conjugation in *trans*) (Table 3.2) and the corresponding *S. coelicolor* mutant. Empty plasmid controls were also introduced into the mutant strains. Complementation was assessed by comparing the phenotypes of the wild-type strain, the mutant, the empty plasmid-containing mutant, and the mutant containing the complementing plasmid, under appropriate growth or stress conditions.

3.3.11 Scanning and transmission electron microscopy

Mutant and wild-type strains were streaked to obtain single colonies on MS agar and grown for 4 to 5 days. Individual colonies were excised from a plate and prepared for scanning electron microscopy (SEM) or transmission electron microscopy (TEM). Samples were fixed overnight in 2% glutaraldehyde, rinsed twice in dH_2O, and post-fixed in 1% osmium tetroxide for 1 h. Samples were then dehydrated using an ethanol gradient (50%, 70%, 95%, and 100% ethanol). SEM samples were transferred to a critical point dryer and, once dry, were mounted

onto SEM stubs and coated with gold before they were viewed using a JEOL JSM 840 SEM. TEM samples were subjected to a final dehydration in 100% propylene oxide, infiltrated with Spurr's resin, and transferred to an embedding mold, where they were polymerized in Spurr's resin at 60°C overnight. Sections were then cut using a Leica UCT ultramicrotome and viewed using a JEOL JEM 1200 TEM. All images were analyzed using ImageJ 1.41a and Adobe Photoshop CS version 8.0 software. The spore diameter and spore wall thickness were calculated for at least 25 spores for each strain.

3.3.12 DAPI staining and light microscopy

Samples for light and fluorescence microscopy were obtained by taking coverslip impressions of samples incubated for 4 days on MS agar. Samples were stained with 4',6-diamidino-2-phenylindole (DAPI). All images were obtained using a Leica wide-field fluorescence microscopy system with a Leica HCS Plan Apo oil immersion objective (magnification, ×100; numerical aperture, 1.4; Leica Microsystems, Welzlar, Germany). Digital images were processed using Adobe Photoshop CS version 8.0 software.

3.3.13 Heat shock assay

Spore suspensions of wild-type and mutant strains were diluted with dH_2O to obtain a final concentration of ~300 spores/50 µl and placed in a 60°C water bath. Fifty-microliter aliquots were plated on MS agar after the incubation times indicated below, and the plates were then incubated at 30°C for ~5 days. Survival rates were calculated by dividing the number of colonies on plates after heat treatment by the number of colonies on plates without heat treatment and were expressed as percentages.

3.3.14 Lysozyme and cell wall antibiotic sensitivity assays

Sensitivities to lysozyme, SDS detergent, and cell wall antibiotics were examined by placing paper disks containing a test compound onto minimal medium agar plates (Kieser *et al.*, 2000) freshly spread with spores to obtain a confluent lawn. After 3 days of incubation at 30°C, zones of growth inhibition were measured for all strains, and the inhibition zones for the mutant strains were compared to those for the wild-type. Lysozyme (BioShop) was tested using 3, 0.3, and 0.03 mg/ml lysozyme; SDS sensitivity was examined using 10%, 1%, and 0.1% SDS; and the antibiotics phosphomycin, vancomycin, cefuroxime, bacitracin, nafcillin, and d-cycloserine were tested by applying 320 µg of each antibiotic to the disks.

3.3.15 Germination assay

To assess the timing of germination in mutant and wild-type strains, spores were plated on MS agar overlaid with cellophane disks and incubated at 30°C. At specific time points (3 h, 5.5 h, 6.5 h, 7.5 h, 9 h, and 11 h), a portion of a cellophane disk (1 cm by 1 cm) was excised and viewed with a light microscope to score germinated spores (indicated by the presence of one or more germ tubes)

and non-germinated spores. The data are representative of at least two independent experiments; a minimum of 200 spores were counted in each experiment.

3.4 RESULTS

3.4.1 *In silico* identification and analysis of cell wall hydrolases in *S. coelicolor*

We anticipated that cell wall remodeling was critical for the growth and morphological development of *S. coelicolor*. Given this, we conducted a survey of the *S. coelicolor* A3(2) genome to identify candidates of potential cell wall lytic enzymes. Using BLASTp analyses and experimentally validated bacterial lytic enzymes as our query sequences, we identified ~60 potential lytic enzymes in *S. coelicolor* having >25% sequence identity to known lytic domains over the majority of the domain sequence. To put this into context relative to other bacteria, *B. subtilis*, another Gram-positive, soil-dwelling, spore-forming bacterium, is predicted to encode 35 cell wall hydrolases (Smith *et al.*, 2000), the Gram-positive *Lactococcus lactis* is predicted to encode only 10 (Steen *et al.*, 2008), while the Gram-negative *E. coli* is predicted to encode 30 (Holtje, 1998). Our own BLASTp analysis estimate that *M. tuberculosis* encodes ~22 cell wall hydrolases (data not shown). *S. coelicolor*, therefore, encodes a significantly greater number of cell wall hydrolases than other bacteria, and this likely reflects the complexity of the *Streptomyces* life cycle. We have assigned the 58 *S. coelicolor* hydrolases to four functional groups: *N*-acetylmuramidases/glucosaminidases, carboxypeptidases, endopeptidases, and amidases (Table 3.1). The group containing the most enzymes was the endopeptidase group, with 23 representatives. Of these, 12 were identified as NlpC/P60-like proteins. The majority of functionally characterized NlpC/P60 enzymes possess endopeptidase activity (Anantharaman & Aravind, 2003), but there are also examples of these enzymes having amidase activity (Firczuk & Bochtler, 2007); for this reason, these proteins were assigned to a distinct subgroup (Table 3.1). The *N*-acetylglucosaminidases/muramidases were also well represented, with 17 predicted enzymes belonging to this group. Five of these enzymes were previously designated members of the Rpf subgroup (Ravagnani *et al.*, 2005). Only 3 of the 58 hydrolases identified in our screen are predicted to possess LysM domains (SCO3097, SCO3098 [both of these are Rpf proteins], and SCO6773) (Table 3.1). These domains are involved in PG binding and are commonly associated with cell wall hydrolases (Buist *et al.*, 2008).

While none of the predicted hydrolases have been experimentally characterized, members of the Rpf class have been studied extensively in other actinomycetes (Mukamolova *et al.*, 1998, Mukamolova *et al.*, 2002b, Mukamolova *et al.*, 2006). Analysis of the *rpf* genes in *S. coelicolor* revealed that the sequence upstream of one gene, SCO3097 (also referred to as *rpfA*), was highly conserved in the upstream (non-coding) regions of six other cell wall

hydrolase genes: SCO1240, SCO4108, SCO4582, SCO4796, SCO5839, and SCO6773 (Fig. 3.1A). The products of these seven genes were predicted to have diverse enzymatic activities (Bateman *et al.*, 2000). *rpfA* encodes one of the Rpf-like enzymes with a LysM PG-binding motif; SCO1240 and SCO4796 encode putative NlpC/P60 endopeptidases/amidases; SCO4582 is predicted to encode an enzyme with lytic transglycosylase activity; and SCO4108, SCO5839 and SCO6773 are predicted to encode endopeptidases (the SCO6773 product also contains a LysM domain) (Fig. 3.1B). We renamed SCO1240 (*swlA*), SCO4582 (*swlB*), and SCO6773 (*swlC*) for reasons described below. The upstream sequence conservation for these seven genes was maintained for orthologous genes in multiple *Streptomyces* species, including *S. avermitilis* and *S. griseus* (Appendix; Fig. 6.1), as well as in *M. tuberculosis* and other more divergent Gram-positive bacteria (Barrick *et al.*, 2004). Barrick *et al.* (2004) identified this upstream sequence as a potential riboswitch. Riboswitches are RNA sequences typically found within the leader UTRs of mRNAs and range in size from 70 to 200 nucleotides (nt) (Tucker & Breaker, 2005, Barrick & Breaker, 2007, Winkler & Breaker, 2005). They adopt structures that bind metabolites with exquisite specificity, and this binding often results in a structural alteration that modulates either the transcription or translation of the associated downstream gene(s) (Fig. 1.7). The products of genes downstream of similar riboswitches usually act in common pathways, and given this, we set out to elucidate the biological roles of these hydrolase genes and their associated products, guided by the expectation that they may act together to facilitate a specific aspect of cell wall remodeling in *Streptomyces*.

3.4.2 Seven cell wall hydrolase genes have distinct transcription profiles

As a first step in characterizing the seven genes, we sought to determine whether they were subject to common transcriptional or posttranscriptional control. To investigate their expression profiles, RNA was harvested from plate-grown cultures at growth stages ranging from early vegetative growth to sporulation. Following harvesting of RNA, semi-quantitative RT-PCR was conducted, and various transcriptional patterns were observed. The expression of four of the genes (*rpfA*, *swlB*, *sco5839*, and *swlC*) peaked at 24 h, after which their expression appeared to decline before increasing again during sporulation (48 h) (Fig. 3.2). A similar profile was observed for *sco4108* and *sco4796*, except that for these two genes the maximal transcript levels were maintained for an extended period (24 to 31 h) before the levels decreased and then increased again during entry into sporulation. In contrast, *sco1240* expression increased throughout development, with maximal transcript abundance occurring at 48 h (spore formation). These expression profiles were reproducibly observed with both experimental and biological replicates. The variable expression patterns observed for the seven genes suggested that they were unlikely to be coordinately regulated at a transcriptional or posttranscriptional (transcript stability) level, although such regulation may be shared by subsets of these seven genes.

3.4.3 The conserved upstream sequence corresponds to an extended 5′ UTR

Given the different transcription profiles observed for the hydrolase-encoding genes, we decided to test whether the conserved upstream sequence did in fact correspond to a leader UTR, as the 'riboswitch' designation was based solely on bioinformatic analyses and there was no experimental data to support its existence. We first investigated whether this sequence could be part of the coding sequence for each gene due to misannotation of translation start sites. We found that each annotated translation start site was preceded by a strong ribosome-binding site and that six of the seven genes either had no alternative start codons within 300 nt of the annotated start, or had a stop codon located between any potential start codon and the annotated start (*rpfA* had an alternative start codon 15 nt upstream of the predicted start site). This suggested that translation was unlikely to initiate within the conserved upstream sequence. Using S1 nuclease mapping and 5′ RACE experiments, we mapped the transcription start sites for each gene and found that each message included an extended 5′ UTR (Table 3.5). The *sco1240* transcript had the shortest 5′ UTR (~100 nt), while the other transcripts had longer leaders, ranging from 162 nt for *sco4582* to 237 nt for *rpfA*. The mapped ends meant the UTRs were ~40 to 50 nt longer than predicted by previous bioinformatic analyses (Barrick *et al.*, 2004) for all seven hydrolase genes except *sco4796*, whose leader sequence was the predicted size, and *sco1240*, whose leader sequence was ~80 nt shorter than the expected size.

3.4.4 Purified cell wall hydrolases cleave *S. coelicolor* cell walls

Having established that each hydrolase gene shared a conserved leader region large enough to include a riboswitch, we turned our attention to the function of the associated gene products. The seven enzymes fell into four distinct functional classes, and in order to focus our investigations, we selected one enzyme from each functional class for further biochemical and biological characterization, as follows: RpfA (LysM-containing Rpf subclass), SCO1240 (NlpC/P60 endopeptidase/amidase), SCO4582 (lytic transglycosylase), and SCO6773 (LysM-containing endopeptidase). To probe the enzymatic functions of these enzymes, they were overexpressed as N-terminal His-tagged fusions (without their signal peptides) and were purified using Ni^{2+} affinity chromatography. Each enzyme was assessed for its ability to cleave purified cell wall preparations from wild-type *S. coelicolor* using zymogram analysis, a standard method for demonstrating cell wall hydrolase activity (Leclerc & Asselin, 1989). All four hydrolases had detectable cleavage activity, as evidenced by zones of clearing on the zymogram (Fig. 3.3), although not all of them were equally effective in their cleavage capabilities. SCO6773 (SwlC) exhibited the most robust cleavage of the four enzymes and was also the most stable, retaining its activity for several weeks, in contrast to the other enzymes, which lost cleavage activity within days. SCO4582 (SwlB) was readily purified; however, it exhibited less activity than equivalent amounts of SCO6773 (SwlC), and obtaining detectable cleavage in the zymogram assays required considerable buffer optimization (see Table 3.4).

SCO1240 (SwlA) and RpfA were the least active of the four hydrolytic enzymes; they were the most challenging to overexpress and purify in an active form and were the least stable of the four enzymes examined in terms of their activity, although detectable zones of cleavage could be observed in the zymograms when freshly purified protein was used (Fig. 3.3). These experiments demonstrated cell wall cleavage capabilities for all four hydrolytic enzymes, and consequently, we propose that SCO1240, SCO4582 and SCO6773 be renamed SwlA, SwlB, and SwlC, respectively (*S*treptomyces cell *w*all *l*ytic enzyme).

3.4.5 SwlB and SwlC are important for branching during vegetative growth

To shed light on the biological role of each of the four representative hydrolases and to determine whether these enzymes acted at similar stages in development, individual and multiple mutant strains were constructed. As we had shown that the hydrolases could metabolize cell walls and demonstrated that transcription of three of the four hydrolases (*rpfA*, *swlB*, and *swlC*) was maximal at 24 h, we reasoned that the absence of these gene products might affect vegetative growth. In examining the vegetative growth of plate-grown cultures, we found that *rpfA* and *swlA* mutants resembled the wild-type strain in their hyphal extension and branching patterns; however, the *swlB* mutant was markedly different. The vegetative hyphae of the *swlB* mutant appeared to be unusually long and straight, and there was a general lack of productive branching: it appeared that branches could be initiated, but continued outgrowth of these hyphae did not occur as robustly as it did in the wild-type strain (Fig. 3.4). A similar phenotype was observed for the *swlC* mutant (data not shown). Both the *swlB* and *swlC* mutants grew at rates similar to the wild-type, and while emergence of the first branch initiated at the same position as in the wild-type (i.e., there was no significant difference in the distance from the tip to the first branch) (data not shown), the resulting branches were significantly shorter for both of these mutants than for the wild-type ($P < 0.01$) (Fig. 3.4D). The vegetative defects of the two mutants could be complemented by introduction of a wild-type copy of the gene into the chromosome (Fig. 3.4; data not shown).

3.4.6 All of the cell wall hydrolase mutants form defective dormant spores

The expression of the four hydrolase genes was also observed to increase during entry into the sporulation stage. Thus, we predicted that the products of these genes might also play a role in spore formation. Dormant *Streptomyces* spores are typically resistant to heat, and heat sensitivity is a hallmark of spore wall defects (Margot *et al.*, 1998, Mazza *et al.*, 2006). We therefore conducted heat shock assays with strains having both individual and multiple hydrolase deletion mutations. All four single mutants were hypersensitive to heat stress: 10 min of exposure to 60°C resulted in ~70% viable wild-type spores, compared with ~30% viable spores for the mutants, while 40 min of heat treatment resulted in ~50% viable wild-type spores and less than 10% viable mutant spores (Fig. 3.5). Introduction of a copy of a wild-type gene into the corresponding mutant strain

complemented the heat sensitivity phenotype of these mutants (data not shown). An *rpfA swlB swlC* triple mutant was more heat sensitive than any of the single mutants (Fig. 3.5). Taken together, these data suggest that the activities of all four cell wall hydrolases are critical for the development of dormant, heat-resistant spores.

We also tested the single and multiple mutants for sensitivity to detergent, lysozyme, and cell wall antibiotics, as spore and cell wall defects have also been associated with increased sensitivity to these chemical insults. None of the mutants were more sensitive to these compounds than the wild-type strain (data not shown).

Given that heat sensitivity is correlated with spore defects, SEM was used to compare the appearances of spores of wild-type and mutant strains (Fig. 3.6). We found that all four single hydrolase mutants exhibited abnormal spore morphologies. The *swlA* mutant spores failed to 'round out' like wild-type spores and were variable in size, suggesting that there was a defect in placement of sporulation septa. The *rpfA*, *swlB*, and *swlC* mutant spores were also heterogeneous in size and displayed a distinctive spore separation that yielded spores having an unusual cylindrical shape (Fig. 3.6). A similar cylindrical spore phenotype was observed for an *rpfA swlB swlC* triple-mutant strain (data not shown). Bright-field light microscopy and DAPI staining of the wild-type and mutant strains confirmed the abnormal shape and size of the mutant spores, revealing that despite the unusual spore separation and septum placement, DNA segregation was unaffected (Fig. 3.6). To further probe the nature of the cylindrical spores observed for *rpfA*, *swlB*, and *swlC* mutants, TEM was conducted. We found that the spores were fully separated but that they were cylindrical when they were in spore chains (Fig. 3.7A) (they appeared to be rectangular in TEM cross sections); these chains were unlikely to represent an early stage of sporulation, as they were typically found together with abundant free spores, which are typically seen in mature sporulating cultures. The cylindrical spore conformation was not maintained following the liberation of individual spores, although some mutant spores appeared to be more oblong than round, which may be a reflection of the different spore sizes (Fig. 3.7A).

To further characterize the mutant spores, we conducted a quantitative examination of spore diameter and spore wall thickness using images obtained by TEM. We found no change in overall spore diameter for any of the mutants compared to the wild-type (data not shown); however, all four individual hydrolase mutants possessed significantly thinner spore walls, which appeared to be on average only approximately one-third as thick as the wild-type spore walls (Fig. 3.7B,C).

3.4.7 *swlA* and *rpfA* mutants are delayed in spore germination

As our investigations suggested that the four hydrolase gene products played a role in both vegetative growth and dormant spore formation, we were interested in determining whether these gene products also contributed to spore germination.

Germination of both wild-type and mutant strains was assessed by incubating spores on MS agar and then scoring the frequency of germ tube emergence. No mutant strain was overwhelmingly defective in germination capability; however, the *swlA* and *rpfA* mutant strains reproducibly initiated germination more slowly than the wild-type, although by 11 h, spores of all strains were fully germinated (Fig. 3.8). The germination delay was, however, statistically significant only at 3 h for both mutant strains ($P < 0.01$). All other mutant strains displayed germination kinetics similar to those of the wild-type strain. The germination defects of the *rpfA* and *swlA* mutants could be complemented by introducing a copy of the wild-type gene into the mutant strain (data not shown).

3.5 DISCUSSION

Because its life cycle comprises several morphologically distinct cell types, we reasoned that *S. coelicolor* must employ a multitude of cell wall hydrolases to facilitate the PG remodeling required to transition from one cell type to the next. Indeed, our bioinformatic analyses suggested that ~58 cell wall hydrolases are encoded within the *S. coelicolor* genome (Table 3.1). The developmental complexity of *S. coelicolor* led us to wonder if there were dedicated roles for at least a subset of these PG hydrolases, and whether there was functional redundancy within these enzymes.

The PG hydrolases characterized in this work share an extended region at the 5' end of the RNA transcripts encoding them. Intriguingly, this region is predicted to house a riboswitch regulatory element (Barrick *et al.*, 2004). Our end-mapping experiments suggest that this conserved region is important as it is transcribed in all cases examined. It has been shown that the products of genes controlled by a given riboswitch are often involved in the same metabolic pathway. The potential for riboswitch regulation is discussed further in Chapter 4, however we first wanted to see if the cell wall hydrolases sharing the conserved (predicted) riboswitch were involved in similar biological/developmental processes. Our study revealed that several single hydrolase deletion strains exhibited morphological defects, a finding that suggests the hydrolases we tested do not carry out completely redundant functions. We also noted that a triple mutant (*rpfA swlB swlC*) is slightly more heat sensitive than the strains harboring individual deletions of each gene; however the spore morphologies of the triple and single mutants look very similar. Because the effects of hydrolase deletion do not seem to be consistently additive, it is possible that the proteins may function in the same pathway or act as part of a complex. Indeed, recent studies have shown that the mycobacterial proteins RpfB and RpfE interact with the endopeptidase RipA (an NlpC/P60-like enzyme similar to SwlA), and that the activity of these hydrolases is enhanced upon RipA interaction (Hett *et al.*, 2007, Hett *et al.*, 2008). Future investigations should include a comprehensive analysis of PG hydrolase interacting partners, as this will undoubtedly shed light on their function and regulation.

In *B. subtilis*, cell wall hydrolases have dedicated roles during defined stages of growth. These include the germination-specific lytic enzymes (GSLEs) that play a specialized role in degrading spore PG (see below), as well as the hydrolases dedicated to cell wall remodeling during vegetative growth (Atrih & Foster, 1999, Smith *et al.*, 2000, Setlow, 2003). In contrast, most of the hydrolase deletion mutants examined here affected multiple growth stages. For example, *swlB* and *swlC* both had vegetative growth defects and formed aberrantly shaped spores, suggesting that they were involved in multiple cellular processes – a finding that is consistent with their transcriptional profiles. Given that we examined only a small fraction of the *S. coelicolor* PG hydrolase complement, it is impossible to say whether this finding extends beyond those that were tested.

We have shown that two cell wall hydrolases (encoded by *rpfA* and *swlA*) contribute to spore germination in *S. coelicolor* by facilitating the efficient outgrowth of germ tubes. Such a role for RpfA is consistent with the observed function of Rpf proteins in other actinomycetes (Mukamolova *et al.*, 1998). *S. coelicolor* encodes five Rpf proteins, and with the functional redundancy observed for the *M. tuberculosis* Rpfs, it is surprising that a single deletion resulted in a (albeit minor) phenotypic change. The RpfA and SwlA enzymes may act directly in degrading spore PG during germination, or they may have a more indirect role. For example, they may be involved in the formation of spore PG and in their absence, an altered substrate for a germination-specific hydrolase may be generated (see below), resulting in less efficient PG hydrolysis during germination.

All four of the cell wall hydrolase mutants examined here were defective in their ability to produce wild-type spores. The two major mutant spore phenotypes we observed were abnormal shape (cylindrical in the mutant as opposed to oval in the wild-type) and incomplete spore separation. Additionally, all of the deletion strains were heat hypersensitive and possessed thinner spore walls than the wild-type. The former observation is consistent with the cell wall hydrolases being involved in the production/remodeling of spore wall PG, however it is unclear why the cell wall hydrolase deletion mutants would possess thinner spore walls. One possibility is that these hydrolases are part of a protein complex that carries out cell wall remodeling and in their absence, complex function is compromised. While this hypothesis remains to be tested experimentally, our suggestion that all the cell wall hydrolases tested here seem to participate in the same pathway is consistent with this idea. Recent work has identified such a complex in *Mycobacterium*, where the hydrolases RipA and RpfB interact with a PBP to coordinate cell wall metabolism (Hett *et al.*, 2010). Additionally, another recent study in *E. coli* showed that the proper functioning of such complexes can depend on the temporal cascade of protein activity (see section 1.4.2) (Uehara *et al.*, 2010).

The crucial role played by cell wall hydrolases, especially in a developmentally complex organism such as *S. coelicolor*, necessitates that their activity be tightly regulated (section 1.4.2). Post-translational regulatory

mechanisms have been described in a few cases; these have come in the form of substrate modification, or modulation through interactions (as described for RpfB/RipA) and localization. A comprehensive analysis of the PG material from the different *S. coelicolor* growth stages will be an important first step toward understanding cell wall hydrolase control in this organism. In addition, co-localization studies examining cell wall hydrolases, cytoskeletal proteins, PBPs and other proteins generally important for cell growth would begin to address whether *S. coelicolor* employs modes of regulation similar to those observed in *E. coli* and *B. subtilis*.

The spore defects observed for the hydrolase mutants (thin cell walls, heat sensitivity, and germination defects) are similar to the phenotypes of other *S. coelicolor* developmental mutants. Both *mreB* and *whiD* mutant spores exhibit irregular morphologies like those seen for the hydrolase mutants examined here. Heat hypersensitivity of spores has been noted previously for *whiD* and *mreB* mutants. In addition, *mreB* mutants are defective in germ tube elongation (a phenotype attributed to improper spore formation), while *whiD* mutant spores have thinner cell walls than wild-type spores (Mazza *et al.*, 2006, Molle *et al.*, 2000). The MreB protein is proposed to polymerize to form an actin-like cytoskeletal scaffold for PG synthesis, which in rod-shaped bacteria primarily occurs at the lateral cell wall (Jones *et al.*, 2001). In *B. subtilis*, for example, the MreB isoform MreBH interacts with the PG-associated hydrolase (LytE); this interaction is predicted to coordinate cell wall hydrolysis with cell wall synthesis (Carballido-Lopez *et al.*, 2006). Moreover, recent work in *Caulobacter crescentus* suggests that MreB dictates glycan strand length by promoting the transglycosylase activity of PBPs (Takacs *et al.*, 2009). The apical tip growth displayed by *S. coelicolor* is not directed by MreB (Daniel & Errington, 2003), but is instead dependent on a coiled-coil protein named DivIVA (Hempel *et al.*, 2008). The *S. coelicolor* MreB homolog is however, important during aerial hypha formation and sporulation (Mazza *et al.*, 2006). Interestingly, a recent study has shown that the individual disruption of the multiple *mre* genes encoded by *S. coelicolor* gives rise to phenotypes similar to the *mreB* deletion strain (Kleinschnitz *et al.*, 2011). Furthermore, the protein products for at least one of these genes (*mreC*) interacts with multiple PBPs (although no PG hydrolase interactions were detected), suggesting the potential for a protein complex directing spore wall synthesis (Kleinschnitz *et al.*, 2011). Finally, another group of proteins that contribute to cell wall remodeling in *S. coelicolor* is the SsgA-like proteins (SALPs) (section 1.2.1.4) (Noens *et al.*, 2005). A model has been proposed in which these proteins balance PG biosynthesis and hydrolysis during sporulation (Noens *et al.*, 2005); however, there is currently no data to support a role for the hydrolases examined here in any SALP-associated process.

Acknowledgements from original manuscript:

We thank Dave Capstick, Julia Swiercz, and Justin Nodwell for critical reading of the manuscript and helpful discussions, Dagmara Jakimowicz for microscopy advice, Dennis Claessen for helpful experimental suggestions, Eric Brown for his generosity in providing antibiotics, Marcia Reid for invaluable assistance with electron microscopy, and Nolan D'Souza, Lauren Brady, and Evelyn Miwa for assistance with experiments.

This work was funded by the Canada Research Chairs program, by a grant from the Natural Sciences and Engineering Research Council of Canada (NSERC discovery grant 312495), and by a seed grant from the Institute for Infectious Disease Research at McMaster University.

3.6 FIGURES AND TABLES

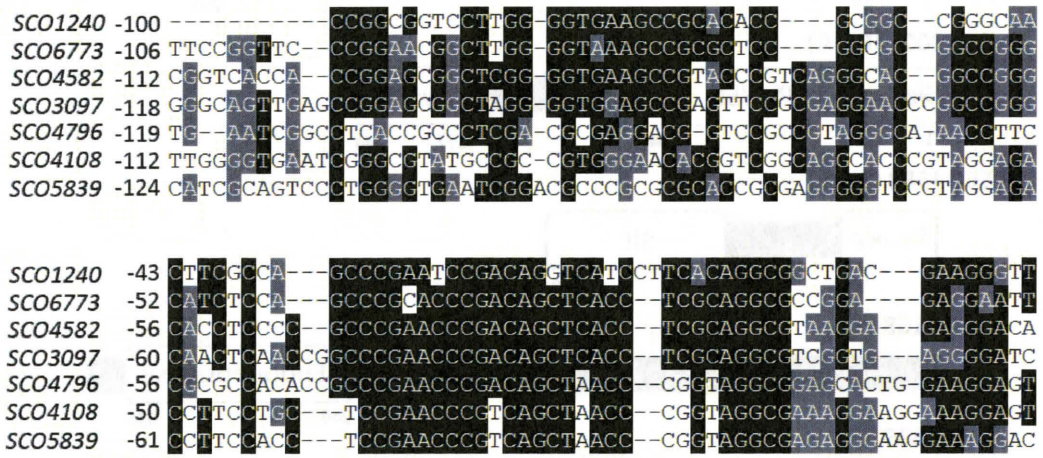

Figure 3.1A. Alignment of upstream non-coding sequences for seven putative cell wall hydrolases. Multiple-sequence alignment of the predicted UTRs for the seven hydrolase-encoding genes. Identical nucleotides are indicated by black shading, while similar nucleotides (purines or pyrimidines) are indicated by gray shading.

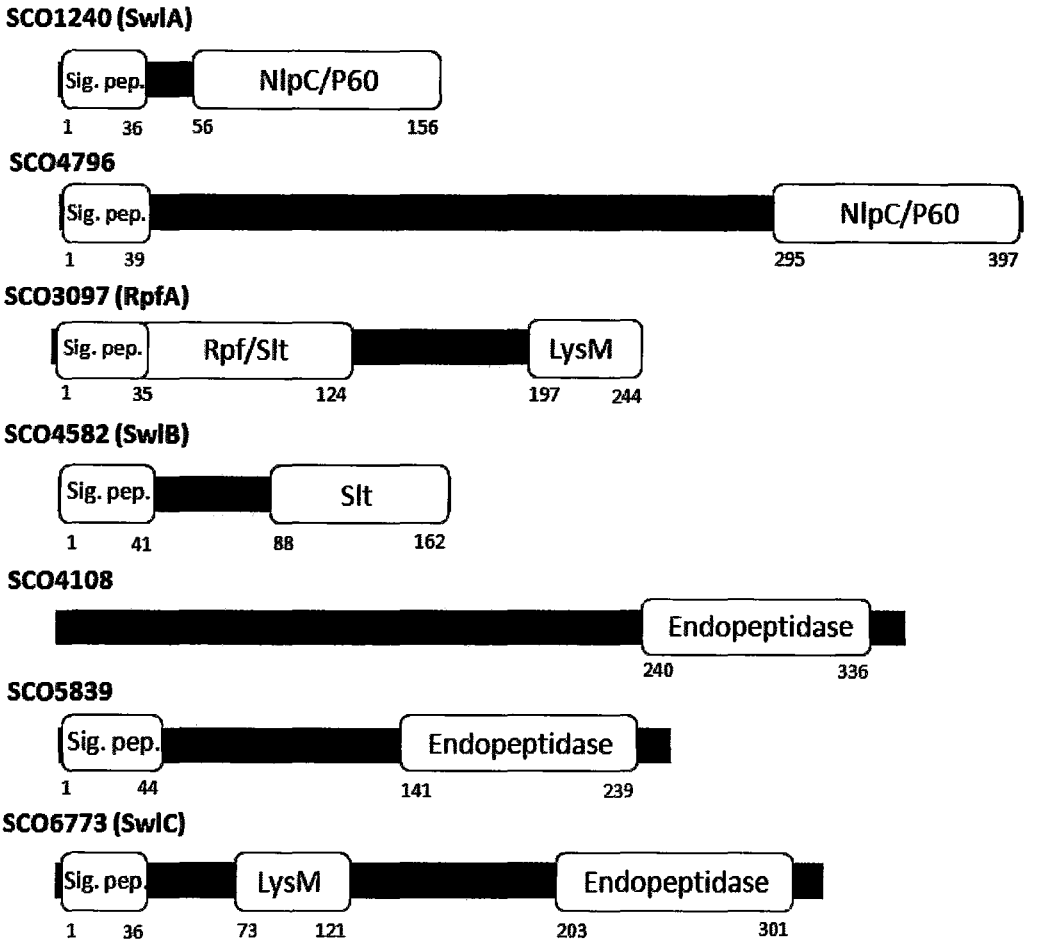

Figure 3.1B. Schematic representation of the functional domains predicted for the seven cell wall hydrolase proteins. Proteins are grouped on the basis of their functional domain, with the relative position of each domain within the protein sequence indicated by the amino acid number at the beginning and end of each domain/motif. Sig. pep. = signal peptide; NlpC/P60 = endopeptidase domain; Slt = soluble lytic transglycosylase; Rpf = resuscitation-promoting factor; LysM = lysin motif (implicated in peptidoglycan binding).

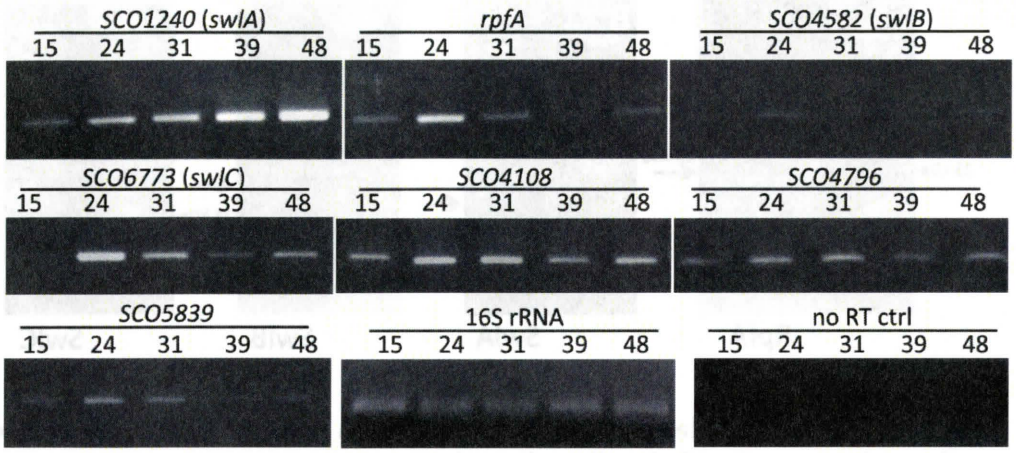

Figure 3.2. Expression profiles of the putative cell wall hydrolase genes during *S. coelicolor* development. RNA was harvested after 15, 24, 31, 39, and 48 h of growth on R5 (rich) medium. Vegetative hyphae were evident at 15 h, aerial hyphae were beginning to form by 24 h, and spores were detectable by 48 h. RNA samples were subjected to RT-PCR using oligonucleotides specific for the coding regions of the seven hydrolase genes. The number of reaction cycles was optimized for each PCR to ensure that the products examined were generated within the linear range of amplification (27 cycles for *sco1240*, *sco4108*, *sco4796*, and *sco5839*; 28 cycles for *rpfA*, *sco4582*, and *sco6773*). 16S cDNA was amplified as a positive control (15 cycles), and a 'no-RT' reaction was conducted using each template-primer combination to ensure there was no DNA contamination of the RNA samples or the PCR reagents (27 or 28 cycles).

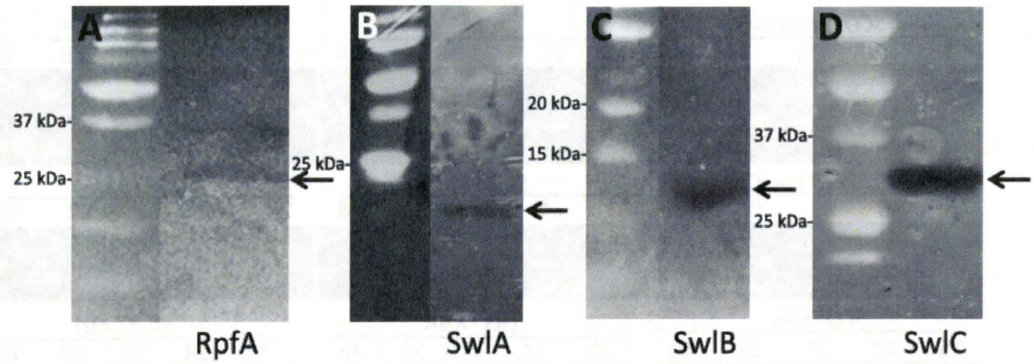

Figure 3.3. Cell wall cleavage assay (zymogram) using *S. coelicolor* cell walls as the substrate. Purified cell wall hydrolases (without their signal peptides) were separated on a 12% or 15% polyacrylamide gel containing 0.2% *S. coelicolor* cell wall. Following electrophoresis, the separated proteins were renatured for 18 h before the gel was stained with methylene blue to reveal zones of clearing, which represented cleavage of the cell wall. Precision Plus protein standards (Bio-Rad) were used as size markers for comparison with the following expected protein sizes: (A) RpfA, 21.7 kDa; (B) SwlA, 13.8 kDa; (C) SwlB, 14.0 kDa; and (D) SwlC, 28.6 kDa. Zones of clearing (indicated by arrows) are seen as black bands on the inverted greyscale images. The second, larger band in panel A was reproducibly detected, but the corresponding protein could not be detected on a Coomassie blue-stained gel.

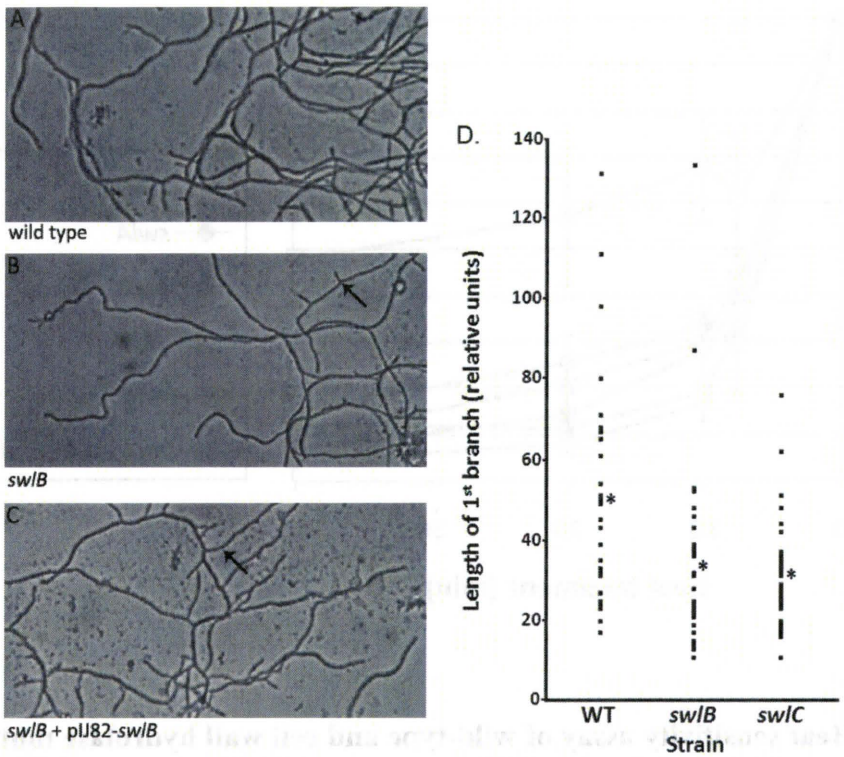

Figure 3.4. Defects in vegetative growth for the *swlB* mutant. Light microscope images of (A) wild-type strain, (B) *swlB* mutant, and (C) *swlB* mutant/pIJ82-*swlB* vegetative hyphae grown for 18 h on coverslips inserted into MS agar plates. While wild-type hyphae frequently extend significant branches, the arrow in panel B indicates the stunted branching observed for the *swlB* mutant. When a wild-type copy of *swlB* was introduced into the mutant on a plasmid, wild-type branching was restored, as indicated by the arrow in panel C. The *swlB* mutant also produced apparently longer hyphae than the wild-type strain. (D) Dot plot of first branch lengths for the wild-type, *swlB*, and *swlC* strains. Asterisks indicate the mean first branch length for each strain. The difference in branch length between each of the mutants and the wild-type was statistically significant ($P < 0.01$). (WT = wild-type)

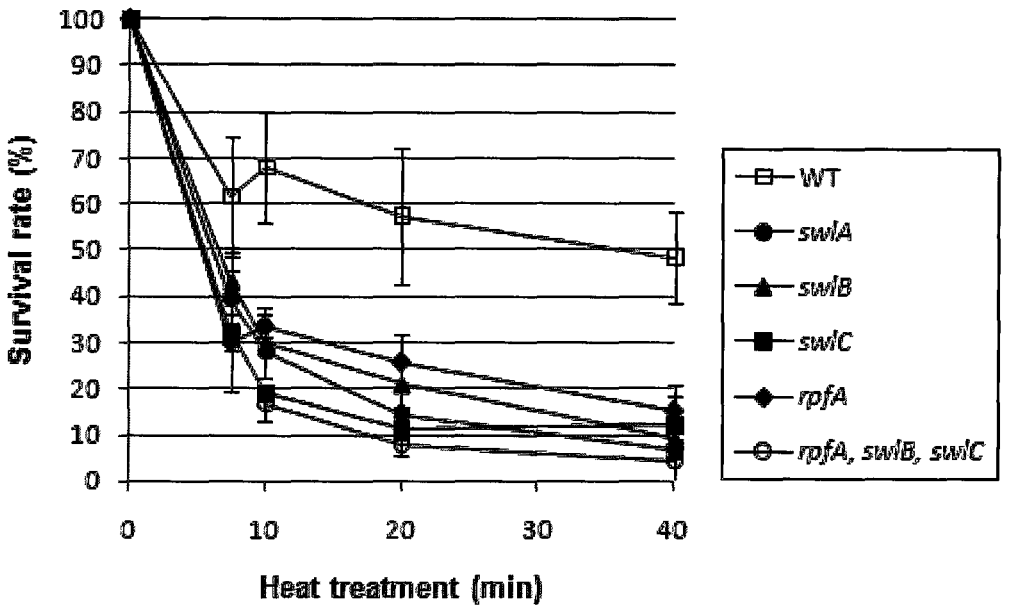

Figure 3.5. Heat sensitivity assay of wild-type and cell wall hydrolase mutant spores. Spores were tested for the ability to survive heat shock at 60°C for the times indicated. Approximately 300 heat-shocked spores were spread on MS agar and incubated for 5 days, and their survival rates were calculated (section 3.3.13). After a 40-min heat treatment, all mutant strains were at least threefold more heat sensitive than the wild-type strain, and the *swlA* mutant was the most heat sensitive of the single mutants, exhibiting a fivefold increase in heat sensitivity. Each value is the average of three replicates, and the standard error was calculated for the survival rate at each time point. (WT = wild-type)

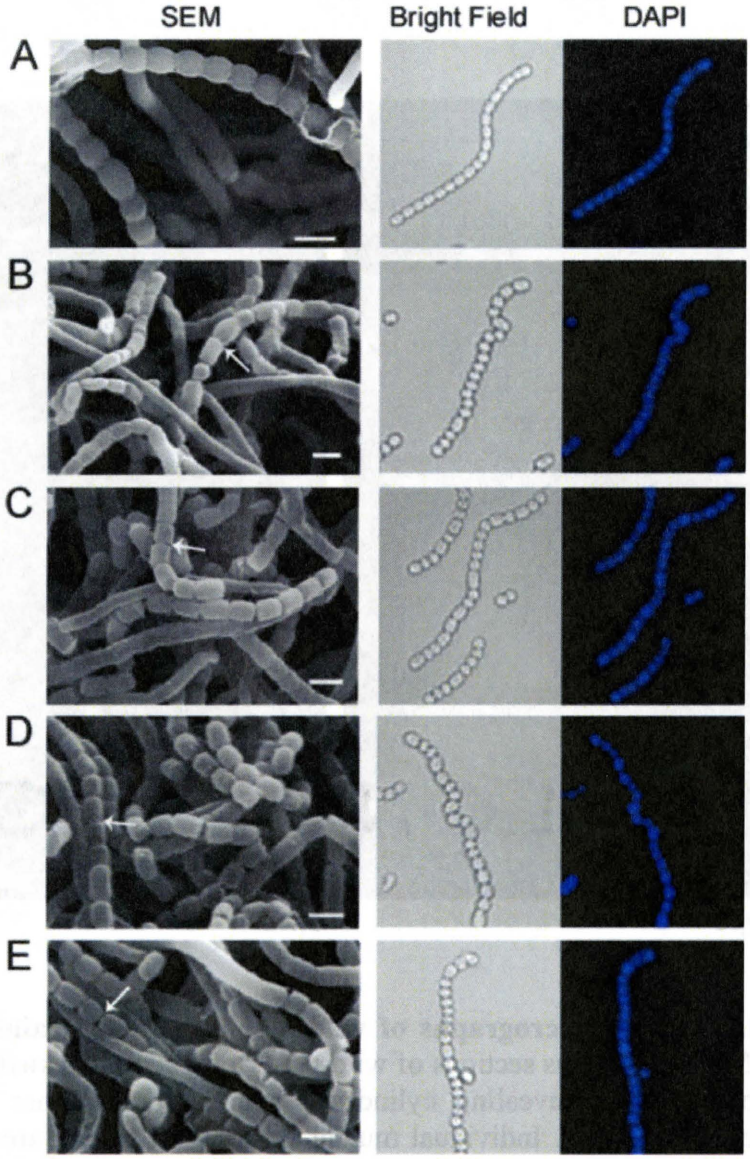

Figure 3.6. Microscope images of (A) wild-type strain and (B) *swlA*, (C) *rpfA*, (D) *swlB*, and (E) *swlC* mutants. The panels on the left show SEM micrographs of wild-type and mutant spores after 5 days of growth on MS agar. While wild-type spores were rounded and a uniform size, the mutant spores were more "box shaped" and were irregularly sized. Bars = 1 μm. The arrows indicate sites of enhanced spore separation. The panels on the right show bright-field images and fluorescence micrographs of wild-type and mutant strains after 4 days of growth on MS agar, followed by DAPI staining of coverslip impressions taken for each strain. Analysis of the mutant spore chains showed irregular spore sizes and shapes but no DNA segregation defects compared to the wild-type spore chains.

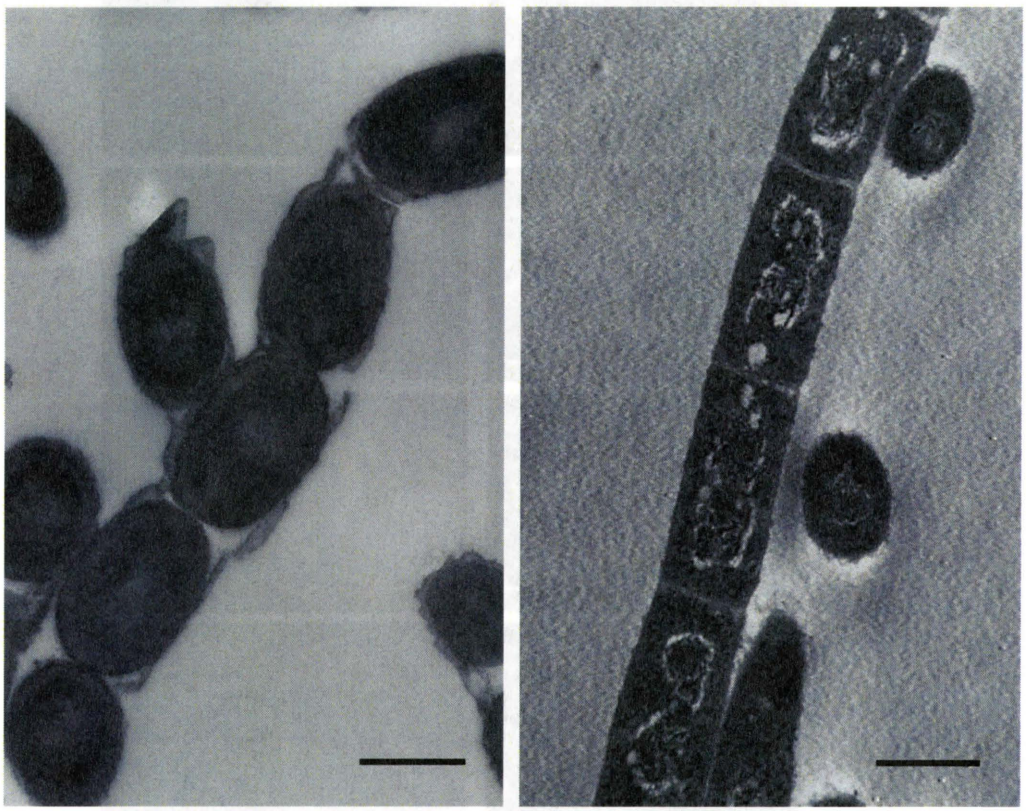

Figure 3.7A. TEM micrographs of wild-type and *swlC* strains grown for 5 days on MS agar. Cross sections of wild-type (left panel) and *swlC* mutant (right panel) spore chains, revealing cylindrical spores in the spore chains of the hydrolase mutant strain. Individual mutant spores, in contrast, are more rounded and are similar to wild-type spores (although they are longer in some cases). (Bars = 500 nm)

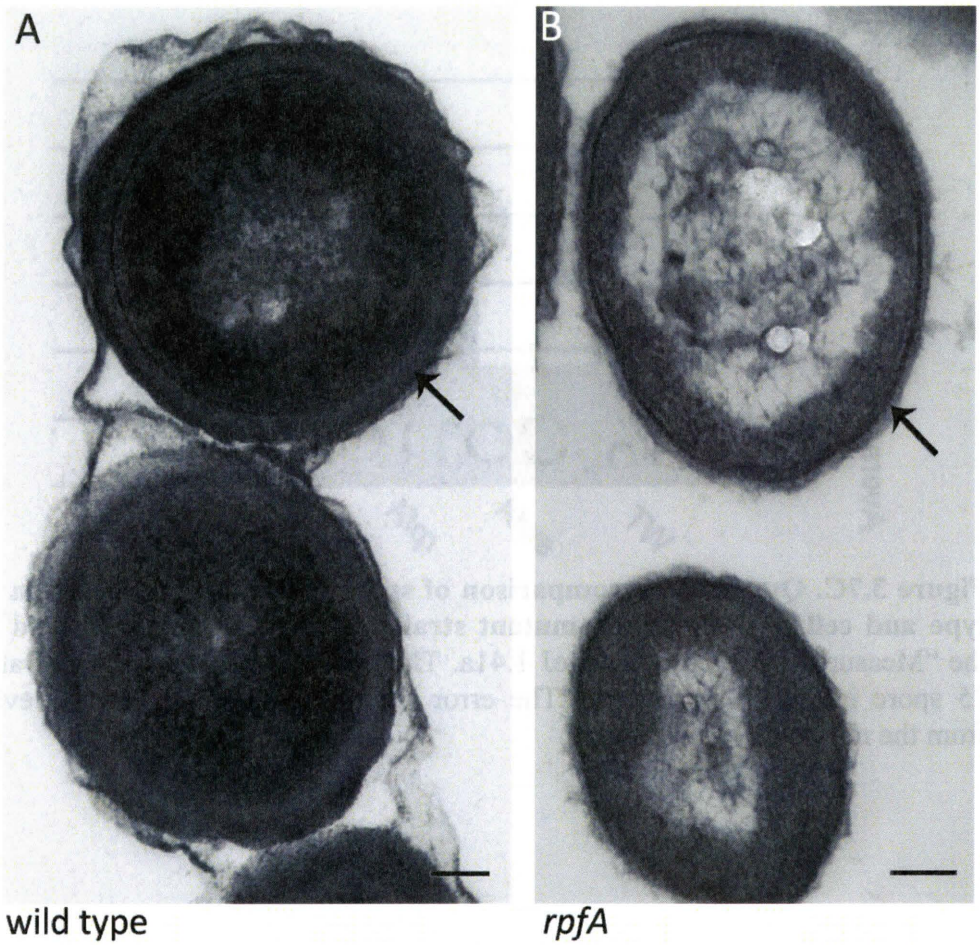

Figure 3.7B. TEM micrographs of wild-type and *rpfA* strains grown for 5 days on MS agar. Wild-type (left panel) and *rpfA* mutant (right panel) spores that are similar sizes but have different spore wall thicknesses (arrows). (Bars = 100 nm)

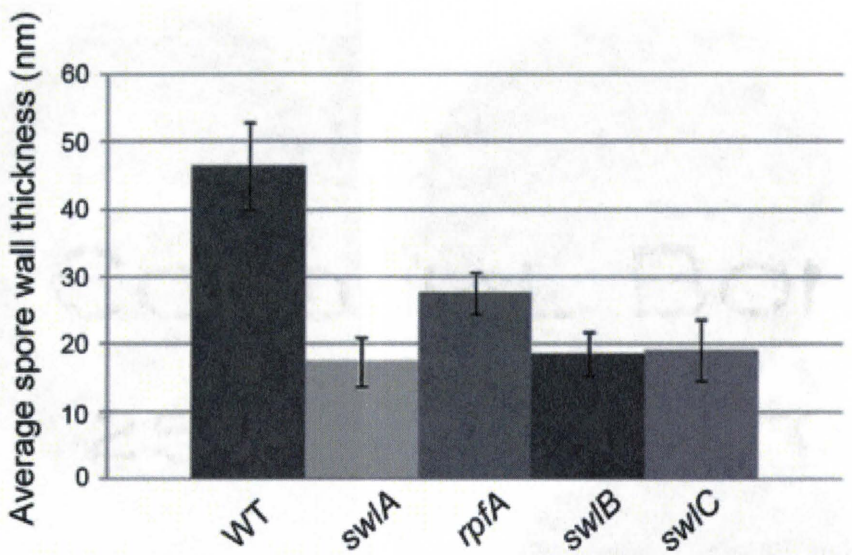

Figure 3.7C. Quantitative comparison of spore wall thickness between wild-type and cell wall hydrolase mutant strains. Cell walls were measured using the "Measure" function of ImageJ 1.41a. The bars indicate the means of at least 25 spore image measurements. The error bars indicate one standard deviation from the mean. (WT = wild-type)

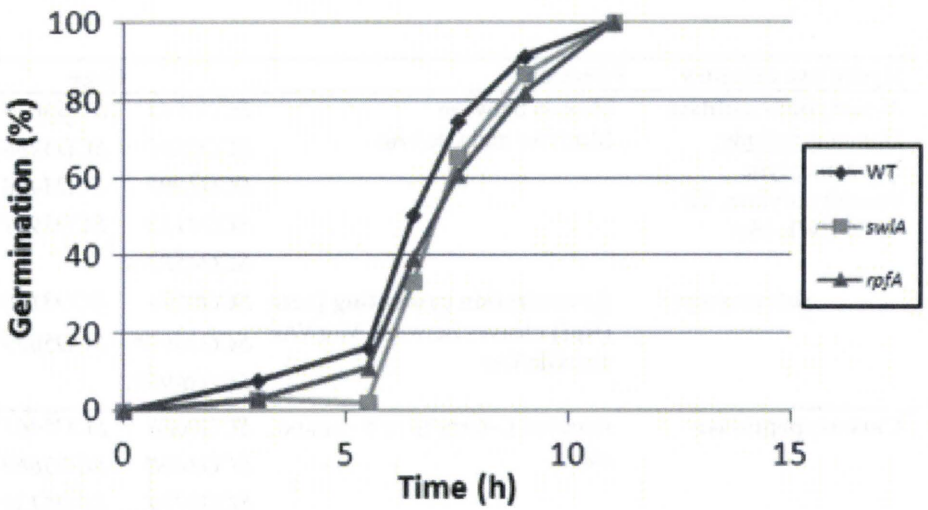

Figure 3.8. Comparison of germination rates of the wild-type strain and *swlA* and *rpfA* mutants. Spores were spread on MS agar and were incubated at 30°C for the indicated periods of time. Germination was assessed using light microscopy. Germination experiments were conducted at least three times using independent spore stocks and involved quantifying the proportion of germinated spores in a population of >200 spores. The curves are representative germination curves and show that the proportion of germinated spores prior to 11 h was reproducibly less for the two mutant strains, although only the difference at 3 h was statistically significant ($P < 0.01$). (WT = wild-type)

Table 3.1. Predicted cell wall hydrolases in *S. coelicolor.* (* Genes encoding a LysM PG-binding domain; references in section 3.3.1)

Hydrolase category	Function	Gene	
***N*-acetylmuramidase** Domains include: lysozyme, lytic transglycosylase, Slt and GEWL-like	cleaves between Mur*N*Ac and Glc*N*Ac	*SCO0543*	*SCO5029*
		SCO0591	*SCO5286*
		SCO1805	*SCO5466*
		SCO4132	*SCO5997*
		SCO4582	
Subcategory:	**Resuscitation promoting factor (Rpf)** cleaves between Mur*N*Ac and Glc*N*Ac	*SCO0974*	*SCO3150*
		*SCO3097**	*SCO5029*
		*SCO3098**	
Carboxypeptidase	removes C-term L- or D- amino acid	*SCO0088*	*SCO5467*
		SCO3408	*SCO5660*
		SCO3774	*SCO6131*
		SCO3811	*SCO6489*
		SCO4439	*SCO7050*
		SCO4847	*SCO7607*
Endopeptidase	cleaves amide bonds in peptides	*SCO2835*	*SCO4672*
		SCO3368	*SCO4798*
		SCO3949	*SCO5623*
		SCO4082	*SCO5839*
		SCO4132	*SCO6773**
		SCO4561	
Subcategory:	**NlpC/P60** endopeptidase/amidase activity	*SCO1240*	*SCO4793*
		SCO2135	*SCO4796*
		SCO2136	*SCO5294*
		SCO3511	*SCO6884*
		SCO4108	*SCO7021*
		SCO4202	*SCP1.148*

Table 3.2. Bacterial strains and plasmids used in this study.

Strain	Genotype/characteristics/use	References
Streptomyces coelicolor		
M145	SCP1- SCP2-	(Kieser, 2000)
E103 (*swlA*)	M145 *SCO1240::aac(3)IV*	This study
E104 (*rpfA*)	M145 *SCO3097::aac(3)IV*	This study
E105 (*swlB*)	M145 *SCO4582::aac(3)IV*	This study
E106 (*swlC*)	M145 *SCO6773::aac(3)IV*	This study
E107 (*rpfA, swlB*)	M145 *SCO3097::vph SCO4582::aac(3)IV*	This study
E108 (*rpfA, swlBC*)	M145 *SCO3097 SCO4582::aac(3)IV SCO6773::vph*	This study
Escherichia coli		
DH5α	Used for routine cloning	
ET12567 (pUZ8002)	*dam-, dcm-*; with *trans*-mobilizing plasmid pUZ8002	(MacNeil *et al.*, 1992, Paget *et al.*, 1999a)
BL21 (DE3) pLysS	Protein over expression host	Novagen
Rosetta 2	Protein over expression host with pRARE2 which supplies 'rare' tRNAs	Novagen
Plasmids		
BT340	FLP recombination plasmid	(Datsenko and Wanner, 2000)
pIJ82	pSET152 derivative, *aac(3)IV* replaced with *hyg* gene	Gift from H. Kieser
pIJ2925	pUC18-based cloning vector	(Janessen and Bibb, 1993)
pET15b	Over expression of His_6-tagged proteins	Novagen

Table 3.3. Oligonucleotides used in this study.

	Sequence 5′ → 3′
Disruption primers	
SCO1240FWD	GGTCATCCTTCACAGCGGCTGACGAAGGGTTGCGCATGATTCCGGGGATCCGTCGACC
SCO1240REV	ACGGCGGGACAGAACGCCGTCACCCCCGCGGGCGGGCTATAGGCTGGAGCTGCTTC
SCO3097FWD	CAGCTCACCTCGCAGGCGTCGGTGAGGGGATCAACCATGATTCCGGGGATCCGTCGACC
SCO3097REV	CACGCACCGGGGCGGGAGTCACGGGACCGCCGCCGCTTATGTAGGCTGGAGCTGCTTC
SCO4582FWD	CAGCTCACCTCGCAGGCGTAAGGAGAGGGACACCGCATGATTCCGGGGATCCGTCGACC
SCO4582REV	CGGTACCTCTTAGGCGAGGTTCGGGCGGCGTACGGCTCATGTAGGCTGGAGCTGCTTC
SCO6773FWD	ACAGCTCACCTCGCAGGCGCCGGAGAGGAATTCACCATGATTCCGGGGATCCGTCGACC
SCO6773REV	GGCCTTCGGTGCGCGGGGGCCGCGCGGAACCGGTCGTCATGTAGGCTGGAGCTGCTTC
S1 mapping/ 5′ RACE primers	
RACE adapters/ primers	see Swiercz *et al.* (2008), and RT-PCR primers below
1240 S1U	CCGCCTGCGGCGGCGTTTCG
1240 S1D	GCCGCGGCCGCCTCGGCGGCGG
3097 S1U	CGGTCAGACGCTCACGGTCACG
3097 S1D	see "3097 crR"
4582 S1U	GCTCACTCCGGGCGACCCGCAG
4582 S1D	see "4582 crR"
6773 S1U	GCGTCATATCCGTGACCGTGCG
6773 S1D	see "6773 RT2"
RT-PCR primers	
16S_L	CCTGATGCCGAGCCGATTGT
16S_R	GGGGCATTTTGCCGAGTTCC
1240 US	ATGTCCGCGCTCAATCGTGTCC
1240 DS	GCGGTACGGGGCGCCCTTCTTGG
3097 crL	AAGGCCACCCGTGTCATC
3097 crR	GTAGTAACCGTTGCCGGTGT
4108 US	GTGGCGTCAAACCGGCCTGC
4108 DS	CGAGTCCGCGCTGCTTGG
4582 crL	CAACGGTCAGAACCGTCAC
4582 crR	GGGTTGCCGGAGGACTCACG
4796 US	TTGGCGTCGCACCGCAAGTCGC
4796 DS	CCTGGCGGTACAGGTCGTCGACC
5839 US	ATGGCGTTCACGCGCGCCACCG
5839 DS	GCCGATGGTGACGACCGGGGTG
6773 RT1	GCCGAGAAGAACTCCGACTC

6773 RT2	CGTCGATCGAGAGCTTGAG

Protein purification primers	
SCO1240PP 5'	CAGTACCATATGGCGAGTCATGCGACGAAAGCC
SCO1240PP 3'	CAGTACGGATCCCTACTTGACCCGGCCGTACCA
SCO3097PP 5'	CAGTACCATATGGCCACCGCGTCCGAGTGGGAC
SCO3097PP 3'	CAGTACGGATCCTTACTTCAGGTGCAGCTGCTG
SCO4582PP 5'	CAGTACCATATGCCGGCCGCCGCCACGACC
SCO4582PP 3'	CAGTACGGATCCTCAGTACGCGCTGAAGAC
SCO6773PP 5'	CAGTACCATATGGCCAACGCCGCTCCCGCGCAC
SCO6773PP 3'	CAGTACGGATCCTCAGACGGAGACGCCGTGCGA

Complementation primers	
1240U	see "1240 S1U"
1240D	GGGGATGGTGATCATTCGCTGGCTGA
4582U	see "4582 S1U"
4582D	GACATCCCGATGTTCCAGTG
3097up	CAGAAGCCGTGATCGTCTTTG
3097end	TTACTTGTCGTCATCGTCCTTGTAGTCGCCGCCGCCCTTCAGGTGCAGCTGCTG
3097FLAG	GGCGGCGGCGACTACAAGGACGATGACGACAAGTAAGCGGCGGCGGTCCCGTGACTC
9798D	CGGTACGGATCCCACGAGCATCTCCTTCTTC
6773U	CGGTACTCTAGACTGTGCGTCTTGGTCCCTTAC
6773D	CGGTACGGATCCGCTGTCACTCTTCGAATCG

Routine cloning	
M13 FWD	GTAAAACGACGGCCAGT
M13 REV	CAGGAAACAGCTATGAC
T7 prom	TAATACGACTCACTATAGGG
T7 term	GCTAGTTATTGCTCAGCGG

Table 3.4. Protein overexpression, and zymogram buffer conditions. (* Values were calculated excluding the signal peptide, but including the His_6 tag)

Protein	size (kDa)*	pI*	[IPTG] (mM)	Induction time (h)	Induction temperature (°C)	Renaturation buffer
SwlA	13.8	10.8	1	2	22	50 mM KH_2PO_4 pH 4.5, 0.1 % Triton X-100, 5 mM $MgCl_2$
RpfA	21.7	6.25	1	2.5	30	25 mM NaP pH 7.0, 0.1 % Triton X-100, 10 mM $MgCl_2$
SwlB	14.0	5.4	1	5	22	25 mM Tris-HCl pH 6.0, 0.2 % Triton X-100, 10 mM $MgCl_2$, 1 mM DTT
SwlC	28.6	6.7	2	3	37	25 mM NaP pH 7.0, 0.1 % Triton X-100, 10 mM $MgCl_2$

Table 3.5. 5' end mapping of the four cell wall hydrolase transcripts.

Gene	Predicted protein domain	Predicted leader size (nt)	UTR size: S1 mapping (nt)	UTR size: 5′ RACE (nt)
swlA	Endopeptidase (NlpC/P60 subgroup)	183	~100	-
rpfA	N-acetylglucosaminidase (Rpf subgroup)	166	~240	237
swlB	N-acetylglucosaminidase	123	-	162
swlC	Endopeptidase	155	-	205

Chapter 4:

TOWARD DECIPHERING THE REGULATION OF RpfA IN *STREPTOMYCES COELICOLOR*

Haiser, H.J., Yousef, M.R., and Elliot, M.A.

Preface:
This chapter presents unpublished work that was the main focous of my Ph.D. studies following the submission of the manuscript presented in the previous chapter. A postdoctoral researcher in the lab (M.R.Y.) completed the work to determine the proposed secondary structure of the 5' untranslated region preceding *rpfA* (Fig. 4.4). The liquid chromatography experiment was done in collaboration with Dr. Kalinka Koteva in the lab of Dr. Gerard Wright, McMaster University. I carried out all other work, including additional structural probing experiments. All authors collaborated on the experimental design and the data interpretation.

4.1 CHAPTER SUMMARY

The resuscitation promoting factor (Rpf) family of cell wall hydrolytic proteins has recently been implicated in the transition from dormant to actively growing bacterial cells. Both *Mycobacterium tuberculosis* and *Streptomyces coelicolor* encode 5 Rpf-like proteins. One of the *rpf* genes (*rpfA*) is of particular interest, as it is predicted to be under the control of a conserved metabolite-sensing riboswitch. The Rpf-associated riboswitch is found upstream of 7 genes in *S. coelicolor*, all of which are predicted to encode products with cell wall cleavage activity. In *M. tuberculosis*, this sequence is only associated with *rpfA*. To begin dissecting *rpfA* regulation, RpfA was fused to a 3×FLAG tag to facilitate the monitoring of *in vivo* protein expression. The RpfA-FLAG fusion is highly expressed early in development, and can be found primarily in the growth medium fraction of liquid-grown cultures; RpfA expression shuts off shortly after the onset of stationary phase (~36-40 h of growth). Exposing 4 h cultures to the supernatant of stationary phase cultures results in complete repression of RpfA expression. The secondary structure of the *rpfA* leader region suggests a translational regulatory role for this putative riboswitch, a hypothesis that is further supported by expression studies of a strain with a mutagenized leader sequence.

4.2 INTRODUCTION

Bacterial dormancy is a widespread phenomenon in which organisms adopt a state of low metabolic activity in order to survive adverse conditions (Dworkin & Shah, 2010, Kell *et al.*, 1998). Dormancy can be manifested in a number of ways including exo/endospore formation, which requires major morphological changes, as well as less morphologically distinct states where cellular metabolism is shut down, but no overt physical changes occur (Dworkin & Shah, 2010). Bacterial cells can exist in dormant states for extended periods of time, and must be stimulated to resume vegetative growth. In the case of most sporulating bacteria, the stimulus is often in the form of a 'germinant' that binds to specific receptors, initiating a cascade of molecular events that result in outgrowth (Setlow, 2003). In other dormant cells, the cues that trigger growth are not as well defined. In the late 1990s, researchers made the exciting discovery that dormant cells of the non-sporulating *Micrococcus luteus* can be stimulated to resume growth by a protein termed the resuscitation-promoting factor (Rpf) (Mukamolova *et al.*, 1998). Further characterization have shown Rpf proteins to have functional and structural similarity to lysozymes – a major family of cell wall hydrolases (Cohen-Gonsaud *et al.*, 2005, Cohen-Gonsaud *et al.*, 2004, Mukamolova *et al.*, 2002a).

Peptidoglycan (PG) is the major component of the Gram-positive cell wall (Figure 1.4) (Schleifer & Kandler, 1972). PG is a dynamic mesh-like polymer composed of parallel glycan strands, comprising alternating *N*-acetylglucosamine (Glc*N*Ac) and *N*-acetylmuramic acid (Mur*N*Ac) residues, held together by Mur*N*Ac-linked peptides (Vollmer *et al.*, 2008a). PG metabolism is necessarily a

stringently controlled process, regulated both spatially and temporally. Transcriptional control of cell wall hydrolases has been investigated in several cases. One of the best understood systems is in *Bacillus subtilis*, where the cell wall hydrolases involved in germination and sporulation are controlled by dedicated sigma factors that are specific for these processes (Sonenshein *et al.*, 2002). The spatial regulation of PG hydrolases can involve the association of the hydrolytic domain with additional domains specialized for cell wall binding, including the 'LysM' domain (Buist *et al.*, 2008) – a domain possessed by many Rpf proteins (Ravagnani *et al.*, 2005).

Genes encoding Rpf proteins are widespread within the Actinobacteria, with *Mycobacterium tuberculosis* and *Streptomyces coelicolor* each possessing 5 Rpf-like proteins (Ravagnani *et al.*, 2005). Importantly, a *M. tuberculosis* strain harbouring a deletion in *rpfB* shows reduced virulence in mouse models (Russell-Goldman *et al.*, 2008, Tufariello *et al.*, 2006), highlighting the pathogenic significance of this protein family. The five Rpfs from *M. tuberculosis* are under independent transcriptional control, suggesting that these proteins may be involved in separate processes (Tufariello *et al.*, 2004, Gupta *et al.*, 2010). While the biochemical function of the Rpfs is well established (Mukamolova *et al.*, 2006), there remain a number of outstanding questions concerning the biological activity and control of these proteins. One of the big questions is: how does cell wall cleavage by the Rpfs successfully trigger growth resuscitation? Two explanations for this have been put forward: in one, Rpf activity may relieve a physical constraint in the cell wall that previously inhibited growth, while in the second, PG hydrolysis may liberate a signaling molecule that initiates a regulatory cascade, leading to the resumption of growth (Keep *et al.*, 2006). A second important question is one that is relevant for many cell wall hydrolases, and that is: what factors contribute to the control of Rpf/hydrolase activity.

Interestingly, several cell wall hydrolases genes, including the *rpfA* gene from both *S. coelicolor* and *M. tuberculosis*, are preceded immediately at their 5' end by a predicted gene control element called a riboswitch (Barrick *et al.*, 2004). Riboswitches are widespread in (but not confined to) prokaryotes where they are usually embedded in 5' untranslated regions (UTRs) of mRNAs. These RNA control elements fold into complex structures and bind specific small molecule metabolites (ligand). Metabolite binding typically results in a conformational 'switch' that alters expression of the associated *cis*-encoded gene in the absence of other cellular factors (Winkler & Breaker, 2005). This 'switch' can be controlled at a transcriptional level (termination/antitermination) or translational level (sequestered/available ribosome binding site) (see Fig. 1.7) (Serganov & Patel, 2007). Fascinatingly, riboswitches typically function in regulatory feedback/forward loops where the product of the gene under riboswitch control, is often involved in the transport or metabolism of the metabolite bound by the riboswitch (Mandal & Breaker, 2004).

In 2004 the *ydaO* riboswitch motif (named for the downstream gene in *B. subtilis*) was computationally predicted to control the expression of several genes

in diverse bacteria, including *Mycobacterium*, *Bacillus*, *Clostridium,* and *Streptomyces* species (Barrick *et al.*, 2004, Altschul *et al.*, 1990). Interestingly, over half of the genes associated with the *ydaO* motif encode cell wall hydrolytic enzymes (Block *et al.*, 2010). Determining the function of this conserved sequence will therefore have broad implications and may reveal a novel control mechanism for cell wall hydrolase expression and activity.

Our interest in the *ydaO* motif began when we identified an antisense RNA sequence that was complementary to the UTR of four of the seven *ydaO* motif-associated genes in *S. coelicolor*. All of the downstream genes are predicted to encode cell wall hydrolase proteins. We used end-mapping experiments to confirm the presence of riboswitch motif-containing UTRs at the 5' end of each primary transcript, and carried out transcriptional profiling experiments that suggested these genes were not subject to identical transcriptional/post-transcriptional control (Haiser *et al.*, 2009). Work from another group has shown that the *ydaO* motif in *B. subtilis* serves as a gene control element, likely acting at the level of transcription (Block *et al.*, 2010). There has not, however, been any *ydaO* motif-specific metabolite identified, and in the absence of such evidence, it is not yet possible to conclude that the *ydaO* motif is a riboswitch regulatory element.

In this work we begin to address questions relating to the regulation of RpfA in *S. coelicolor*. We have established growth conditions that result in the specific repression of RpfA expression, and through structural probing experiments, have determined that the *ydaO* motif may exert its regulatory effects at a translational level.

4.3 Materials and Methods

4.3.1 Bacterial strains, plasmids, media, and growth conditions used in this study

S. coelicolor A3(2) wild-type strain M145 and all mutant derivatives were grown on R2YE and MS (mannitol-soy flour) solid growth media (Kieser *et al.*, 2000). All experiments involving liquid growth medium used a 50:50 mixture of yeast extract/malt extract (YEME) and tryptic soy broth (TSB) medium (Sambrook & Russell, 2001, Kieser *et al.*, 2000). Antibiotic selection was maintained when appropriate (Kieser *et al.*, 2000). *E. coli* strains were grown in LB broth/agar at 37°C, following standard conditions (Sambrook & Russell, 2001). All bacterial strains and plasmids used in this study are described in Table 4.1.

4.3.2 Polymerase chain reaction and oligonucleotides

All polymerase chain reaction (PCR) experiments were carried out using the iProof polymerase system (Bio-Rad), following the manufacturers instructions. In most cases the 'HF' buffer was used, although in cases of low yield, the 'GC' buffer was used. The concentration of dimethyl sulfoxide (DMSO) added to reactions varied from 5-10%. In all cases, cloning products were verified by DNA sequencing. The sequences of all oligonucleotides are provided in Table 4.2.

4.3.3 Synthesis and construction of the RpfA-FLAG strain

To follow RpfA expression, we constructed a 3×FLAG-tagged variant that we could detect via immunoblotting (Fig. 4.1A). To facilitate the subsequent generation of UTR mutant strains, we had this sequence synthesized by Genscript. The synthesized RpfA-FLAG DNA included 159 nucleotides (nt) upstream of the *rpfA* transcription start site, and 264 nt downstream of the *rpfA* stop codon. This sequence was flanked on either end by *Bgl*II sequences, to enable ready transfer into *Streptomyces* conjugative vectors, and was cloned into the *Kpn*I/*Hin*dIII sites of pUC57. Upon receipt of this construct, we sub-cloned this fragment into the *Kpn*I/*Hin*dIII site of pBluescriptII-KS– (Kieser *et al.*, 2000), to facilitate further manipulation.

The 3×FLAG-tag (DYKDHDGDYKDHDIDYKDDDDK) DNA sequence was introduced before the *rpfA* stop codon, and was flanked on either side by *Xho*I sites to facilitate its removal for use in other constructs. Additionally, a region encoding three glycine residues was included immediately upstream of the tag to act as a flexible linker.

Because we were interested in creating versions of the RpfA-FLAG strain both with and without the 5' UTR, the majority of the 5' UTR sequence was omitted during DNA synthesis. To facilitate cloning of the 5' UTR into the construct, we modified a single base 10 nt downstream of the *rpfA* transcription start site (changed a cytosine to a guanine), creating an *Nco*I site. Additionally, we modified the 3 nt immediately upstream of the *rpfA* start codon from AAC to CAT, creating an *Nde*I site. DNA corresponding to the 5' UTR was PCR amplified from wild-type chromosomal DNA, with oligonucleotides containing *Nco*I and *Nde*I sites at their 5' ends (*rpfA*UTR5' and *rpfA*UTR3' respectively; Table 4.2). Following amplification and digestion, the resulting fragment could then be cloned into the corresponding sites in the vector containing RpfA-FLAG.

To reduce synthesis cost, we initially excluded a large portion of sequence corresponding to the *rpfA* coding-region. This sequence was later incorporated by exploiting a naturally occurring *Sal*I site near the 3' end of the *rpfA* gene. The DNA corresponding to the coding region was PCR amplified with oligonucleotides 3097-PP5' and 9798D (Table 4.2). The resulting fragment was digested with *Nde*I and *Sal*I, and the 693 nt product was cloned into the corresponding site of the vector harbouring the synthesized RpfA-FLAG fragment.

The RpfA-FLAG sequence including the 5' UTR and full *rpfA* sequence in pBluescriptII-KS– was named pBlue-RpfA-FLAG+ and correspondingly, the version lacking the 5' UTR was named pBlue-RpfA-FLAG- (Table 4.1). Before moving these vectors into the *rpfA* deletion strain, they were further sub-cloned into the integrating vector pIJ82 (Table 4.1). To facilitate conjugal transfer into *Streptomyces*, the plasmids were transformed into the *E. coli* strain ET12567/pUZ8002 (which mobilizes the *oriT*-containing pIJ82 for transfer into *Streptomyces*; Table 4.1). In all cases, empty plasmid controls were introduced

into the same *S. coelicolor* strains. Complementation of the *rpfA* heat sensitivity phenotype was assessed as previously described (section 3.3.13) (Haiser *et al.*, 2009).

4.3.4 Deletions and substitutions of the 5' UTR sequence

The following steps were taken to construct a version of the RpfA-FLAG strain lacking the first stem structure (ΔP1RpfA-FLAG) (Fig. 4.6). An oligonucleotide (P1*rpfA*5'; Table 4.3) was designed that began 45 nt after the *rpfA* transcription start site, and contained an *Nco*I site at its 5' end. The truncated fragment was PCR amplified from chromosomal DNA using the oligonucleotides P1*rpfA*5'/*rpfA*UTR3' (Table 4.2). Following digestion with *NcoI*/*Nde*I, the fragment was cloned into the corresponding site of pIJ82-RpfA-FLAG-; this resulted in a 5' UTR lacking residues 7-45 (construct ΔP1). The plasmid construct was then transferred to *Streptomyces* by conjugation as described above.

Six other modifications to the wild type 5' UTR sequence were generated, and are summarized in Fig. 4.6. The construction of each variant involved site-directed mutagenesis using two long, reverse complementary oligonucleotides having the desired deletion or nucleotide changes incorporated into the centre of the oligonucleotide sequence. Two PCR products were amplified: the first using the oligonucleotide *rpfA*UTR5' in combination with a reverse-facing oligonucleotide harbouring the desired modification (ΔP7-*rpfA*Rev or M*x*-*rpfA*Rev), and the second with a forward-facing oligonucleotide containing the desired modification (ΔP7-*rpfA*Fwd or M*x*-*rpfA*Fwd), in combination with *rpfA*UTR3' (Table 4.2). The two PCR products were then checked on an agarose gel, PCR-purified (QIAGEN), and combined in approximately equal amounts before being subjected to PCR amplification using the oligonucleotides *rpfA*UTR5'/*rpfA*UTR3'. The resulting PCR product was then cloned into pIJ82-RpfA-FLAG- and moved into *Streptomyces* as described for the ΔP1 mutation.

4.3.5 Protein isolation

Cells from liquid-grown *Streptomyces* cultures were collected by centrifugation at 4°C, while solid-grown cultures were harvested by scraping growth from cellophane-covered plates. For the isolation of cytoplasmic and insoluble proteins, cells were first washed in 10.3% sucrose, followed by re-suspension in phosphate-buffered saline (PBS) containing a cOmplete, Mini, EDTA-free protease inhibitor cocktail (Roche) tablet (1 tablet/10 ml of buffer) and lysozyme to a final concentration of 1 mg/ml. Following a 20 minute incubation at 37°C, the cells were subjected to microtip sonication on ice (50% Power level, 40% Duty; 8-10 cycles of 5 s continuous bursts, alternating with 10 s rest periods). Cell debris was separated from soluble proteins by centrifugation (10,344×g, 15 min, 4°C). Both the pellet (insoluble proteins and cell debris) and aliquots of the supernatant (soluble cytoplasmic proteins) were resuspended in Laemmli buffer (Laemmli, 1970). In some cases protein concentrations were determined using the method of Bradford (Bio-Rad; (Bradford, 1976)) to ensure equal loading of polyacrylamide

gels, while for others, aliquots were normalized based on wet cell weight, or adjusted based on Coomassie staining sample aliquots separated on polyacrylamide gels.

Secreted proteins for liquid-grown *Streptomyces* cultures were harvested by pelleting cells from one milliliter of culture by centrifugation (10,344×g, 5 min, 4°C). Following this, 800 µl of supernatant was removed, and supernatant-associated proteins were concentrated by adding one-quarter volume (200 µl) of 100% (w/v) trichloroacetic acid (TCA). The TCA-supernatant mixture was incubated for 30 min at 4°C before proteins were recovered by centrifugation (10,344×g, 5 min, 4°C). Protein pellets were washed twice with chilled acetone before being dried at room temperature and re-solubilized in 80 µl Laemmli buffer.

4.3.6 Immunoblot analysis

Samples were subjected to electrophoresis in 12% (w/v) denaturing SDS-polyacrylamide gels at 200 V for ~1 h. Gels and 0.45 µm PVDF-Plus transfer membranes (GE) were soaked in 10% methanol before being equilibrated in transfer buffer (25 mM Tris, 192 mM glycine, 10% methanol) for 30 min. The transfer of proteins from gels to membranes was accomplished using the Trans-Blot semi-dry transfer cell (Bio-Rad) (15 V for ~1 h). Membranes were blocked in Tris-buffered saline and 0.05% Tween 20 (TBS-T) with 5% low fat milk for 1 h, and were then incubated, with shaking, overnight with the primary 'anti-FLAG' (DYKDDDDK) Tag antibody (1:1500 dilution; Cell Signaling, cat. # 2368) at 4°C. Membranes were washed with TBS-T (3 x 5 min) at room temperature, before being incubated with an anti-Rabbit IgG horseradish peroxidase-linked secondary antibody (1:3000 dilution; Cell Signaling, cat. #7074) for 1 h at room temperature. After membranes were washed (3 x 5 min), detection was carried out using Amersham ECL™ Western Blotting Detection Reagents (GE Healthcare) following the manufacturers instructions. Blots were imaged using X-Omat LS film (Kodak).

4.3.7 Preparation of conditioned growth medium

Cells were removed from conditioned growth medium by centrifugation (4,000 rpm, 5 min, 4°C). The resulting supernatant was filter sterilized twice (0.45 and then 0.2 µm filter; Pall) before being passed through the Ultracel – 3000 molecular weight cut-off centrifugal filter (Amicon®Ultra), following the manufacturers instructions, to give two fractions: < 3kDa and >3 kDa.

4.3.8 Liquid chromatography

The <3 kDa fraction of conditioned growth medium (see above) was subjected to reverse-phase HPLC using the ISCO CombiFlash® purification system, and a 4.3g C18 RediSep column. Fractions were collected at one-minute intervals under the following conditions: solvent A (water) and solvent B (acetonitrile) followed a linear gradient (flow rate of 10 ml/min) from 0 to 100% B over 14.4 min. A

Genevac solvent evaporator was used to dry the resulting fractions, after which they were resuspended in 100% DMSO for further testing. A DMSO control was included in all downstream experiments.

4.3.9 *In vitro* transcription

To generate the DNA template for *in vitro* transcription (IVT), oligonucleotides IVT*rpfA*UTR5' (containing the T7 RNA polymerase promoter site) and IVT*rpfA*UTR3' (Table 4.2) were used for PCR amplification from chromosomal DNA. The MEGAshortscript™ kit (Applied Biosystems) was then used for *in vitro* transcription, following the manufacturers instructions with minor modifications. Briefly, the IVT reaction volume was doubled from 20 µl to 40 µl, and included 1 µl gel-purified (QIAGEN) DNA template (~100 nM), 1 × T7 Reaction buffer, 7.5 mM each ATP, CTP, GTP, and UTP, 1 mM GMP, and the T7 enzyme mixture. The reaction was then incubated for four hours at 37°C before being treated with DNase. DNA-free IVT reactions were separated on 6% polyacrylamide gels, and the RNA bands of interest were visualized using UV-shadowing. The band corresponding to the full-length transcript was excised and eluted from the gel slice in buffer containing 0.4 M sodium acetate and 1 mM EDTA, and the RNA was recovered by ethanol precipitation following standard methods (Sambrook & Russell, 2001), resuspended in dH_2O, and quantified by UV spectroscopy using an Ultraspec 3100 pro (Biochrom).

4.3.10 Structural probing experiments

Gel-purified RNA for structural probing experiments was 5' end-labeled using the KinaseMax™ Kit (Applied Biosystems) with minor modifications. Briefly, ~50 pmol of RNA was first de-phosphorylated by treatment with calf intestine alkaline phosphatase, doubling the volumes of all reaction components indicated in the manufacturers instructions. This was followed by T4 polynucleotide kinase reaction, to add a 5' [γ-^{32}P]dATP residue (Perkin Elmer), and removal of excess label using NucAway™ Spin Columns (Applied Biosystems) following the manufacturers instructions. The end-labeled RNA was then gel-purified from a polyacrylamide gel as described for the unlabeled RNA, except that autoradiography was used to detect the full-length RNA transcript.

'In-line' probing reactions were set up using 1 µl of gel-purified end-labeled RNA, 4 µl 2.5 × reaction buffer (125 mM Tris pH 8.3, 250 mM KCl_2, 100 mM $MgCl_2$), and where indicated, including 4 µl conditioned growth medium. Reactions were incubated at 65°C for 5 minutes, after which they were slow cooled to room temperature, where they were then maintained for ~40 hours to allow self-cleavage to occur. RNA ladders were prepared using RNase T1 treated and alkali hydrolyzed RNA, as described in the RNase T1 Biochemistry Grade kit (Applied Biosystems). A 10-bp ladder (Invitrogen) was also prepared by radio end-labeling, following the manufacturers instructions. After incubation, all samples were precipitated, separated in 6% polyacrylamide sequencing gels and visualized using a phosphorimager as previously described (Haiser *et al.*, 2008).

4.4 RESULTS

4.4.1 RpfA is a secreted protein that is expressed in liquid-grown cultures

The RpfA protein encoded by *S. coelicolor* possesses an N-terminal signal peptide that is predicted to target this protein for extracellular secretion (Bateman *et al.*, 2000). To confirm this prediction and to follow *in vivo* RpfA expression over a time course experiment, we constructed a fusion between the C-terminus of RpfA and a 3× FLAG-tag epitope (hereinafter referred to as 'RpfA-FLAG'; section 4.3.3) (Fig. 4.1A). The RpfA-FLAG fusion was transferred into the *rpfA* mutant strain (Haiser *et al.*, 2009) on an integrating plasmid vector (see materials and methods). Following strain construction, we observed that RpfA-FLAG provided nearly full complementation of the *rpfA* heat sensitivity phenotype (data not shown), and thus we reasoned that the fusion did not disrupt RpfA function. Next, we assessed solid (MS and R2YE agar) and liquid-grown (YEME/TSB) cultures for RpfA-FLAG expression and found that RpfA-FLAG was not detected in the total cellular protein, cytoplasmic or membrane fractions of solid-grown cultures (data not shown). In contrast, RpfA-FLAG was readily detected in the secreted fraction of liquid-grown cultures (Fig. 4.1B). This localization pattern is consistent with observations for cell wall hydrolases from other organisms (193, 203), including the RpfA protein from *Micrococcus luteus*, which was originally purified from conditioned growth medium (Mukamolova *et al.*, 1998). Time course experiments revealed that RpfA-FLAG was expressed as early as 4-hours after initiating growth in liquid culture, and was detectable until ~36-40 h of growth (Fig. 4.1B).

4.4.2 Conditioned growth medium represses RpfA-FLAG expression

We successfully identified conditions where RpfA-FLAG was expressed, but found it to be no longer detectable after ~40 h of growth. There were a number of possible explanations for this observation. Transcription may have simply ceased, or alternatively, the 5' UTR of *rpfA* may have sensed a metabolite that resulted in riboswitch-mediated repression. To test the latter hypothesis, we grew cultures of RpfA-FLAG for 4 h, as we had established that there was abundant RpfA-FLAG being secreted into the growth medium at this time (Fig. 4.1B). After collecting and washing the 4 h cells, they were resuspended in one of three media-types: fresh growth medium (YEME/TSB); 40 hour cell-free conditioned growth medium from wild-type *S. coelicolor*; or a mixture of fresh growth medium and cytoplasmic extracts from 40 hour wild-type cells. Following an additional 3 hours of growth, secreted proteins were collected and RpfA-FLAG expression was assessed by immunoblotting (section 4.3.6; Fig. 4.2A). The striking observation was that cells resuspended in conditioned growth medium failed to express RpfA-FLAG, while those resuspended in either fresh medium or fresh medium and cytoplasmic extracts, expressed RpfA-FLAG at near wild type levels (Fig. 4.2B).

To ensure that changes in the conditioned growth medium did not affect general protein expression, and were in fact specific for RpfA-FLAG expression, we tested the expression of another FLAG-tagged secreted protein (SCO3098) when grown in the conditioned medium. Importantly, *sco3098* encodes an Rpf protein that shares extensive amino acid and functional domain similarity to RpfA, but lacks the *ydaO* leader preceding its coding sequence (Ravagnani *et al.*, 2005, Altschul *et al.*, 1990). Following growth for ~14 h, to a point where SCO3098-FLAG was readily detectable (data not shown), secreted proteins were harvested and SCO3098-FLAG expression was analyzed. In contrast to what we observed for RpfA-FLAG, we found that SCO3098-FLAG expression following growth in conditioned medium was comparable to that observed following growth in fresh medium (Fig. 4.2C). Taken together, these results suggest that a molecule within the conditioned growth medium of 40-hour cultures represses RpfA expression, either directly or indirectly.

4.4.3 RpfA is repressed by a heat-labile small molecule

Given that riboswitches are often part of feedback/forward loops, studying the genetic context of representative members of a given riboswitch class can often reveal candidate metabolites (Dambach & Winkler, 2009). The diversity of genes associated with the *ydaO* leader makes for a challenging exception to this general rule. Nevertheless, we reasoned that if the products of the genes potentially under riboswitch control were involved in producing the factor that imparts repression, then deletion of these genes might result in a strain deficient for the repressing ligand. To test this idea, we prepared cell-free conditioned growth medium from cultures of the *rpfA* deletion strain (Haiser *et al.*, 2009) and evaluated RpfA-FLAG expression when grown in this medium (see above). The mutant-conditioned medium repressed RpfA-FLAG expression, similar to that observed for wild-type grown control samples (data not shown), suggesting that RpfA alone is not responsible for generating the repressing metabolite.

Next, we focused on assessing the physical and chemical nature of the factor that repressed RpfA expression. To this end we separated conditioned medium samples based on their retention in various molecular weight cut-off spin columns, and then tested these fractions for their ability to repress RpfA-FLAG expression (see above). Using a 3 kDa size exclusion column, we found that the >3 kDa fraction did not affect RpfA-FLAG expression, whereas the flow-through fraction (<3 kDa) completely inhibited expression (Fig. 4.3). We also tested the stability of the small molecule inhibitor present in the <3 kDa fraction, and found that after boiling for 15 minutes, repression of RpfA-FLAG expression was no longer observed (Fig. 4.3). Cumulatively, these findings suggest that a small, heat-labile molecule accumulates during liquid-culture growth, and represses RpfA expression.

Lacking a strain deficient in the production of the molecule of interest has hampered molecule identification through comparative chromatographic methods. Thus, we carried out fractionation experiments using the < 3 kDa

fraction of the wild-type conditioned medium samples previously shown to repress RpfA-FLAG expression. For this, reverse-phase HPLC was used to separate the samples using an acetonitrile gradient to facilitate elution through a C18 column. This resulted in 15 fractions, each separated on the basis of charge. The fractions were re-solubilized in DMSO, and added individually to cultures expressing RpfA-FLAG (see above). Initially, our results suggested that some of the fractions possessed 'activity' (i.e. they repressed RpfA-FLAG expression); however, these results were not reproducible, as subsequent fractionation experiments identified different active fractions (data not shown).

4.4.4 A proposed secondary structure for the *rpfA* leader region suggests translational regulation

Mechanistic insight into the regulatory mode employed by riboswitches is often obtained by comparing RNA secondary structures in the presence and absence of its cognate ligand (Winkler & Breaker, 2005). Even though the identity of the ligand is unknown in this case, we reasoned that secondary structural analysis could provide insight into the functioning of this highly conserved RNA region. Thus, through a combination of bioinformatic analyses, published structural data (Barrick *et al.*, 2004, Block *et al.*, 2010), and RNA structural probing experiments (RNase T1 cleavage and "in-line" probing; see materials and methods), we assembled a secondary structure model for the *rpfA* 5' UTR in *S. coelicolor* (Fig. 4.4). A number of interesting features stand out in the analysis of this structure. First, there are no secondary structure motifs like terminators/anti-terminators that characterize transcription-based regulation within the proposed structure. We also observed the potential for base pairing between the loop that is associated with stem P7, and the predicted ribosome-binding site (RBS) for the *rpfA* transcript. This predicted pairing could lead to RBS occlusion and translation inhibition. The different transcriptional profiles observed for the four hydrolase-encoding gene transcripts sharing this same 5' UTR (Fig. 3.2), the lack of terminator/antiterminator structures, and the potential for pairing with the RBS all suggest a translation-based regulatory mechanism for this RNA motif in *S. coelicolor*.

Finally, there exists an extended single stranded region, joining stems P3 and P5 (Fig. 4.4B [residues 199-208]). This region has been highlighted previously (Block *et al.*, 2010), as being one that is highly conserved in the *ydaO* motif of many species. This is particularly interesting in light of the fact that metabolite-binding riboswitches often interact with their cognate ligands in highly conserved single stranded regions (Blouin *et al.*, 2010).

4.4.5 Conditioned growth medium induces structural changes in the *rpfA* 5' UTR

RNA structural changes that occur in response to ligand binding are ideally assessed by incubating *in vitro* transcribed RNA with candidate metabolites. Since our fractionation attempts did not yield any obvious candidate metabolites,

we decided to test whether *rpfA* leader RNA undergoes structural rearrangements when incubated with conditioned growth medium. This was accomplished by incubating the <3 kDa fraction of conditioned (40-hour) wild-type growth medium, together with end-labeled RNA corresponding to the *rpfA* 5' UTR, and allowing spontaneous 'in line' cleavage to occur (section 4.3.10). Our results are preliminary in nature, as we did not achieve the single nucleotide resolution required to identify the subtle changes that typically occur in response to ligand binding. However, we did reproducibly identify regions of increased protection from spontaneous cleavage, between residues 110-210 of the *rpfA* 5' UTR (Fig. 4.5). Importantly, this region includes both the loop associated with stem P7, and the highly conserved single-stranded region. As such, we decided to further examine these regions to assess their functional importance.

4.4.6 Dissection of the requirements for regulation and expression of the *rpfA* 5' UTR

With evidence mounting to suggest that the *rpfA* 5' UTR is a gene control element, we sought to determine the effects of altering the UTR sequence, on RpfA-FLAG expression. We began our analysis by constructing variants of the RpfA-FLAG strain having either full or partial deletions of the native 5' UTR sequence, and additional variants possessing single nucleotide deletions/alterations (see materials and methods for details on strains construction; see Fig. 4.6 for a summary of all mutations made). Each of the resulting strains were assessed for RpfA-FLAG expression over time, and changes in RpfA-FLAG expression when grown in conditioned growth medium.

We included the following deletion strains in our analysis: ΔP7-RpfA-FLAG - lacks the stem-loop in the P7 region (Δ residues 176 – 195), ΔP1-RpfA-FLAG - lacks stem P1 (Δ residues ~7 – 45), and ΔUTR-RpfA-FLAG – lacks residues 10 – 225) (Fig. 4.6). These three variants include both the *rpfA* promoter region and RBS. Interestingly, the RpfA-FLAG protein was not detectable in either the ΔP1 or ΔUTR-RpfA-FLAG strains (data not shown), suggesting that the regions deleted in these strains are important for the transcription and/or translation of *rpfA*. In contrast, RpfA-FLAG was detectable in the growth medium of ΔP7-RpfA-FLAG cultures; moreover, a short time course experiment revealed that expression continues beyond the 40-hour time point (Fig. 4.7A). Given that repression is absent (or at least delayed) in >40-hour ΔP7-RpfA-FLAG cultures, we decided to test the effects of adding conditioned growth medium to these cells. This experiment revealed that the repression typically imparted by conditioned growth medium was much less pronounced in the ΔP7 strain (Fig. 4.7B). Thus, these results suggested that the P7 region of the *rpfA* 5' UTR was important for repression, and this repression could be mediated thorough base pairing of the loop associated with stem P7 with the RBS. These results encouraged us to more precisely define the regions contributing to the altered expression of the ΔP7 strain. Additionally, we wanted to test for expression changes resulting from altering the sequence of the highly conserved

single-stranded region, since this area may be important for ligand-interaction. To this end, we constructed five strains, each harbouring mutations in either the P7 stem loop or the conserved single stranded region. Most strains had single nucleotide deletions or base substitutions, although up to four nucleotides were changed in one strain (Fig. 4.6). All resulting strains exhibited expression patterns (both in the presence and absence of conditioned medium) identical to that observed when the native 5' UTR was present (data not shown). Thus, despite identifying stem loop P7 as a region of importance for *rpfA* repression, the mechanism through which repression occurs, and the identities of the nucleotides important for repression remain unknown.

4.4.6 Expression of the *ydaO* antisense RNA

In a small RNA cloning experiment (section 2.4.2) we identified a 27 nt antisense RNA fragment that was complementary to the *ydaO* motif (*α-ydaO*). We confirmed the expression of this *α-ydaO* RNA via northern blotting (see section 2.3.6 for method) of RNA isolated from wild-type *S. coelicolor* cells grown on minimal and rich medium. Although originally cloned from an RNA population isolated from cells grown on minimal medium, *α-ydaO* is primarily transcribed on rich growth medium, where it exists as a ~75 nt transcript (Fig. 4.8A; data not shown). The positioning of *α-ydaO* with respect to the downstream coding sequences (Fig. 1.8) suggests that deletion of these genes should eliminate *α-ydaO* expression (through removal of its promoter region). However, an analysis of *α-ydaO* expression in single and multiple deletion mutants showed no significant changes in *α-ydaO* expression (Fig. 4.8B). Furthermore, attempts to map the 5' end of *α-ydaO* using 5' RACE (section 3.3.4) were unsuccessful (data not shown). For additional discussion on the role of *α-ydaO*, see section 5.1.1.

4.5 Discussion

The *ydaO* motif belongs to a class of "orphaned" riboswitches for which the structural change-inducing ligand is currently unknown (Barrick *et al.*, 2004). In previous work, we found that seven *S. coelicolor* cell wall hydrolase genes were preceded by a conserved DNA sequence containing the *ydaO* motif (Haiser *et al.*, 2009). End-mapping experiments revealed these regions to be downstream of the transcription start sites. We also determined the transcriptional profiles for all seven genes during growth on solid medium, and characterized the biological role of the protein products encoded by four of these genes (Haiser *et al.*, 2009). Interestingly, we identified the *rpfA* gene product to be important during at least two stages of growth in *S. coelicolor* – germination and sporulation (Haiser *et al.*, 2009).

4.5.1 RpfA expression and biological function

In this work, we began to address the potential regulatory role of the conserved 5' UTR preceding *rpfA* by following *in vivo* RpfA expression. Our results indicate

that in liquid culture, RpfA is expressed immediately following germination and hyphal outgrowth and is detectable for another ~36 hours (Fig. 4.1B). Attempts to follow *rpfA* transcription in liquid culture were not successful. In solid culture, *rpfA* transcription follows a defined temporal pattern – expression peaks after 24 h of growth, followed by a period of decreased expression, and then an increase as the cultures approach sporulation (Haiser *et al.*, 2009). We did not however, detect RpfA-FLAG from cultures grown on solid medium.

4.5.2 A proposed model for the riboswitch regulation of *rpfA*

Our most exciting finding is perhaps that conditioned *S. coelicolor* growth medium specifically inhibits RpfA expression (Fig. 4.2B). Although it is tempting to propose that repression is mediated through a riboswitch regulatory mechanism, our speculation should be tempered with the following caveat: riboswitch regulation can only be definitively concluded once a change in RNA structure following specific ligand-binding is shown. This structural change must also coincide with a corresponding change in expression of the associated downstream gene. Our findings could have broad implications with respect to the *ydaO* riboswitch class, as we would expect ligand identity to be conserved for all members of this group, based on what is known about previously characterized riboswitches (Roth & Breaker, 2009).

Riboswitches are often part of feed back/feed forward loops, where the genes controlled by the upstream UTR encode products involved in the transport or metabolism of the cognate ligand (Fig 1.7). Based on an analysis of genome sequences, Block *et al.* (2010) determined that almost half of the ~580 genes preceded by the *ydaO* motif are predicted to encode cell wall hydrolases. Interestingly, many of the *ydaO* examples in *Bacillus* sp. and *Clostridium* sp. precede genes encoding amino acid or ion (potassium) transporters (although some precede hydrolase genes), while all of the examples in the Actinobacteria are associated with cell wall hydrolase genes (Block *et al.*, 2010). Importantly, many of these genes are of pathogenic significance including the *rpfA* homolog in *M. tuberculosis* and a gene encoding a germination-specific hydrolase from *Clostridium botulinum* (Altschul *et al.*, 1990). Taking these predicted gene functions into account – an attractive hypothesis is that the small molecule that inhibits RpfA expression is a component of PG itself, such as a muropeptide (see Fig. 4.9 for model). In this way, the expression of the cell wall hydrolases controlled by the *ydaO* motif would be directly coupled to the status of the cell wall.

4.5.3 Feasibility of the proposed model

The proposed model for the riboswitch regulation of *rpfA* would depend on both the shedding of PG, and a method of re-uptake. Indeed, during a single cell division cycle, Gram-positive (Mauck *et al.*, 1971) and Gram-negative (Uehara *et al.*, 2005) bacteria can turn over as much as 50% of their PG material. In Gram-negative bacteria, the bulk of the old material gets trapped in the periplasmic

space and is efficiently recycled (Park & Uehara, 2008). Due to fundamental differences in their cell envelope structure (namely the lack of an outer membrane in Gram-positive bacteria) (Fig. 1.4), it was long thought that PG recycling systems were absent from Gram-positive bacteria. However, a recent study has challenged this idea by presenting evidence for a PG recycling pathway in *B. subtilis*. The *B. subtilis* pathway involves proteins distinct from the *E. coli* pathway, but plays a functionally analogous role (Litzinger *et al.*, 2010). BLASTp searches querying the amino acid sequences of the proteins comprising the *B. subtilis* pathway did not reveal any significant similarity to *S. coelicolor* proteins (data not shown); however, this does not exclude the possibility of an analogous system in this organism.

It is worth noting that in addition to maintaining cell structure, there is precedent for PG (or PG fragments) serving as a signaling molecule. This is exemplified by the mammalian and insect proteins NOD1 and 2 that sense bacterial PG and promote immune responses (Viala *et al.*, 2004, Chaput & Boneca, 2007, Wray *et al.*, 2001). Moreover, within bacteria, PG triggers 'rippling behavior' in *Myxococcus xanthus* cell populations (Shimkets & Kaiser, 1982a, Shimkets & Kaiser, 1982b), induces secondary metabolite production and beta-lactamase expression in *Pseudomonas aeruginosa* and *Escherichia coli*, respectively (Korgaonkar & Whiteley, 2011, Jacobs *et al.*, 1994), and has recently been shown to act as a germinant in *B. subtilis* (Shah *et al.*, 2008). In this last example, a eukaryotic-like serine/threonine (Ser/Thr) kinase protein (PrkC) can bind specific PG fragments through its multiple extracellular PASTA (penicillin and Ser/Thr kinase associated) domain repeats. This binding results in the phosphorylation of an essential ribosome GTPase that presumably initiates a cascade leading to spore germination (Shah *et al.*, 2008).

4.5.4 A possible connection to PASTA domain-containing Ser/Thr kinases

Regulatory proteins possessing PASTA domains coupled with Ser/Thr kinase domains are widespread among the Actinomycetes and Firmicutes (Yeats *et al.*, 2002, Molle & Kremer, 2010). Indeed, *S. coelicolor*, encodes three such proteins (Jones & Dyson, 2006, Bateman *et al.*, 2000, Petrickova & Petricek, 2003). Several studies have implicated Ser/Thr kinases in the transcriptional regulation of enzymes involved in cell wall metabolism, including PknA and PknB in *M. tuberculosis,* which control the cell wall biosynthetic enzyme MurD (Thakur & Chakraborti, 2008), and a PBP involved in cell division (Dasgupta *et al.*, 2006), respectively. A recent metabolomic study in *Staphylococcus aureus* has shown that a Ser/Thr kinase deletion strain has altered intracellular levels of PG precursor metabolites (Liebeke *et al.*, 2010). In *B. subtilis,* PrkC, the PASTA-domain containing protein that facilitates PG-induced germination (Shah *et al.*, 2008), was recently shown to transcriptionally activate the cell wall hydrolase YocH, and this activation was induced by PG fragments (Shah & Dworkin, 2010). YocH possesses a 'Stationary phase survival' (Sps) domain (Shah & Dworkin, 2010). The Sps and Rpf proteins are both secreted cell wall hydrolases

with a role in maintaining viability following exponential phase, and it has been suggested these proteins are functionally analogous (Shah & Dworkin, 2010), although they are not defined as homologues based on amino acid sequence similarity (Ravagnani *et al.*, 2005). The connection between PASTA domain-containing Ser/Thr kinases and the activation of Rpf-like proteins sets up an intriguing premise for *rpfA* regulation in *S. coelicolor*, one that is not necessarily mutually exclusive from the proposed model.

To test a possible role for PASTA-containing Ser/Thr kinases in *rpfA* regulation, we assessed RpfA-FLAG expression in a strain lacking the three PASTA-containing Ser/Thr kinases in *S. coelicolor* (Δ*sco2110*, *3821*, and *3848*; a gift from Dr. M.J. Buttner). We observed no differences in RpfA-FLAG expression in the triple PASTA mutant background compared with that of the *rpfA* mutant background (data not shown). Moreover, in the triple PASTA mutant, RpfA-FLAG expression was still repressed in the presence of conditioned growth medium (data not shown), suggesting the PASTA proteins are not involved in mediating this response.

Of note, *S. coelicolor* encodes at least two additional Ser/Thr kinases that are not associated with PASTA domains, but are predicted to be involved in cell wall metabolism (Petrickova & Petricek, 2003). Indeed, *sco4817* and *4820* encode Ser/Thr kinases possessing additional PG-binding and cell wall hydrolytic domains respectively (Petrickova & Petricek, 2003). Moreover, the genetic context of these genes suggests that they may be involved in the production of the osmoprotectant glycine betaine (Boch *et al.*, 1997, Petrickova & Petricek, 2003). This is interesting since the *ydaO* motif was originally predicted to be responsive to an osmoprotectant, due to its association with genes encoding transporters implicated in responding to osmotic shock in *Bacillus* (Barrick *et al.*, 2004). It should however be noted that Block *et al.* (2010) tested glycine betaine, ecotine, trehalose and maltose, all of which are metabolites involved in osmoprotection, but none of these induced structural arrangements in the *ydaO* motif. Nevertheless, the hypothesis that PG sensing by a membrane-bound Ser/Thr kinase regulates cell wall hydrolase expression through an osmoprotectant-sensing riboswitch warrants further study.

4.5.5 Other possibilities for *rpfA* regulation

Based on our deletion analyses, we have demonstrated a role for the *rpfA* 5' UTR in affecting downstream gene expression. While concluding that this regulation is mediated by a riboswitch-based mechanism is premature, the widespread conservation of its 5' UTR strongly suggests an important function for this region. It could for example, serve as a target for binding by a regulatory factor such as an RNA-binding protein, small regulatory RNA, or downstream transcriptional activator. Our transcriptional profiling results argue against a common mode of transcriptional control for these *ydaO*-associated genes in *S. coelicolor*. Nevertheless, in cases where the transcriptional control of cell wall hydrolases has been studied, two-component systems have been identified as key

players. In addition being controlled by PrkC, the *B. subtilis* Sps protein YocH is activated by the two-component system (TCS) YycFG, in response to an unknown signal (Howell *et al.*, 2003). The homologous TCS in *Staphylococcus aureus* (WalKR) is a master regulator of cell wall metabolism (Dubrac *et al.*, 2007, Dubrac *et al.*, 2008). However, in neither of these cases have there been reports involving transcriptional regulatory factors binding downstream of the transcription start site. In *S. coelicolor*, cell wall homeostasis is controlled in part by the sigma factor s^E. *sigE* mutants have an altered PG composition compared with wild type strains, presumably due to changes in cell wall hydrolase expression (Paget *et al.*, 1999b, Paget *et al.*, 1999a). However, the promoter region of *rpfA*, and of all of cell wall hydrolases sharing the conserved 5' UTR, does not resemble the s^E consensus sequence (data not shown) (Paget *et al.*, 1999a).

4.5.6 Does conditioned growth medium induce transcriptional or translational level repression?

Analysis of the secondary structure prediction for the *rpfA* 5' UTR indicates the potential for base pairing between the loop associated with stem P7 and the RBS for this gene (Fig. 4.4). We addressed the importance of stem-loop P7 during a deletion experiment where we showed that the repression of RpfA via conditioned growth medium is reduced in the absence of this structure (Fig. 4.7B). These findings suggest a translational regulatory method; however, they are not definitive. In an attempt to directly address transcriptional vs. translational regulation, we have attempted to compare changes in RpfA protein expression with RNA transcript levels, but to date these experiments have been inconclusive (data not shown). An experiment that would allow us to distinguish between these two regulatory modes would be to create strains in which RpfA-FLAG (both with and without the 5' UTR) was placed under the control of a constitutive promoter. If growing these strains in the presence of conditioned growth medium resulted in repression only when the 5' UTR was present, this would support the proposal that the *ydaO* motif functions as riboswitch to repress translation. We have constructed and begun testing strains to test this hypothesis; however more rigorous analysis is needed before definitive conclusions can be drawn.

4.5.7 Conclusions and future work

This work provides an important step towards understanding the factors responsible for the complex regulation of *rpfA*. Despite providing evidence that the RpfA protein in *S. coelicolor* is repressed, likely at the translational level, by a component of conditioned growth medium, this work leaves several unanswered questions. A top priority for future work is to identify the component of conditioned growth medium that imparts repression on RpfA. These experiments will likely involve more thorough chromatographic separations, followed by 'activity' testing, and downstream characterization/identification of

any repressing molecule using electron spray ionization mass spectrometry. Once these preliminary studies have been carried out in *S. coelicolor*, it will be interesting to test whether these findings can be extended to the broad range of bacteria possessing the *ydaO* motif.

4.6 FIGURES AND TABLES

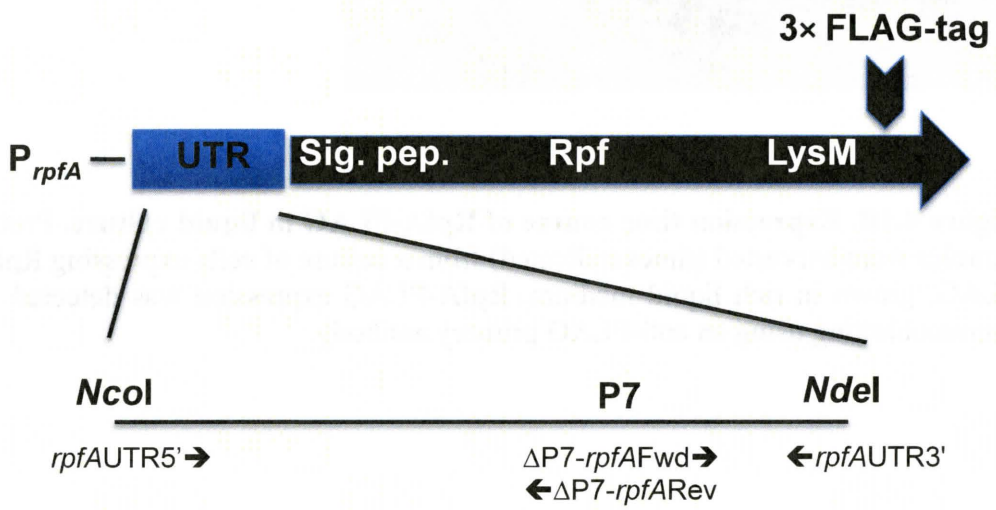

Figure 4.1A. Schematic diagram of RpfA-FLAG. Shown are the approximate locations of the important elements comprising the RpfA-FLAG construct (top panel). The bottom panel illustrates the locations of the oligonucleotides used to create the ΔP7RpfA-FLAG strain (section 4.3.4). A similar approach was taken for the construction of all deletion/truncation strains. (P_{rpfA} = the *rpfA* promoter region; Sig. pep. = signal peptide; Rpf = Rpf domain; LysM = cell wall binding domain; Note: image not drawn to scale)

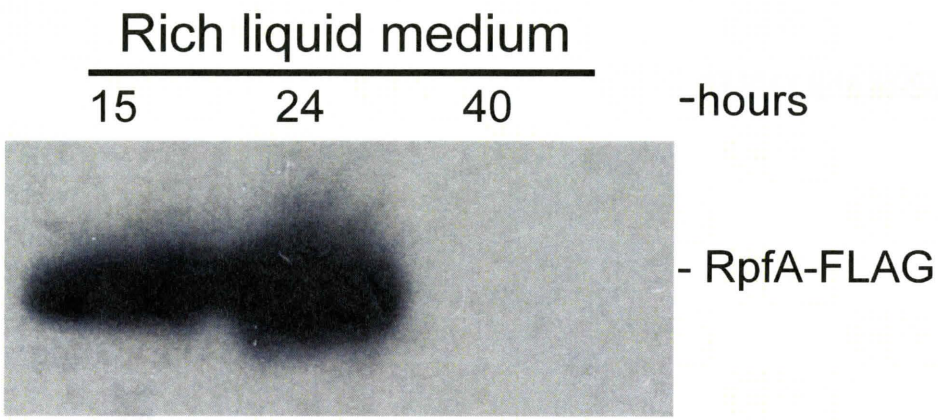

Figure 4.1B. Expression time course of RpfA-FLAG in liquid culture. Protein samples were harvested (times indicated) from a culture of cells expressing RpfA-FLAG, grown in rich liquid medium. RpfA-FLAG expression was detected via immunoblotting using an anti-FLAG primary antibody.

Figure 4.2A.

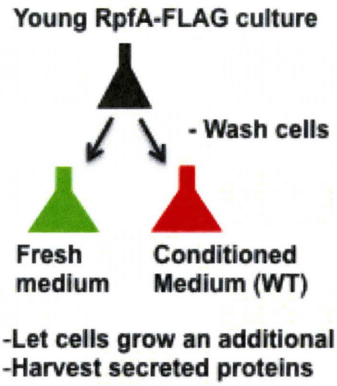
Young RpfA-FLAG culture
- Wash cells
Fresh medium
Conditioned Medium (WT)
-Let cells grow an additional 2 h
-Harvest secreted proteins

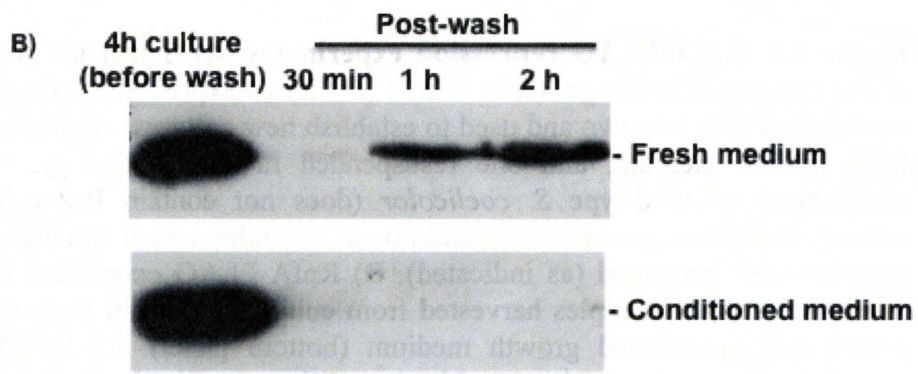
B)
4h culture (before wash)
Post-wash
30 min
1 h
2 h
- Fresh medium
- Conditioned medium

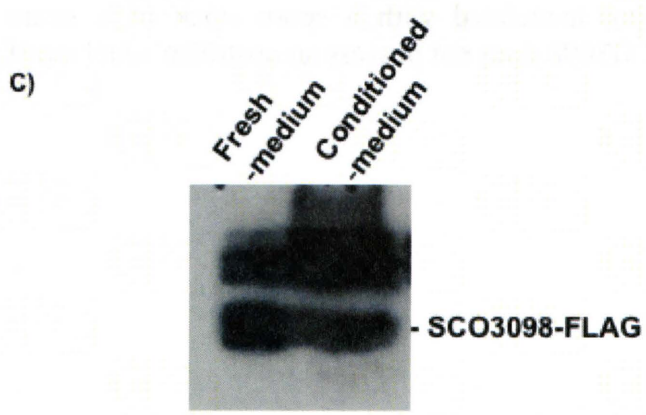
C)
Fresh -medium
Conditioned -medium
- SCO3098-FLAG

Figure 4.2. RpfA-FLAG repression experiment. A) Schematic representation of the experimental design. Cells from 4 h cultures expressing RpfA-FLAG were washed and split into two and used to establish new cultures – one resuspended in fresh growth medium, and one resuspended in conditioned growth medium conditioned by wild-type *S. coelicolor* (does not contain RpfA-FLAG). The cultures were then grown for an additional 2 h, after which samples of secreted proteins were harvested (as indicated). B) RpfA-FLAG expression detected via immunoblotting of samples harvested from cultures grown in fresh medium (top panel) and conditioned growth medium (bottom panel). C) SCO3098-FLAG expression detected via immunoblotting. Filter sterilized conditioned growth medium samples were inoculated with a spore stock of a strain expressing SCO3098-FLAG. SCO3098 does not possess an upstream *ydaO* motif.

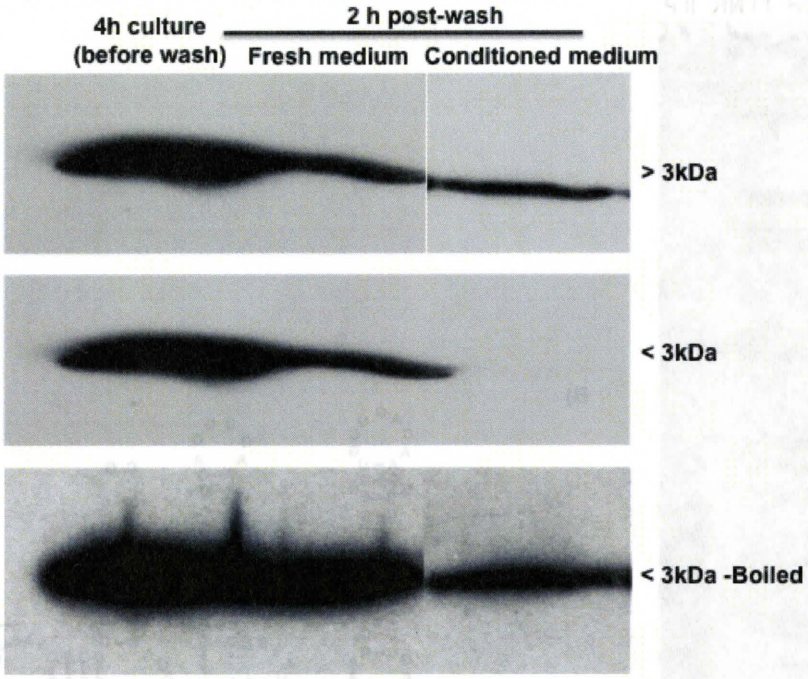

Figure 4.3. RpfA-FLAG is repressed by a heat-labile small molecule. Following the experimental design in Fig. 4.2A, RpfA-FLAG expression in the presence of fresh medium (middle column in all panels), and the >3 kDa fraction of conditioned medium (right column, top panel), the <3 kDa fraction of conditioned medium (right column, middle panel), and boiled conditioned medium (right column, bottom panel). The left column in all panels shows RpfA-FLAG expression in cells before the wash step.

Figure 4.4. A)

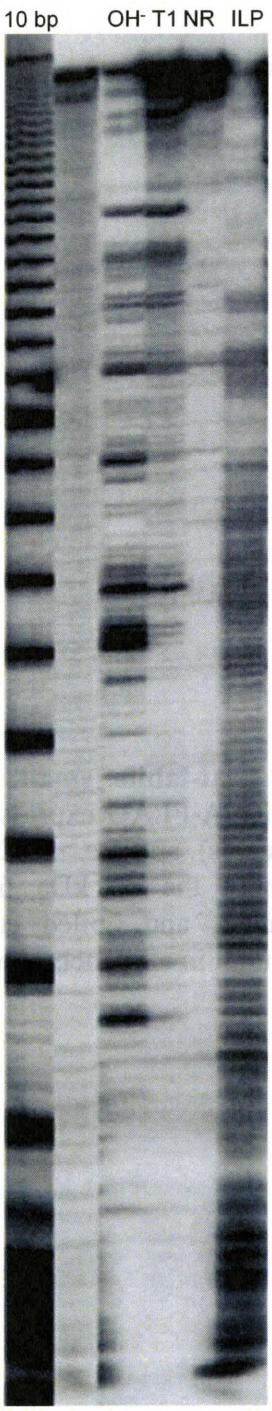

B)

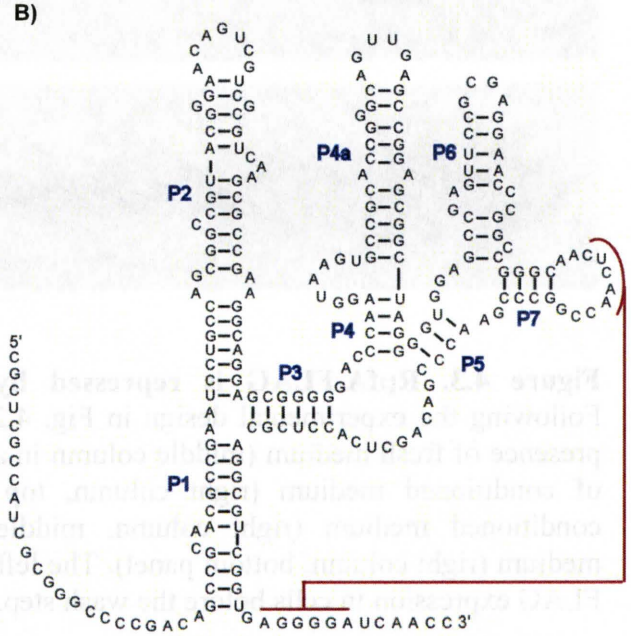

Figure 4.4. Secondary structure analysis of the *rpfA* 5' UTR. A) In-line probing experiment exploiting the differences in the rate of spontaneous cleavage between unpaired and structurally constrained ribonucleotides. 10 bp = 10 base-pair ladder; OH^- = sodium hydroxide treatment; T1 = RNase T1 cleavage (G residues); ILP = in-line probing reaction. B) The proposed secondary structure model for the *rpfA* 5' UTR, with stems indicated as "P*x*". The potential pairing between the P7-associated loop and the RpfA ribosome-binding site is indicated by the red line. (Note: figure modified from data provided by Dr. Mary Yousef)

Figure 4.5.

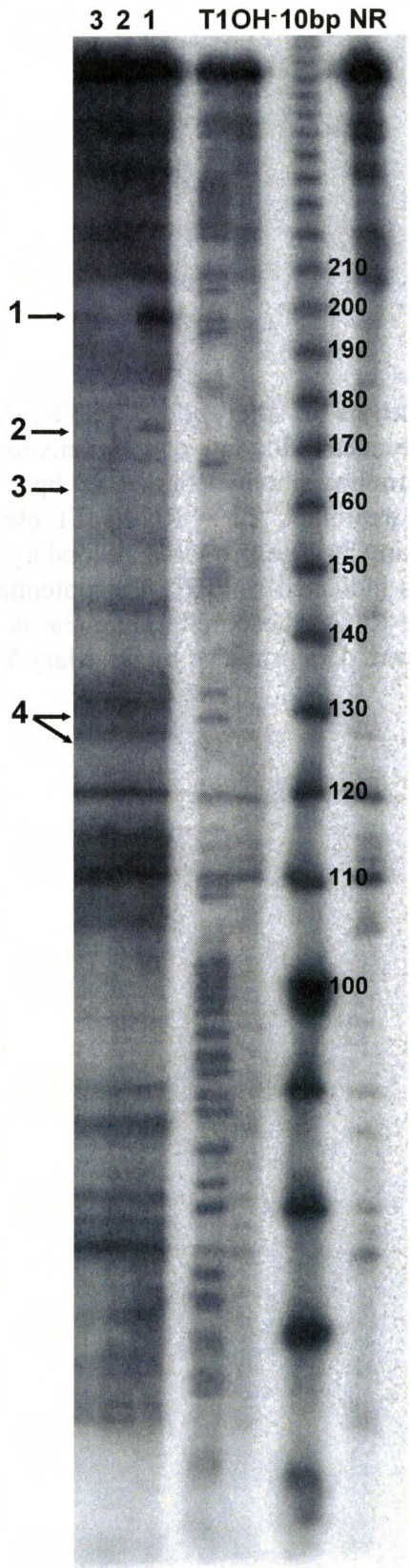
3 2 1
T1
OH-
10bp
NR
1
2
3
4
210
200
190
180
170
160
150
140
130
120
110
100

Figure 4.5. *rpfA* 5' UTR structural alterations in the presence of conditioned medium. An in-line probing experiment was carried out using RNA corresponding the *rpfA* 5' UTR in the absence of growth medium (lane 1), presence of fresh growth medium (lane 2), and presence of conditioned growth medium (lane 3). The numbered arrows on the left side indicate areas showing structural rearrangements in the presence of conditioned growth medium. All of these changes are between 110 and 201 nt in the proposed structure (Fig. 4.4B). 10 bp = 10 base-pair ladder; OH^- = sodium hydroxide treatment; T1 = RNase T1 cleavage (G residues).

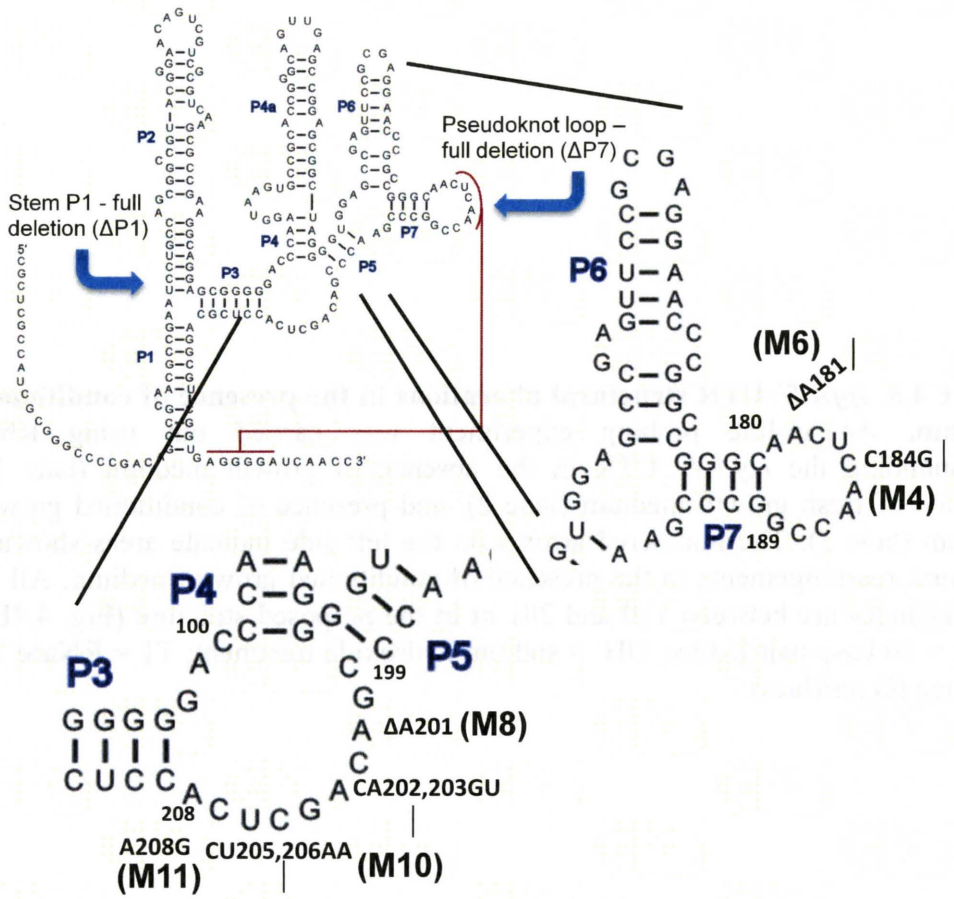

Figure 4.6. Schematic diagram highlighting areas of the *rpfA* 5' UTR subject to deletion/mutation analysis. M4 = C184G; M6 = ΔA181 + C184G; M8 = ΔA201; M10 = CA202,203GU + CU205,206AA; M11 = A208G.

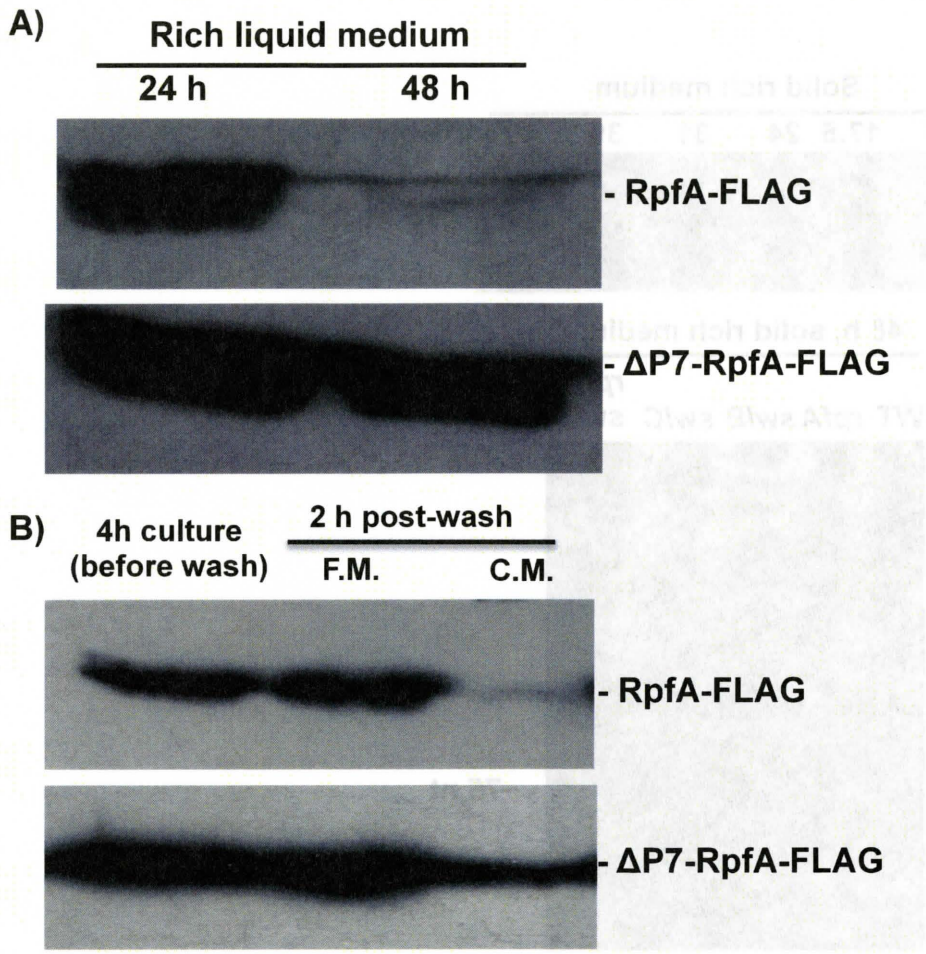

Figure 4.7. Expression analysis of P7 deletion strain. A) Time course experiment showing the immunoblot analysis of RpfA-FLAG (top panel), and ΔP7-RpfA-FLAG expression after 24 and 48 h (as indicated) B) Comparison of the effect of adding conditioned growth medium to the RpfA-FLAG strain and the ΔP7-RpfA-FLAG strain. The experimental protocol outlined in Fig. 2.2A was followed for this experiment. F.M. = fresh growth medium; C.M. = conditioned growth medium [wild-type]

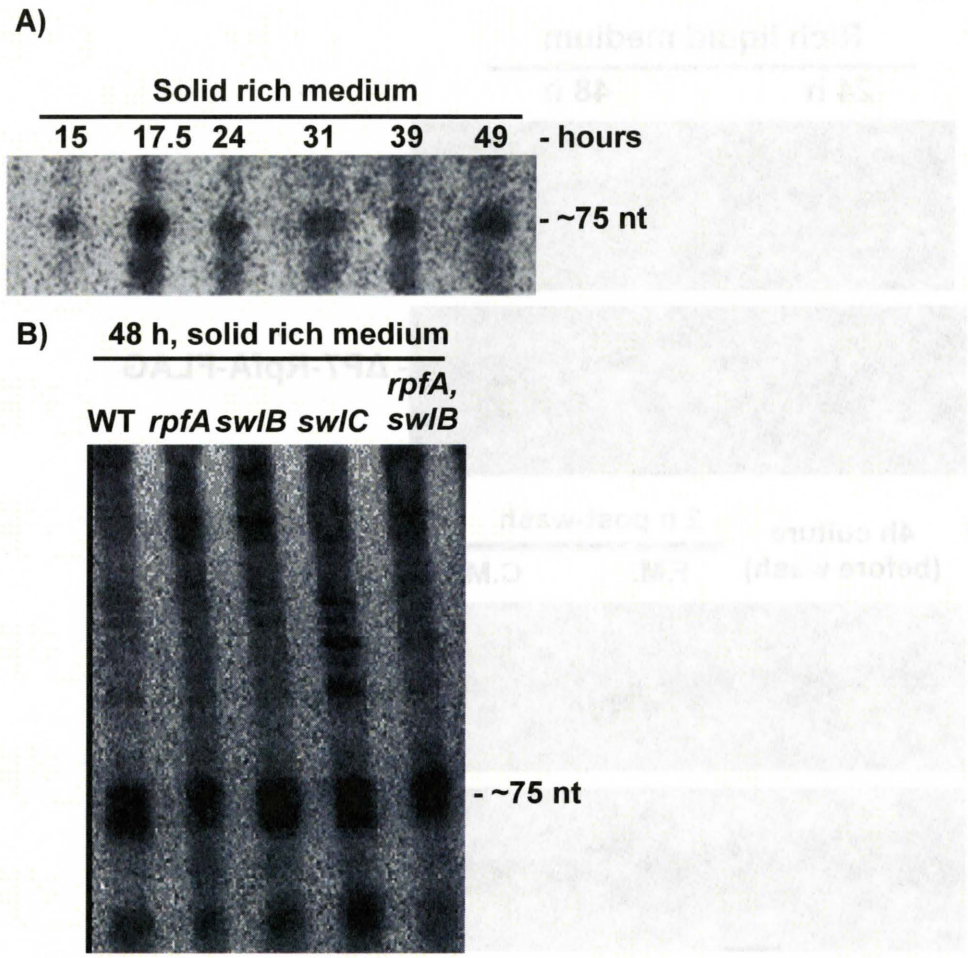

Figure 4.8. Northern blot analysis of *α-ydaO*. A) Total RNA was isolated from wild-type rich medium-grown cultures after the indicated periods of time. The RNA was separated on 6% polyacrylamide gels and was subjected to northern blotting using the oligonucleotide *α-ydaO* before being exposed to X-ray film. B) *α-ydaO* was detected as described in A) except that RNA from wild-type, and the indicated cell wall hydrolase deletion mutant strains were used. WT = wild-type.

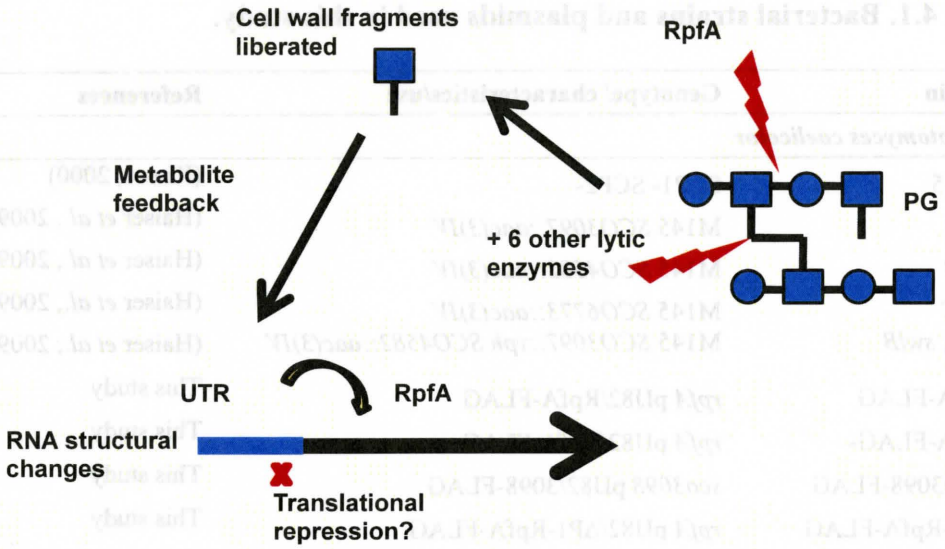

Figure 4.9. Proposed model for the riboswitch regulation for *rpfA*. A model for the interplay between all of the components contributing to riboswitch-regulation of *rpfA*. In this model, the translation of *rpfA* and six other cell wall hydrolase-encoding mRNAs are effectively translated. The associated gene-products cleave the cell wall peptidoglycan resulting in the release of peptidoglycan fragments (metabolites). The fragments, either directly or indirectly, feedback to the metabolite-sensing domain of the riboswitch, causing structural changes in the expression platform domain of the riboswitch. The regulatory consequence of this is translational repression through ribosome occlusion.

Table 4.1. Bacterial strains and plasmids used in this study.

Strain	Genotype/ characteristics/use	References
Streptomyces coelicolor		
M145	SCP1- SCP2-	(Kieser, 2000)
rpfA	M145 *SCO3097::aac(3)IV*	(Haiser *et al.*, 2009)
swlB	M145 *SCO4582::aac(3)IV*	(Haiser *et al.*, 2009)
swlC	M145 *SCO6773::aac(3)IV*	(Haiser *et al.*, 2009)
rpfA, swlB	M145 *SCO3097::vph SCO4582::aac(3)IV*	(Haiser *et al.*, 2009)
RpfA-FLAG	*rpfA* pIJ82/RpfA-FLAG	This study
RpfA-FLAG-SCO3098-FLAG	*rpfA* pIJ82/RpfA-FLAG-*sco3098* pIJ82/3098-FLAG	This study
ΔP1-RpfA-FLAG	*rpfA* pIJ82/ΔP1-RpfA-FLAG	This study
ΔP7-RpfA-FLAG	*rpfA* pIJ82/ΔP7-RpfA-FLAG	This study
M4-RpfA-FLAG	*rpfA* pIJ82/M4-RpfA-FLAG	This study
M6-RpfA-FLAG	*rpfA* pIJ82/M6-RpfA-FLAG	This study
M8-RpfA-FLAG	*rpfA* pIJ82/M8-RpfA-FLAG	This study
M10-RpfA-FLAG	*rpfA* pIJ82/M10-RpfA-FLAG	This study
M11-RpfA-FLAG	*rpfA* pIJ82/M11-RpfA-FLAG	This study
Escherichia coli		
DH5α	Used for routine cloning	
ET12567 (pUZ8002)	*dam-, dcm-*; with *trans*-mobilizing plasmid pUZ8002	(MacNeil *et al.*, 1992, Paget *et al.*, 1999a)
Plasmids		
pIJ82	pSET152 derivative, *aac(3)IV* replaced with *hyg* gene	Gift from H. Kieser
pBluescriptKS-	General cloning vector	(Alting-Mees and Short, 1989)
pBlue-RpfA-FLAG+	pBluescript + RpfA-3xFLAG	This study
pBlue-RpfA-FLAG-	pBluescript + RpfA-3xFLAG (minus 5' UTR)	This study

Table 4.2. Oligonucleotides used in this study.

	Sequence 5′ → 3′
Cloning of RpfA-FLAG and variants thereof	
*rpfA*UTR5'	CAGTACCCATGGCCATCGCGGGCCCCGACAGC
*rpfA*UTR3'	CAGTACCATATGTGATCCCCTCACCGACGC
3097PP5'	CAGTACCATATGGCCACCGCGTCCGAGTGGGAC
9798D	CGGTACGGATCCCACGAGCATCTCCTTCTTC
P1*rpfA*5'	CAGTACCCATGGGAATCCTGCCAGCGGCCG
P7*rpfA*5'	GTTCCGCGAGGAACCCGGCCGAACCCGACAGCTCACCTC
P7*rpfA*3'	GAGGTGAGCTGTCGGGTTCGGCCGGGTTCCTCGCGGAAC
M4*rpfA*5'	CCGGGCAACTGAACCGGCCC
M4*rpfA*3'	GGGCCGGTTCAGTTGCCCGG
M6*rpfA*5'	CCCGGCCGGGCACTGAACCGGCCCGAAC
M6*rpfA*3'	GTTCGGGCCGGTTCAGTGCCCGGCCGGG
M8*rpfA*5'	CCCGAACCCGCAGCTCACCTC
M8*rpfA*3'	GAGGTGAGCTGCGGGTTCGGG
M10*rpfA*5'	CCGAACCCGAGTGAACACCTCGCAG
M10*rpfA*3'	CTGCGAGGTGTTCACTCGGGTTCGG
M11*rpfA*5'	CCGACAGCTCGCCTCGCAGGC
M11*rpfA*3'	GCCTGCGAGGCGAGCTGTCGG
***In vitro* transcription**	
IVTrpfAUTR5'	TAATACGACTCACTATAGGGCGCTCGCCATCGCGGGCCC
IVTrpfAUTR3'	GGACGGACGACGGTGCTTGCCCTTGC

CHAPTER 5:
CONCLUSIONS AND FUTURE DIRECTIONS

With evidence continually mounting to show that small regulatory RNAs (sRNAs) play an important role in eukaryotic, as well as prokaryotic gene regulation, we hypothesized that sRNAs act as regulators in *Streptomyces coelicolor*. To begin testing this hypothesis, we conducted a cloning-based screen to identify novel sRNAs. This experiment revealed a population of stable tRNA cleavage products, along with an antisense RNA encoded on the strand opposite a predicted riboswitch regulatory element (the '*ydaO*' motif). We went on to determine that the cloned tRNAs represented a unique 'tRNA half' population, which appeared in a growth phase-dependent manner (Chapter 2). Following this work we shifted our focus to the riboswitch-associated cell wall hydrolases, and identified roles for these proteins in *Streptomyces* development (Chapter 3). Finally, we selected a representative cell wall hydrolase, RpfA, to begin addressing the hypothesis that its expression is controlled by a riboswitch regulatory element (Chapter 4).

5.1 CONTEXT AND FOUNDATIONS FOR FUTURE WORK

5.1.1 Small RNAs in *Streptomyces*

Following our initial identification of the tRNA halves, we discovered that cleavage resulting in these fragments occurred when cultures were propagated on minimal growth medium, but not rich medium. However, attempts to identify a nutrient component of the rich medium that effectively prevented cleavage were unsuccessful. While all tRNAs appeared to be susceptible to cleavage, there was a bias toward cleavage of tRNAs for more frequently used codons. We did not identify an enzyme responsible for carrying out tRNA cleavage, although we have some evidence suggesting that is unlikely to be the single stranded ribonuclease, RNase E. Finally, we observed a delay in tRNA cleavage in strains arrested in development before aerial hyphae formation, but not in those with a developmental block at the sporulation stage. Our discovery was followed by several other studies that indicated that tRNA cleavage was a widespread and conserved phenomenon in extremely divergent organisms. The two major outstanding questions concerning this work are: the identity of the ribonuclease that cleaves the tRNAs, and the biological consequences of tRNA cleavage. A thorough discussion of how our findings fit into the context of other works describing tRNA cleavage, and the prospects for future work in this area is presented in Chapter 2.

In 2008, we published a summary of our computational and direct cloning screens, along with the further characterization of some candidate sRNAs (Swiercz *et al.*, 2008). Coworkers Julia Swiercz and Hindra, who shared co-first authorship on the manuscript, carried out the majority of the downstream characterization. This work was only the second published investigation of

sRNAs in *S. coelicolor*, where the first was a largely computational screen that included experimental verification of sRNA expression for a small subset of their candidates (Panek *et al.*, 2008). Since the publication of these studies, sRNAs have been reported in additional actinomycetes, including *S. griseus* (Tezuka *et al.*, 2009) and *M. tuberculosis*, (Arnvig & Young, 2009). In an interesting comparison, Tezuka *et al.* (Tezuka *et al.*, 2009) showed that only one predicted sRNA overlapped between the three *Streptomyces* sRNA studies described above. This is probably a result of the fact that each group employed different bioinformatic search parameters, but it highlights the fact sRNA identification in *Streptomyces* is not yet saturated and there are likely many more candidates to be discovered.

In addition to the antisense RNA encoded on the opposite strand of the predicted *ydaO* riboswitch, our cloning-based screen also revealed an antisense RNA gene later renamed *α-abeA* (Hindra *et al.*, 2010). This sRNA is encoded on the opposite strand of the first gene in a four-gene operon; interestingly, overexpression of the operon led to an increase in antibiotic production (Hindra *et al.*, 2010). Careful characterization of the antisense RNA suggested that, unexpectedly, *α-abeA* did not appear to be involved in regulating the gene cluster. In a recent study involving another *cis*-encoded antisense RNA in *Streptomyces*, D'Alia *et al.* (2010) showed that overexpression of an sRNA encoded antisense to the glutamate synthase I gene prevented antibiotic production, and resulted in other physiological defects. This group also computationally predicted over 3,500 *cis*-encoded sRNAs in *S. coelicolor*, although they confirmed the expression of only 13 of these candidates (D'Alia *et al.*, 2010).

Genetic characterization of *α-ydaO* was hindered by unsuccessful attempts to map the promoter region, determine the precise size of the RNA, and construct deletion or overexpression strains (section 4.4.6). While we have been unable to assign a function to this RNA, its role in the regulation of *ydaO*-associated genes cannot be discounted at this point. Riboswitch regulation, coupled with a regulatory antisense RNA, would represent a completely novel and complex form of RNA regulation. Two recent discoveries highlight the complexity of riboswitch regulation. The first involves the Mg^{2+}-sensing riboswitch that regulates expression of the Mg^{2+} transporter encoded by the *mgtA* gene in *Salmonella* (Cromie *et al.*, 2006). When initially discovered, this system seemed to operate via a classic riboswitch mechanism: transcription of the *mgtA*-encoding transporter was regulated by the concentration of the metal that it transported (Mg^{2+}). However, a more recent discovery has added to the complexity of this system. In addition to sensing intracellular Mg^{2+}, the *mgtA* leader region also encodes a short proline-rich peptide (MgtL), the expression of which is controlled by intracellular proline concentrations. When proline is depleted, MgtL is not translated, causing an increase in *mgtA* expression (Park *et al.*, 2010). *mgtA* expression is thus controlled by two disparate signals, sensed in different ways within the same 'UTR'. Although the physiological significance of this is not yet understood, it highlights the regulatory potential contained within

leader regions. The second example involves the *S*-adenosyl methionine (SAM)-sensing riboswitch in *Listeria monocytogenes*, which controls the expression of two ABC-transporters (SreA and B). Analogous to the Mg^{2+}-sensing riboswitch, SAM binding causes transcriptional termination and thus prevents transporter expression. However, further investigation revealed that transcriptional termination generates a ~230 nt RNA fragment (the UTR portion of the transcript), which then functions as a *trans*-acting sRNA that represses the expression of the master virulence regulator PrfA (Loh *et al.*, 2009). This striking example of dual functionality by a regulatory RNA highlights the seemingly limitless complexity of these systems.

We cannot exclude the possibility that *α-ydaO* is the product of so-called 'transcriptional noise' or a degradation product thereof (as it was isolated only once in a direct cloning screen of total RNA). Over the last decade, abundant non-genic RNAs lacking any ascribed function have been expanding in RNA sequence databases (Huttenhofer *et al.*, 2005, Costa, 2007). Indeed, one study found that ~94% of the *Bacillus anthracis* genome is transcribed in at least one of growth conditions (Passalacqua *et al.*, 2009). These and other observations have fuelled debate over the functional relevance of these non-coding RNA transcripts. While some argue that these RNAs deserve robust characterization (Costa, 2007), others have suggested the low abundance of these transcripts might indicate that they may have a limited functional role (Babak *et al.*, 2005). A close examination of genetic context, use of target prediction programs, and detection using northern blotting will aid in evaluating the significance of these transcripts in future studies.

5.1.2 Is the *ydaO* motif a riboswitch regulatory element?

Our study aimed at identifying factors important for the regulation of the cell wall hydrolases began with end-mapping experiments, which confirmed the existence of extended leader transcripts at the 5' end of the hydrolase-encoding mRNAs. We further showed that conditioned growth medium represses the expression of at least one of the hydrolases, RpfA, but were unable to isolate the component responsible for this action. We examined the RNA secondary structure of the untranslated region (UTR) preceding the *rpfA* gene, and found that it folds into a structure having the potential for translational riboswitch-regulation, mediated by ribosome-binding site blockage. Finally, we identified a stem/loop structure within the riboswitch sequence that seems to be important for the response to conditioned growth medium.

Deciphering the role of the *ydaO* motif in controlling cell wall hydrolase expression in *S. coelicolor* is of significant interest. As a first step, it is important to obtain more robust evidence to support the hypothesis that repression is mediated by the *ydaO* motif in *S. coelicolor*. Work is in progress that will allow us to directly address this issue. We have placed the *rpfA* gene downstream of a constitutive promoter, both with and without the *ydaO* motif. The effect of conditioned growth medium on RpfA expression in these backgrounds should

effectively differentiate between regulation at the level of transcriptional initiation, versus post-transcriptional/translational. It should be noted that while our secondary structure model suggests translational level repression, the findings of Block *et al.* (2010), suggest that the *ydaO* motif acts at the level of transcriptional attenuation. This discrepancy is not unprecedented in riboswitch regulation, as the same B_{12}-sensing riboswitch that regulates the *btuB* gene at a transcriptional level in *Bacillus*, modulates translation initiation in Gram-negative bacteria (Nahvi *et al.*, 2004).

In addition to deciphering the regulatory mechanism exerted by the *ydaO* motif, future work should be aimed at identifying the specific component of spent medium that causes repression of RpfA. The approach taken during our preliminary chromatographic separation attempts (section 4.4.3) could be improved upon by taking advantage of the fact that riboswitches often function as part of autoregulatory loops. One way to accomplish this would be to create multi-fold deletion strains comprising combinations of the seven genes encoded downstream of the *ydaO* motif. Conditioned medium resulting from the growth of these strains could then be tested to see if they repress RpfA expression. In the event that such a strain fails to promote repression, LC/MS could be harnessed to compare the metabolite profile of this strain, with that of the wild-type strain. Obvious differences (e.g. a peak in the repressing fraction that is absent in the non-repressing fraction) could be exploited for further characterization using techniques such as electron spray ionization mass spectrometry, to identify the metabolite.

We chose to study the *ydaO* motif corresponding to *rpfA* as we had already established the biological significance of the cell wall hydrolase it encoded. In addition, its homolog in *Mycobacterium tuberculosis*, which is also preceded by a *ydaO* motif, is important for TB pathogenesis (Kana *et al.*, 2008, Russell-Goldman *et al.*, 2008). It will be important to test whether studies involving $ydaO_{Sc}$ can be extended to $ydaO_{Mtb}$. Efforts to do this have already been initiated through the creation of a strain in which $ydaO_{Sc}$ is replaced by $ydaO_{Mtb}$. Testing whether both motifs respond similarly to conditioned growth medium will be an important first step in assessing the widespread significance of our findings.

5.1.3 Cell wall hydrolases in *Streptomyces* development

An examination of the genetic context corresponding to *α-ydaO* revealed the association of this RNA with a predicted riboswitch regulatory element found upstream of multiple genes encoding cell wall hydrolase proteins. Intrigued by the fact that proteins of this type had not yet been studied in *S. coelicolor*, we systematically predicted the coding potential for cell wall hydrolases in this organism (section 3.4.1). Our analysis revealed an unprecedented number of putative cell wall hydrolases, reflecting the complex lifecycle of *S. coelicolor*. Our characterization of the riboswitch-associated cell wall hydrolases also included the first biochemical demonstration of PG cleavage capabilities for cell wall hydrolases in *S. coelicolor*. After creating and characterizing several cell

wall hydrolase deletion mutant strains, we determined that the spores of these strains were heat hypersensitive. A closer examination using electron microscopy revealed that the spores of all mutant stains had thinner spore walls compared to that of their parent strain. A more detailed look at development in each of the mutant strains revealed that at least two strains, *rpfA* and *swlA*, were slightly delayed in their ability to germinate. Moreover, the *swlB* strain exhibited defects in hyphal branching during vegetative growth. Transcriptional profiling complemented our phenotypic analyses, and revealed variable patterns of expression for the riboswitch-associated hydrolases. Additional investigation in this area will undoubtedly fill in some of the gaps in *Streptomyces* cell biology, especially those studies focusing on hydrolase localization.

Largely owing to advances in fluorescence microscopy, we are beginning to understand the elegant coordination of events during growth and cell division in bacteria (Margolin, 2009). The fundamental importance of cell wall hydrolases in these processes has already been established in previous sections. During *Streptomyces* exospore formation, cell wall hydrolases would be required for cell division, spore maturation, and spore separation/release. All four of the mutant strains we constructed (*rpfA*, *swlA*, *swlB*, and *swlC*) possessed sporulation defects, manifested as heat sensitivity, abnormal spore morphology, and thinner spore walls in comparison to that of the wild-type strain. An important and outstanding question is how these enzymes are temporally and spatially localized. As already discussed in Chapter 3, some likely candidates for coordinating cell wall hydrolases during sporulation include the Mre, and Ssg proteins. A recent study highlighted the utility of two-hybrid interaction, as multiple binding partners were found the Mre proteins, including proteins involved in cell wall biosynthesis (Kleinschnitz *et al.*, 2011). Furthermore, the combined use of genetic, biochemical, and fluorescence microscopy-based studies, has also advanced our understanding of the Ssg proteins, and how they coordinate cell division during sporulation (Willemse *et al.*, 2011). The techniques presented in these studies are highly applicable to further characterizing the role of cell wall hydrolases in *S. coelicolor* cell biology.

APPENDIX

Table 6.1. Complete list of cloned RNA fragments.

tRNA	Sequence (5' to 3')
3'His GTG	TCCAGGATGCCGCGGGTTCAAGTCCCGTCACTCACCCC
	TCCAGGATGCCGCGGGTTCAAGTCCCGTCACTCACCCC
	TCCAGGATGCCGCGGGTTCAAGTCCCGTCACTCACCCC
	TCCAGGATGCCGCGGGTTCAAGTCCCGTCACTCACCCC
	TCCAGGATGCCGCGGGTTCAAGTCCCGTCACTCACCCC
	TCCAGGATGCCGCGGGTTCAAGTCCCGTCACTCACCCC
	TCCAGGATGCCGCGGGTTCAAGTCCCGTCACTCACCCC
	TCCAGGATGCCGCGGGTTCAAGTCCCGTCACTCACCCC
	TCCAGGATGCCGCGGGTTCAAGTCCCGTCACTCACCCC
	TCCAGGATGCCGCGGGTTCAAGTCCCGTCACTCACCCC
	TCCAGGATGCCGCGGGTTCAAGTCCCGTCACTCACCCC
	TCCAGGATGCCGCGGGTTCAAGTCCCGTCACTCA
	GTCCAGAATGCCGCGGGTTCAAGTCCCGTCACTCACCCC
	GTCCAGGATGCCGCGGGTTCAAGTCCCGTCACTCACCCC
	GTCCAGGATGCCGCGGGTTCAAGTCCCGTCACTCACCC
	TCCAGGATGCCGCGGGTTCAAGTCCCGTCACTCACCC
	TCCAGGATGCCGCGGGTTCAAGTCCCGTCACTCACCC
	TCCAGGATGCCGCGGGTTCAAGTCCCGTCACTCACCC
	TCCAGGATGCCGCGGGTTCAAGTCCCGTCACTCACCC
	GTCCAGGATGCCGCGGGTTCAAGTCCCGTCACTCACCC
	TCCAGGATGCCGCGG-GTTCAAGTCCCGTCACTCACCCC
	TCCAGGATGCCGCGG-GTTCAAGTCCCGTCACTCACCCC
	TCCAGGATGCCGCGG-GTTCAAGTCCCGTCACTCACCCC
	TCCAGGATGCCGCGG-GTTCAAGTCCCGTCACTCACCCC
	TCCAGGATGCCGCGG-GTTCAAGTCCCGTCACTCACCCC
	TCCAGGATGCCGCGG-GTTCAAGTCCCGTCACTCACCCC
	TCCAGGATGCCGCGG-GTTCAAGTCCCGTCACTCACCCC
	TCCAGGATGCCGCGG-GTTCAAGTCCCGTCACTCACCCC
	TCCAGGATGCCGCGG-GTTCAAGTCCCGTCACTCACCCC
	TCCAGGATGCCGCGG-GTTCAAGTCCCGTCACTCACCCC
	GTCCAGGATGCCGCGG-GTTCAAGTCCCGTCACTCACCC
	TCCAGGATGCCGCGG-GTTCAAGTCCCGTCACTCACCC
	TTCAGGATGCCGCGG-GTTCAAGTCCCGTCACTCACCCC
	TACAGGATGCCGCGG-GTTCAAGTCCCATCACTCACCC
	TCCAGGATGCCGCGG-GTTCAAGTCCCGTCACTCACTT
	TCCAGGATGCGGGGG-GTTCAATTCCGTTCATTCACCC
5'Met CAT	CGCGGGGTGGAGCAGCTCGGTAGCTCGCTGGGCT
	CGCGGGGTGGAGCAGCTCGGTAGCTCGCTGG
	CGCGGGGTGGAGCAGCTCGGTAGCTCGCTGGGCT
	CGCGGGGTGGAGCAGCTCGGTAGCTCGCTGGGC
	CGCGGGGTGGAGCAGCTCGGTAGCTCGCTGGGC
	CGCGGGGTGGAGCAGCTCGGTAGCTCGCTGGGC
	CGCGGGGTGGAGCAGCTCGGTAGCTCGCTGGGC
	CGCGGGGTGGAGCAGCTCGGTAGCTCGCTGGGC

CGCGGGGTGGAGCAGCTCGGTAGCTCGCTGGGC
CGCGGGGTGGAGCAGCTCGGTAGCTCGCTGGGC
GCGGGGTGGAGCAGCTCGGTAGCTCGCTGGGC
CGCGGGGTGGAGCAGCTCGGTAGATCGCTGGGCT
CGCGGGGTGGAGCAGCTCGGTAGCTCGCTGGGCT
GCGGGGTGGAGCAGCTCGGTAGCTCGCTGGGCT
GCGGGGTGGAGCAGCTCGGTAGCTCGCTGGGCT
GCGGGGTGGAGCAGCTCGGTAGCTCGCTGGGC
GCGGGGTGGAGCAGCTCGGTAGCTCGCTGGGC
GCGGGGTGGAGCAGCTCGGTAGCTCGCTGGGCT
GCGGGGTGGAGCAGCTCGGTAGCTCGCTGGGCT
CGCGGGGTGGAGCAGCTCGGTAGCTCGCTGGGCT
CGCGGGGTGGAGCAGCTCGGTAGCTCGCTGGGCT
GCGGGGTGGAGCAGCTCGGTAGCTCGCTGGGC
GCGGGGTGGAGCAGCTCGGTAGCTCGCTGGGC
CGCGGGGTGGAGCAGCTCGGTAGCTCGCTGGGC
CGCGGGGTGGAGCAGCTCGGTAGCTCGCTGGGC
CGCGGGGTGGAGCAGCTCGGTAGCTCGCTGGGC
CGCGGGGTGGAGCAGCTCGGTAGCTCGCTGGGCG
CGCGGGGTGGAGCAGCTCGGTAGCTCGCTGG
CGCGGGGTGGAGCAGCTCGGTAGCTCGCTGG
GCGAGGTGGAGCAGCTCGGTAGCTCGCTGGGCT
CGCGGGGTGGAGCAGCTCGGTAGCTCGCCGGGCT
CGCGGGGGGGGAGCACCTCGGTAGCTCGCTGGGCT
CGCGGGGGGGGAGCAGCTCGGTAGCTCGCTGGACT
GCGGGGTGGAACAACTCCGTAACTCCCTGGGGTC

3'Asn GTT ACCGGCAGGTTACTG-GTTCGAGTCCAGTCGGGGGAGC
CGGCAGGTTACTG-GTTCGAGTCCAGTCGGGGGAGC
CGGCAGGTTACTG-GTTCGAGTCCAGTCGGGGGA
CGGCAGGTTACTG-GTTCGAGTCCAGTCGGGGGAGCC
CGGCAGGTTACTG-GTTCGAGTCCAGTCGGGGGAGCC
CGGCAGGTTACTG-GTTCGAGTCCAGTCGGGGG
CGGCAGGTTACTG-GTTCGAGTCCAGTCGGGG
CGGCAGGTTACTG-GTTCGAGTCCAGTCCGGGGAGC
CGGCAGGTTACTG-GTTCGAGTCCAGTCCGGGGAGC
CGGCAGGTTACTG-GTTCGAGTCCTGTCGGGGGAGCC
CATGCAGGTTACTG-GTTCGAGTCCAGTCGGGGGAGCC
GCAGGTTACTG-GTTCGTGTCCAGTCCGGGGAGCCA
CGGCAGGTTAGTGGTTAGAGTCCAGTCCGGGG
CCGGCAGGTTACTGGTTCGAGTCCAGTCGGGG
CCGGCAGGTTACTGGTTCGAGTCCAGTCGGGGGAGC
CGGCAGGTTACTGGTTCGAGTCCAGTCGGGG
CGGCAGGTTACTGGTTCGAGTCCAGTCGGGGGAGC
CGGCAGGTTACTGGTTCGAGTCCAGTCGGGGG
CGGCAGGTTACTGGTTCGAGTCCAGTCGGGGG
CGGCAGGTTACTGGTTCGAGTCCGGTCGGGGG
CAGGTTACTGGTTCGAGTCCAGTCCGGGGAGCCA
GCAGGTTACTGGTTCGAGTCCAGTCCGGGGAGCCA
TGGCAGGTTACTGGTTTGAGTCCAGTCCGGGGAGC

5'Ser TGA	GGTGGGTTGCCCGAGCGGCCTAAGGGAACGGTC
	GGTGGGTTGCCCGAGCGGCCTAAGGGAACGGTCT
	GGTGGGTTGCCCGAGCGGCCTAAGGGAACGGTC
	GGTGGGTTGCCCGAGCGGCCTAAGGGAACGGTC
	GGTGGGTTGCCCGAGCGGCCTAAGGGAACGGTC
	GGTGGGTTGCCCGAGCGGCCTAAGGGAACGGTC
	GGTGGGTTGCCCGAGCGGCCTAAGGGAACGGTC
	GGTGGGTTGCCCGAGCGGCCTAAGGGAACGGTC
	GGTGGGTTGCCCGAGCGGCCTAAGGGAACGGTC
	GGCGGGTTGCCCGAGCGGCCTAAGGGAACGGTCT
	GGTGGGTGGACCGACCGGCCTACTGGATCGGTC
	GGTGGGTGGCCGGAGCGGCTTAAGGAAACGTTC
	GGTGGGTTGCCCGAGCGGCCTAAGGGAACGGTC
	GGTGGGTTGCCCGAGCGGCCTAAGGGAACGGTC
	GGTGGGTTGCCCGAGCGGCCTAAGGGAACGGTC
	GGTGGGTTGCCCGAGCGGCCTAAGGGAACGGTC
	GGTGGGTTGCCCGAGCGGCCTAAGGGAACGGTC
	GGTGGGTTGCCCGAGCGGCCTAAGGGAACGGTC
	GGTGGGTTGCCCGAGCGGCCTAAGGGAACGGTC
	GGTGGGTTGCCCGAGCGGCCTAGGGGAACGGTC
5'His GTG	GGTGGGTGTAGCTCAGCTGGTAGAGCACCTGGTTGT
	GGTGGGTGTAGCTCAGCTGGTAGAGCACCTGGTT
	GGTGGGTGTAGCTCAGCTGGTAGAGCACCTGGTT
	GGTGGGTGTAGCTCAGCTGGTAGAGCACCTCGTTGT
	GGTGGGTGTAGCTCAGCTGGTAGAGCACCTGGT
	GGTGGGTGCAGCTCAGCTGGTAGAGCACCTGGTT
	GGTGGGTGTAGCTCAGC-TGGTAGAGCACCTGGTT
	GGTGGGTGTAGCTCAGC-TGGTAGAGCACCTGGTT
	GGTGGGTGTAGCTCAGC-TGGTAGAGCACCTGGTT
	GGTGGGTGTAGCTCAGC-TGGTAGAGCACCTGGTT
	GGTGGGTGTAGCTCAGC-TGGTAGAGCACCTGGT
	GGTGGGTGTAGCTCAGC-TGGTAGAGCACCTGGT
	GGTGGGGGTAGCGGATC-TGGTACAGCACGGGGA
5'Gln CTG	TGGCCTATGGTGTAATTGGCAGCACGACTG
	TGGCCTATGGTGTAATTGGCAGCACGACTGATT
	TGGCCTATGGTGTAATTGGCAGCACGACT
	TGGCCTATGGTGTA-ATTGGCAGCACGACTGATT
	TGGCCTATGGTGTA-ATTGGCAGCACGACTGATT
	TGGCCTATGGTGTA-ATTGGCAGCACGACTGAT
	TGGCCTATGGTGTA-ATTGGCAGCACGACTGA
	TGGCCTATGGTGTA-ATTGGCAGCACGACT
	TGGCCTATGGTGTA-ATTGGCAGCACGAC
3'Arg CCT	AAGCGGGTGTCGCAG-GTTCGAATCCTGCCGGGGGC
	AAGCGGGTGTCGCAG-GTTCGAATCCTGCCGGGGGCACC
	AGCGGGTGTCGCAG-GTTCGAATCCTGCCGGGGGC
	AGCGGGTGTCGCAG-GTTCGAATCCTGCCGGGGGC
	AAAGCGGGTGTCGCAG-GTTCGAATCCTGCCGGGG

	TAAAGCGGGTGTCGCAG-GTTCGAATCCTGCCGG
	AGCGGGTGTCGCAGGTTCGAATCCTGCCGGGGGC
	AAGCGGGTGTCGCAGGTTCGAATCCTGCCGGGGGC
5'Leu GAG	CGGGTGGCGGA-AT-GGCAGACGTGCTAGCTTGA
	CGGGTGGCGGA-AT-GGCAGACGTGCTAGCTTGA
	GTCCGGGTGGCGGA-AT-GGCAGACGCGCTAGCTT
	CCGGGTGGCGTA-AT-GGCAGACGCGCTA
	GTCCGGGTGGCGGAATGGCAGACGCGCTAGCTT
	GTCCGGGTGGCGGAATGGCAGACGCGCTAGCTT
5'Pro CGG	CGGGGTGTGGCGCAGCTTGGTAGCGCGCTTCGTT
	CGGGGTGTGGCGCAGCTTGGTAGCGCGCTTCGTT
	CGGGGTGTGGCGCAGCTTGGTAGCGCGCTTCGTT
	CGGGGTGTGGCGCAGCTTGGTAGCGCGCTTCGTT
	CGGGGTGTGGCGCAGCTTGGTAGCGCGCGTCGTTCGC
	CGGGGTGTGGCGCAGCCTGGTAGCGCACTCTGT
3'Glu CTC	AGGCGGTAGCGCCGGTTCGATTCCGGTCGGGGGTAC
	AGGCGGTAGCGCCGGTTCG--TCCGGTCGGGGGTA
	GGTAGCGCCGGTTAGAATCCGGTCGGGGGTGCCA
3'Thr GGT	GGAGAAGGTCAACG-GTTCGATTCCGTTTTGGGGCTC
	GGAGAAGGTCAACG-GTTCGTTTCCGTTTGGGGGCT
3'Glu TTC	AGGCGGTAGCACGGGTTCGAGTCCCGTTGGGGGCTC
	AGGCGGTAGCACGGGTTCGAATCCCGTTGGGGGCA
3'Val CAC	CCGAAGAGGTCACTGGTTCGAACCCAGTATCGCCCACC
	CACACCGAAGAGGTCACTG-GTTCGAATCCAGTATCGCCC
5'Leu TAG	GCGGCC-GTGGTGGA-ATTGGCAGTCACGCTG
5'Gly GCC	GCGGACGTAACTCA-CTTGGTAGAGCGCAACCTTGC
5'Leu CAG	AAGCGGGTGGCGGA-ATAGGCAAACGCGCTGG
5'Phe GAA	GGGTGGGTAGCTCAGTTGGTACGACCGATCGCCT
3'Lys CTT	ATCAGCGGGT--CCGGG-GTTCGAGTCCCTGGCGGCGCACC
Gly GCC??	*GGGGAAGGCGCAGTGTGCAATTCCTGTCACCCGCTCCA*
(no good match)	*GGGGAAGGCGCAGTGTGCAATTCCTGTCACCCGCTCCA*
	GGGGAAGGCGCAGTGTGCAATTCCTGTCACCCGCTCCA
	GGGGAAGGCGCAGTGTGCAATTCCTGTCACCCGCTGCA
	CAAGGTTGAGGTCGCGAGTTCGAGCCTCGTCGTCCG
	GCGGACGTAGCTCAGTTGGTAGAGCGCAACCTTGC
	GCGAACGTAGCTCAGTTGGTAGAGCGCAACCTTGC

Figure 6.1.

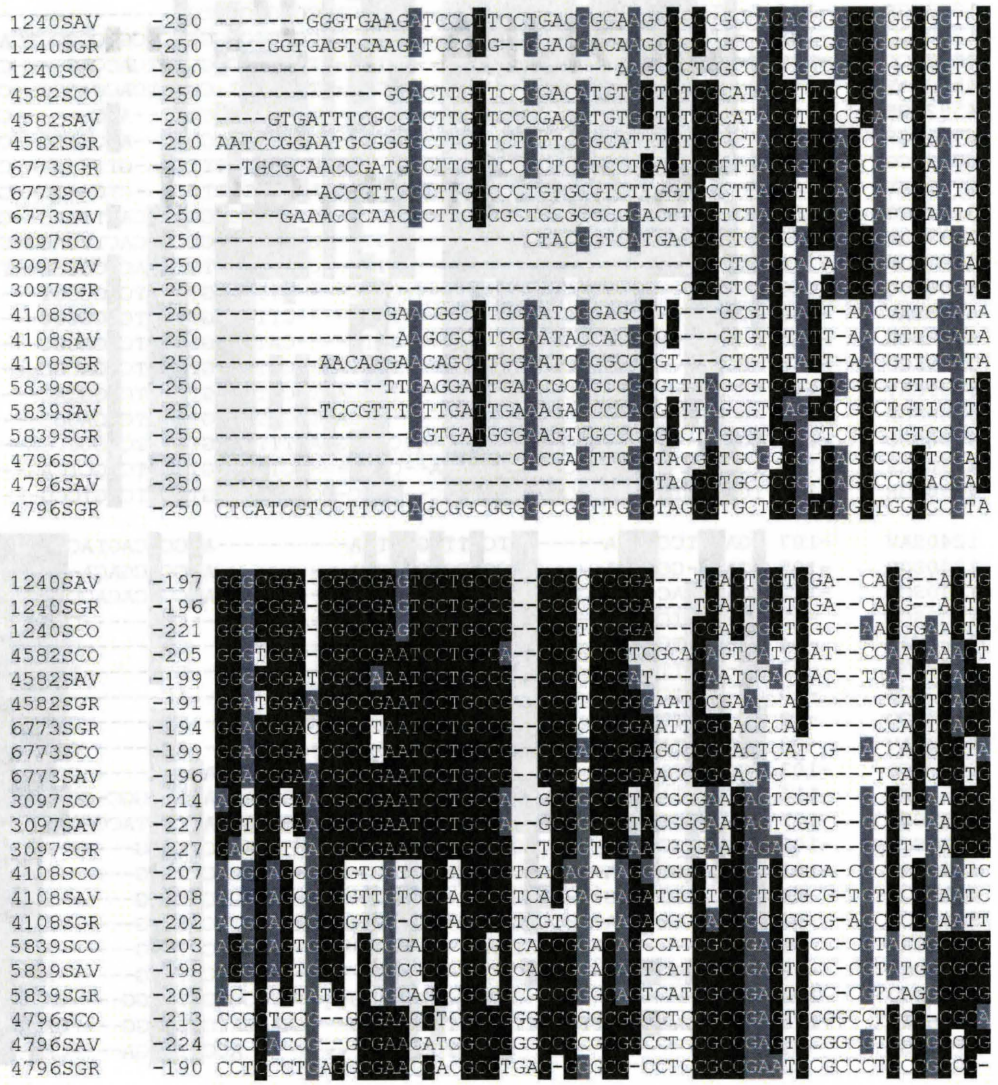
1240SAV -250
1240SGR -250
1240SCO -250
4582SCO -250
4582SAV -250
4582SGR -250
6773SGR -250
6773SCO -250
6773SAV -250
3097SCO -250
3097SAV -250
3097SGR -250
4108SCO -250
4108SAV -250
4108SGR -250
5839SCO -250
5839SAV -250
5839SGR -250
4796SCO -250
4796SAV -250
4796SGR -250
1240SAV -197
1240SGR -196
1240SCO -221
4582SCO -205
4582SAV -199
4582SGR -191
6773SGR -194
6773SCO -199
6773SAV -196
3097SCO -214
3097SAV -227
3097SGR -227
4108SCO -207
4108SAV -208
4108SGR -202
5839SCO -203
5839SAV -198
5839SGR -205
4796SCO -213
4796SAV -224
4796SGR -190

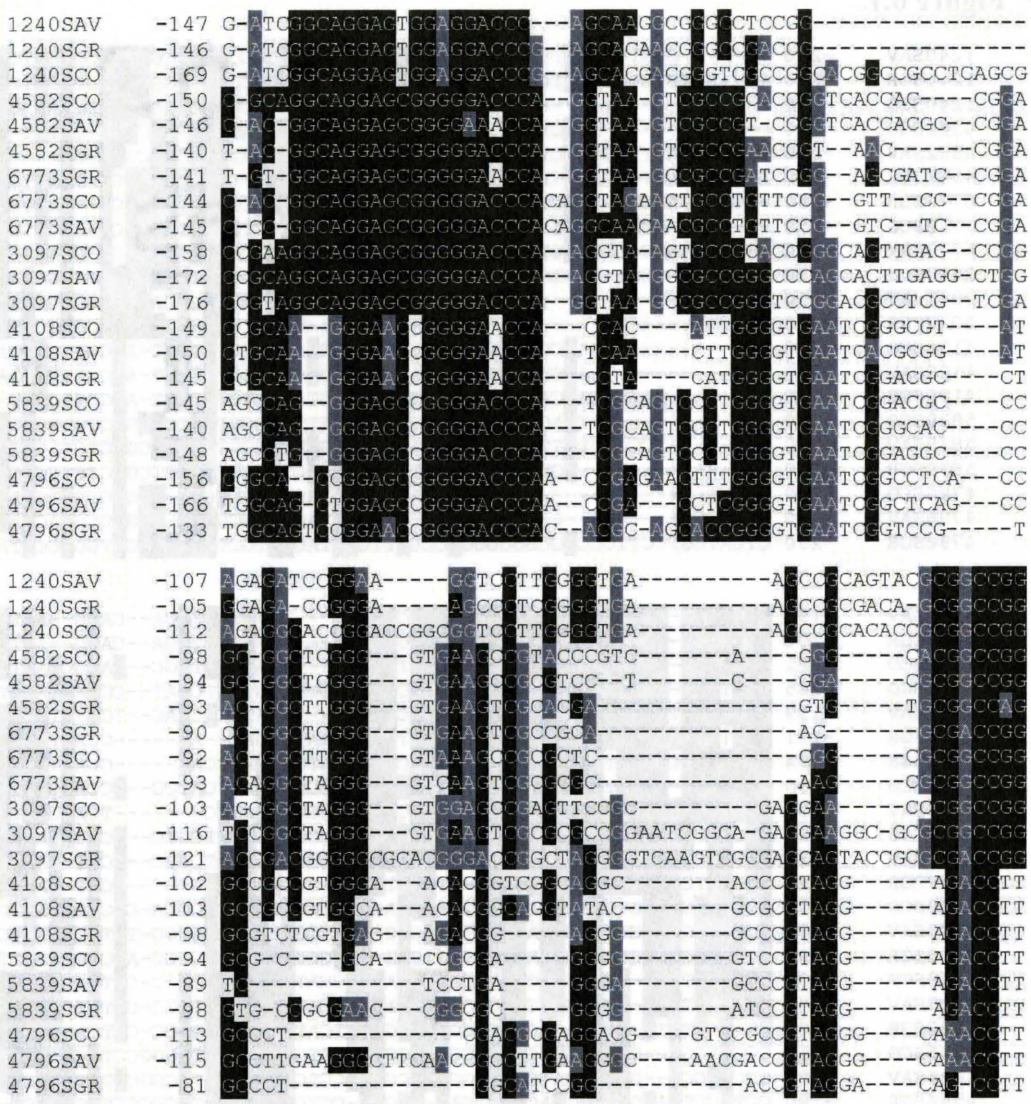

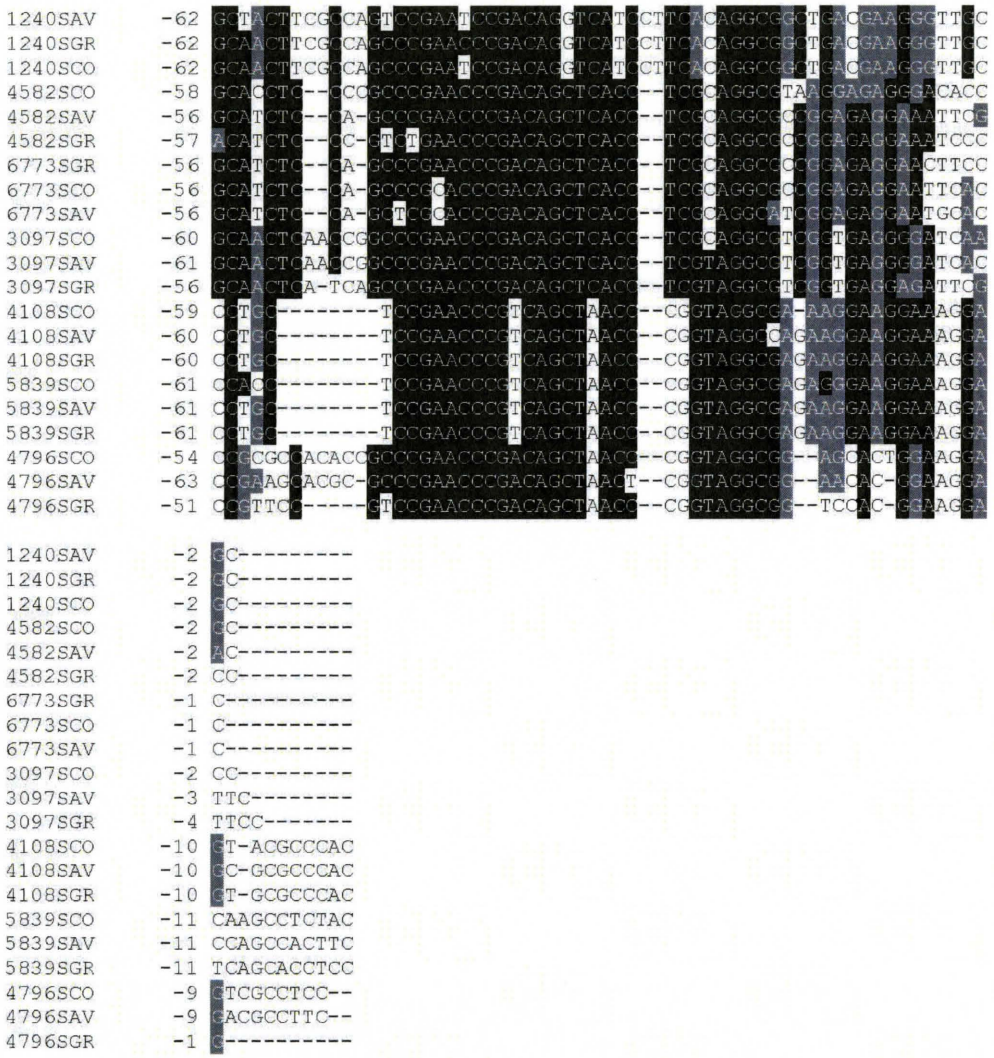

Figure 6.1. Alignment of upstream non-coding sequences for seven putative cell wall hydrolases in multiple *Streptomyces* species. Multiple sequence alignment of the predicted untranslated regions of the seven hydrolase-encoding genes in *S. coelicolor*, and the orthologous genes from the closely related *S. avermitilis*, and *S. griseus*. Identical nucleotides are indicated in black, while similar nucleotides (purines versus pyrimidines) are shaded in grey.

REFERENCES

Alting-Mees, M. A. & J. M. Short, (1989) pBluescript II: gene mapping vectors. *Nucleic Acids Res* **17**: 1.

Altschul, S. F., W. Gish, W. Miller, E. W. Myers & D. J. Lipman, (1990) Basic local alignment search tool. *J Mol Biol* **215**: 403-410.

Amano, K., H. Hayashi, Y. Araki & E. Ito, (1977) The action of lysozyme on peptidoglycan with *N*-unsubstituted glucosamine residues. Isolation of glycan fragments and their susceptibility to lysozyme. *Eur J Biochem* **76**: 299-307.

Anantharaman, V. & L. Aravind, (2003) Evolutionary history, structural features and biochemical diversity of the NlpC/P60 superfamily of enzymes. *Genome Biol* **4**: R11.

Araki, Y., T. Nakatani, H. Hayashi & E. Ito, (1971) Occurrence of non-*N*-substituted glucosamine residues in lysozyme-resistant peptidoglycan from *Bacillus cereus* cell walls. *Biochem Biophys Res Commun* **42**: 691-697.

Aravin, A. A., M. Lagos-Quintana, A. Yalcin, M. Zavolan, D. Marks, B. Snyder, T. Gaasterland, J. Meyer & T. Tuschl, (2003) The small RNA profile during *Drosophila melanogaster* development. *Dev Cell* **5**: 337-350.

Argaman, L., R. Hershberg, J. Vogel, G. Bejerano, E. G. Wagner, H. Margalit & S. Altuvia, (2001) Novel small RNA-encoding genes in the intergenic regions of *Escherichia coli*. *Curr Biol* **11**: 941-950.

Arnvig, K. B. & D. B. Young, (2009) Identification of small RNAs in *Mycobacterium tuberculosis*. *Mol Microbiol* **73**: 397-408.

Atrih, A. & S. J. Foster, (1999) The role of peptidoglycan structure and structural dynamics during endospore dormancy and germination. *Antonie Van Leeuwenhoek* **75**: 299-307.

Babak, T., B. J. Blencowe & T. R. Hughes, (2005) A systematic search for new mammalian noncoding RNAs indicates little conserved intergenic transcription. *BMC Genomics* **6**: 104.

Barnard, A., A. Wolfe & S. Busby, (2004) Regulation at complex bacterial promoters: how bacteria use different promoter organizations to produce different regulatory outcomes. *Curr Opin Microbiol* **7**: 102-108.

Barreteau, H., A. Kovac, A. Boniface, M. Sova, S. Gobec & D. Blanot, (2008) Cytoplasmic steps of peptidoglycan biosynthesis. *FEMS Microbiol Rev* **32**: 168-207.

Barrick, J. E. & R. R. Breaker, (2007) The distributions, mechanisms, and structures of metabolite-binding riboswitches. *Genome Biol* **8**: R239.

Barrick, J. E., K. A. Corbino, W. C. Winkler, A. Nahvi, M. Mandal, J. Collins, M. Lee, A. Roth, N. Sudarsan, I. Jona, J. K. Wickiser & R. R. Breaker, (2004) New RNA motifs suggest an expanded scope for riboswitches in bacterial genetic control. *Proc Natl Acad Sci U S A* **101**: 6421-6426.

Barry, C. E., 3rd, H. I. Boshoff, V. Dartois, T. Dick, S. Ehrt, J. Flynn, D. Schnappinger, R. J. Wilkinson & D. Young, (2009) The spectrum of latent tuberculosis: rethinking the biology and intervention strategies. *Nat Rev Microbiol* **7**: 845-855.

Bateman, A., E. Birney, R. Durbin, S. R. Eddy, K. L. Howe & E. L. Sonnhammer, (2000) The Pfam protein families database. *Nucleic Acids Res* **28**: 263-266.

Bendtsen, J. D., H. Nielsen, G. von Heijne & S. Brunak, (2004) Improved prediction of signal peptides: SignalP 3.0. *J Mol Biol* **340**: 783-795.

Bentley, S. D., K. F. Chater, A. M. Cerdeno-Tarraga, G. L. Challis, N. R. Thomson, K. D. James, D. E. Harris, M. A. Quail, H. Kieser, D. Harper, A. Bateman, S. Brown, G. Chandra, C. W. Chen, M. Collins, A. Cronin, A. Fraser, A. Goble, J. Hidalgo, T. Hornsby, S. Howarth, C. H. Huang, T. Kieser, L. Larke, L. Murphy, K. Oliver, S. O'Neil, E. Rabbinowitsch, M. A. Rajandream, K. Rutherford, S. Rutter, K. Seeger, D. Saunders, S. Sharp, R. Squares, S. Squares, K. Taylor, T. Warren, A. Wietzorrek, J. Woodward, B. G. Barrell, J. Parkhill & D. A. Hopwood, (2002) Complete genome sequence of the model actinomycete *Streptomyces coelicolor* A3(2). *Nature* **417**: 141-147.

Bernhardt, T. G. & P. A. J. de Boer, (2003) The *Escherichia coli* amidase AmiC is a periplasmic septal ring component exported via the twin-arginine transport pathway. *Mol Microbiol* **48**: 1171-1182.

Beveridge, T. J., (1990) Mechanism of gram variability in select bacteria. *J Bacteriol* **172**: 1609-1620.

Bilgin, N., A. A. Richter, M. Ehrenberg, A. E. Dahlberg & C. G. Kurland, (1990) Ribosomal RNA and protein mutants resistant to spectinomycin. *EMBO J* **9**: 735-739.

Block, K. F., M. C. Hammond & R. R. Breaker, (2010) Evidence for widespread gene control function by the *ydaO* riboswitch candidate. *J Bacteriol* **192**: 3983-3989.

Blouin, S., R. Chinnappan & D. A. Lafontaine, (2010) Folding of the lysine riboswitch: importance of peripheral elements for transcriptional regulation. *Nucleic Acids Res.*

Boch, J., G. Nau-Wagner, S. Kneip & E. Bremer, (1997) Glycine betaine aldehyde dehydrogenase from *Bacillus subtilis*: characterization of an enzyme required for the synthesis of the osmoprotectant glycine betaine. *Arch Microbiol* **168**: 282-289.

Bouhss, A., A. E. Trunkfield, T. D. Bugg & D. Mengin-Lecreulx, (2008) The biosynthesis of peptidoglycan lipid-linked intermediates. *FEMS Microbiol Rev* **32**: 208-233.

Bradford, M. M., (1976) A rapid and sensitive method for the quantitation of microgram quantities of protein utilizing the principle of protein-dye binding. *Anal Biochem* **72**: 248-254.

Brun, Y. & L. J. Shimkets, (2000) *Prokaryotic development,* p. xiv, 477 p. ASM Press, Washington, DC.

Buist, G., A. Steen, J. Kok & O. P. Kuipers, (2008) LysM, a widely distributed protein motif for binding to (peptido)glycans. *Mol Microbiol* **68**: 838-847.

Cabeen, M. T. & C. Jacobs-Wagner, (2005) Bacterial cell shape. *Nat Rev Microbiol* **3**: 601-610.

Cabeen, M. T. & C. Jacobs-Wagner, (2007) Skin and bones: the bacterial cytoskeleton, cell wall, and cell morphogenesis. *J Cell Biol* **179**: 381-387.

Calamita, H. G. & R. J. Doyle, (2002) Regulation of autolysins in teichuronic acid-containing *Bacillus subtilis* cells. *Mol Microbiol* **44**: 601-606.

Capstick, D. S., J. M. Willey, M. J. Buttner & M. A. Elliot, (2007) SapB and the chaplins: connections between morphogenetic proteins in *Streptomyces coelicolor*. *Mol Microbiol* **64**: 602-613.

Carballido-Lopez, R. & J. Errington, (2003) The bacterial cytoskeleton: in vivo dynamics of the actin-like protein Mbl of *Bacillus subtilis*. *Dev Cell* **4**: 19-28.

Carballido-Lopez, R., A. Formstone, Y. Li, S. D. Ehrlich, P. Noirot & J. Errington, (2006) Actin homolog MreBH governs cell morphogenesis by localization of the cell wall hydrolase LytE. *Dev Cell* **11**: 399-409.

Chakraburtty, R. & M. Bibb, (1997) The ppGpp synthetase gene (*relA*) of *Streptomyces coelicolor* A3(2) plays a conditional role in antibiotic production and morphological differentiation. *J Bacteriol* **179**: 5854-5861.

Challis, G. L. & D. A. Hopwood, (2003) Synergy and contingency as driving forces for the evolution of multiple secondary metabolite production by *Streptomyces* species. *Proc Natl Acad Sci U S A* **100 Suppl 2**: 14555-14561.

Champness, W. C., (1988) New loci required for *Streptomyces coelicolor* morphological and physiological differentiation. *J Bacteriol* **170**: 1168-1174.

Chaput, C. & I. G. Boneca, (2007) Peptidoglycan detection by mammals and flies. *Microbes Infect* **9**: 637-647.

Chater, K., (1999) David Hopwood and the emergence of *Streptomyces* genetics. *Int Microbiol* **2**: 61-68.

Chater, K. F., (1993) Genetics of differentiation in *Streptomyces*. *Annu Rev Microbiol* **47**: 685-713.

Chater, K. F., S. Biro, K. J. Lee, T. Palmer & H. Schrempf, (2010) The complex extracellular biology of *Streptomyces*. *FEMS Microbiol Rev* **34**: 171-198.

Chater, K. F., C. J. Bruton, A. A. King & J. E. Suarez, (1982) The expression of *Streptomyces* and *Escherichia coli* drug-resistance determinants cloned into the *Streptomyces* phage phi C31. *Gene* **19**: 21-32.

Chatterji, D. & A. K. Ojha, (2001) Revisiting the stringent response, ppGpp and starvation signaling. *Curr Opin Microbiol* **4**: 160-165.

Claessen, D., W. de Jong, L. Dijkhuizen & H. A. Wosten, (2006) Regulation of *Streptomyces* development: reach for the sky! *Trends Microbiol* **14**: 313-319.

Clarke, A. J. & C. Dupont, (1992) *O*-acetylated peptidoglycan: its occurrence, pathobiological significance, and biosynthesis. *Can J Microbiol* **38**: 85-91.

Cohen, S. N. & K. J. McDowall, (1997) RNase E: still a wonderfully mysterious enzyme. *Mol Microbiol* **23**: 1099-1106.

Cohen-Gonsaud, M., P. Barthe, C. Bagneris, B. Henderson, J. Ward, C. Roumestand & N. H. Keep, (2005) The structure of a resuscitation-promoting factor domain from *Mycobacterium tuberculosis* shows homology to lysozymes. *Nat Struct Mol Biol* **12**: 270-273.

Cohen-Gonsaud, M., N. H. Keep, A. P. Davies, J. Ward, B. Henderson & G. Labesse, (2004) Resuscitation-promoting factors possess a lysozyme-like domain. *Trends Biochem Sci* **29**: 7-10.

Cohn, F. J., (1875) Untersuchungen ueber Bakterien. Beitraege zur Biologie der Planzen. In: Milestones in Microbiology: 1556 to 1940. T. D. Brock (ed). ASM, pp. 127-222

Condon, C., (2007) Maturation and degradation of RNA in bacteria. *Curr Opin Microbiol* **10**: 271-278.

Condon, C. & H. Putzer, (2002) The phylogenetic distribution of bacterial ribonucleases. *Nucleic Acids Res* **30**: 5339-5346.

Costa, F. F., (2007) Non-coding RNAs: lost in translation? *Gene* **386**: 1-10.

Cromie, M. J., Y. Shi, T. Latifi & E. A. Groisman, (2006) An RNA sensor for intracellular Mg(2+). *Cell* **125**: 71-84.

Cunningham, A. F. & C. L. Spreadbury, (1998) Mycobacterial stationary phase induced by low oxygen tension: cell wall thickening and localization of the 16-kilodalton alpha-crystallin homolog. *J Bacteriol* **180**: 801-808.

D'Alia, D., K. Nieselt, S. Steigele, J. Müller, I. Verburg & E. Takano, (2010) Noncoding RNA of glutamine synthetase I modulates antibiotic production in *Streptomyces coelicolor* A3(2). *J Bacteriol* **192**: 1160-1164.

D'Elia, M. A., K. E. Millar, T. J. Beveridge & E. D. Brown, (2006) Wall teichoic acid polymers are dispensable for cell viability in *Bacillus subtilis*. *J Bacteriol* **188**: 8313-8316.

Dambach, M. D. & W. C. Winkler, (2009) Expanding roles for metabolite-sensing regulatory RNAs. *Curr Opin Microbiol* **12**: 161-169.

Daniel, R. A. & J. Errington, (2003) Control of cell morphogenesis in bacteria: two distinct ways to make a rod-shaped cell. *Cell* **113**: 767-776.

Dasgupta, A., P. Datta, M. Kundu & J. Basu, (2006) The serine/threonine kinase PknB of *Mycobacterium tuberculosis* phosphorylates PBPA, a penicillin-binding protein required for cell division. *Microbiology* **152**: 493-504.

Datsenko, K. A. & B. L. Wanner, (2000) One-step inactivation of chromosomal genes in *Escherichia coli* K-12 using PCR products. *Proc Natl Acad Sci U S A* **97**: 6640-6645.

de Jong, W., A. Manteca, J. Sanchez, G. Bucca, C. P. Smith, L. Dijkhuizen, D. Claessen & H. A. Wosten, (2009) NepA is a structural cell wall protein involved in maintenance of spore dormancy in *Streptomyces coelicolor*. *Mol Microbiol* **71**: 1591-1603.

Deana, A., H. Celesnik & J. G. Belasco, (2008) The bacterial enzyme RppH triggers messenger RNA degradation by 5' pyrophosphate removal. *Nature* **451**: 355-358.

Derouaux, A., S. Halici, H. Nothaft, T. Neutelings, G. Moutzourelis, J. Dusart, F. Titgemeyer & S. Rigali, (2004) Deletion of a cyclic AMP receptor protein homologue diminishes germination and affects morphological development of *Streptomyces coelicolor*. *J Bacteriol* **186**: 1893-1897.

Deutscher, M. P., (2003) Degradation of stable RNA in bacteria. *J Biol Chem* **278**: 45041-45044.

Deutscher, M. P., (2006) Degradation of RNA in bacteria: comparison of mRNA and stable RNA. *Nucleic Acids Res* **34**: 659-666.

Dubrac, S., P. Bisicchia, K. M. Devine & T. Msadek, (2008) A matter of life and death: cell wall homeostasis and the WalKR (YycGF) essential signal transduction pathway. *Mol Microbiol* **70**: 1307-1322.

Dubrac, S., I. G. Boneca, O. Poupel & T. Msadek, (2007) New insights into the WalK/WalR (YycG/YycF) essential signal transduction pathway reveal a major role in controlling cell wall metabolism and biofilm formation in *Staphylococcus aureus*. *J Bacteriol* **189**: 8257-8269.

Dworkin, J. & I. M. Shah, (2010) Exit from dormancy in microbial organisms. *Nat Rev Microbiol* **8**: 890-896.

Elliot, M., M. Buttner & J. Nodwell, (2008) Multicellular development in *Streptomyces*. *Myxobacteria: Multicellularity and Differentiation*: 419–438.

Elliot, M. A., N. Karoonuthaisiri, J. Huang, M. J. Bibb, S. N. Cohen, C. M. Kao & M. J. Buttner, (2003) The chaplins: a family of hydrophobic cell-surface proteins involved in aerial mycelium formation in *Streptomyces coelicolor*. *Genes Dev* **17**: 1727-1740.

Elliot, M. A. & N. J. Talbot, (2004) Building filaments in the air: aerial morphogenesis in bacteria and fungi. *Curr Opin Microbiol* **7**: 594-601.

Engel, H., B. Kazemier & W. Keck, (1991) Murein-metabolizing enzymes from *Escherichia coli*: sequence analysis and controlled overexpression of the slt gene, which encodes the soluble lytic transglycosylase. *J Bacteriol* **173**: 6773-6782.

Ensign, J. C., (1978) Formation, properties, and germination of actinomycete spores. *Annu Rev Microbiol* **32**: 185-219.

Firczuk, M. & M. Bochtler, (2007) Folds and activities of peptidoglycan amidases. *FEMS Microbiol Rev* **31**: 676-691.

Fischer, W., P. Rosel & H. U. Koch, (1981) Effect of alanine ester substitution and other structural features of lipoteichoic acids on their inhibitory activity against autolysins of *Staphylococcus aureus*. *J Bacteriol* **146**: 467-475.

Flärdh, K., (2003a) Essential role of DivIVA in polar growth and morphogenesis in *Streptomyces coelicolor* A3(2). *Mol Microbiol* **49**: 1523-1536.

Flärdh, K., (2003b) Growth polarity and cell division in *Streptomyces*. *Curr Opin Microbiol* **6**: 564-571.

Flärdh, K. & M. J. Buttner, (2009) *Streptomyces* morphogenetics: dissecting differentiation in a filamentous bacterium. *Nat Rev Microbiol* **7**: 36-49.

Flärdh, K., K. C. Findlay & K. F. Chater, (1999) Association of early sporulation genes with suggested developmental decision points in *Streptomyces coelicolor* A3(2). *Microbiology* **145 (Pt 9)**: 2229-2243.

Fournier, M. J. & H. Ozeki, (1985) Structure and organization of the transfer ribonucleic acid genes of *Escherichia coli* K-12. *Microbiol Rev* **49**: 379-397.

Fu, H., J. Feng, Q. Liu, F. Sun, Y. Tie, J. Zhu, R. Xing, Z. Sun & X. Zheng, (2009) Stress induces tRNA cleavage by angiogenin in mammalian cells. *FEBS Letters* **583**: 437-442.

Ghosh, S. & P. Setlow, (2009) Isolation and characterization of superdormant spores of *Bacillus* species. *J Bacteriol* **191**: 1787-1797.

Gilbert, P., P. J. Collier & M. R. Brown, (1990) Influence of growth rate on susceptibility to antimicrobial agents: biofilms, cell cycle, dormancy, and stringent response. *Antimicrob Agents Chemother* **34**: 1865-1868.

Gottesman, S., C. A. McCullen, M. Guillier, C. K. Vanderpool, N. Majdalani, J. Benhammou, K. M. Thompson, P. C. FitzGerald, N. A. Sowa & D. J. FitzGerald, (2006) Small RNA regulators and the bacterial response to stress. *Cold Spring Harb Symp Quant Biol* **71**: 1-11.

Gram, H. C., (1884) Uber die isolierte Farbung der Schizomyceten in Schnitt - und Trockenpraparaten. *Fortschritte der Medizin* **2**: 185-189.

Gupta, R. K., B. S. Srivastava & R. Srivastava, (2010) Comparative expression analysis of rpf-like genes of *Mycobacterium tuberculosis* H37Rv under different physiological stress and growth conditions. *Microbiology* **156**: 2714-2722.

Gust, B., G. L. Challis, K. Fowler, T. Kieser & K. F. Chater, (2003) PCR-targeted *Streptomyces* gene replacement identifies a protein domain needed for biosynthesis of the sesquiterpene soil odor geosmin. *Proc Natl Acad Sci U S A* **100**: 1541-1546.

Hagège, J. M. & S. N. Cohen, (1997) A developmentally regulated *Streptomyces* endoribonuclease resembles ribonuclease E of *Escherichia coli*. *Mol Microbiol* **25**: 1077-1090.

Haiser, H. J., F. V. Karginov, G. J. Hannon & M. A. Elliot, (2008) Developmentally regulated cleavage of tRNAs in the bacterium *Streptomyces coelicolor*. *Nucleic Acids Res* **36**: 732-741.

Haiser, H. J., M. R. Yousef & M. A. Elliot, (2009) Cell wall hydrolases affect germination, vegetative growth, and sporulation in *Streptomyces coelicolor*. *J Bacteriol* **191**: 6501-6512.

Heffron, J. D., B. Orsburn & D. L. Popham, (2009) Roles of germination-specific lytic enzymes CwlJ and SleB in *Bacillus anthracis*. *J Bacteriol* **191**: 2237-2247.

Helmann, J. D., (2002) The extracytoplasmic function (ECF) sigma factors. *Adv Microb Physiol* **46**: 47-110.

Hempel, A. M., S. B. Wang, M. Letek, J. A. Gil & K. Flärdh, (2008) Assemblies of DivIVA mark sites for hyphal branching and can establish new zones of cell wall growth in *Streptomyces coelicolor*. *J Bacteriol* **190**: 7579-7583.

Hesketh, A., W. J. Chen, J. Ryding, S. Chang & M. Bibb, (2007) The global role of ppGpp synthesis in morphological differentiation and antibiotic production in *Streptomyces coelicolor* A3(2). *Genome Biol* **8**: R161.

Hett, E. C., M. C. Chao, L. L. Deng & E. J. Rubin, (2008) A mycobacterial enzyme essential for cell division synergizes with resuscitation-promoting factor. *PLoS Pathog* **4**: e1000001.

Hett, E. C., M. C. Chao & E. J. Rubin, (2010) Interaction and modulation of two antagonistic cell wall enzymes of mycobacteria. *PLoS Pathog* **6**: e1001020.

Hett, E. C., M. C. Chao, A. J. Steyn, S. M. Fortune, L. L. Deng & E. J. Rubin, (2007) A partner for the resuscitation-promoting factors of *Mycobacterium tuberculosis*. *Mol Microbiol* **66**: 658-668.

Hindra, P. Pak & M. A. Elliot, (2010) Regulation of a novel gene cluster involved in secondary metabolite production in *Streptomyces coelicolor*. *J Bacteriol* **192**: 4973-4982.

Hladny, J., K. H. Schleifer & O. Kandler, (1972) Amino acid sequence of the threonine containing mureins of some species of *Streptococcus*. *Arch Mikrobiol* **85**: 23-38.

Holtje, J. V., (1998) Growth of the stress-bearing and shape-maintaining murein sacculus of *Escherichia coli*. *Microbiol Mol Biol Rev* **62**: 181-203.

Holtje, J. V., D. Mirelman, N. Sharon & U. Schwarz, (1975) Novel type of murein transglycosylase in *Escherichia coli*. *J Bacteriol* **124**: 1067-1076.

Hoppner, C., A. Carle, D. Sivanesan, S. Hoeppner & C. Baron, (2005) The putative lytic transglycosylase VirB1 from *Brucella suis* interacts with the type IV secretion system core components VirB8, VirB9 and VirB11. *Microbiology* **151**: 3469-3482.

Hopwood, D. A., (1999) Forty years of genetics with *Streptomyces*: from in vivo through in vitro to in silico. *Microbiology* **145 (Pt 9)**: 2183-2202.

Hopwood, D. A., (2007) *Streptomyces in nature and medicine : the antibiotic makers,* p. viii, 250 p., [258] p. of plates. Oxford University Press, Oxford ; New York.

Hopwood DA, B. M., Chater KF, Kieser T, Bruton CJ, Kieser HM, Lydiate DJ, Smith CP, Ward JM, Schrempf H, (1985) *Genetic manipulation of Streptomyces – A laboratory manual.* The John Innes Foundation, Norwich, U.K.

Howell, A., S. Dubrac, K. K. Andersen, D. Noone, J. Fert, T. Msadek & K. Devine, (2003) Genes controlled by the essential YycG/YycF two-component system of *Bacillus subtilis* revealed through a novel hybrid regulator approach. *Mol Microbiol* **49**: 1639-1655.

Hunt, A. C., L. Servin-Gonzalez, G. H. Kelemen & M. J. Buttner, (2005) The bldC developmental locus of *Streptomyces coelicolor* encodes a member of a family of small DNA-binding proteins related to the DNA-binding domains of the MerR family. *J Bacteriol* **187**: 716-728.

Huttenhofer, A., P. Schattner & N. Polacek, (2005) Non-coding RNAs: hope or hype? *Trends Genet* **21**: 289-297.

Jacobs, C., L. J. Huang, E. Bartowsky, S. Normark & J. T. Park, (1994) Bacterial cell wall recycling provides cytosolic muropeptides as effectors for beta-lactamase induction. *EMBO J* **13**: 4684-4694.

Jacobs, C., B. Joris, M. Jamin, K. Klarsov, J. Van Beeumen, D. Mengin-Lecreulx, J. van Heijenoort, J. T. Park, S. Normark & J. M. Frere, (1995) AmpD, essential for both beta-lactamase regulation and cell wall recycling, is a novel cytosolic *N*-acetylmuramyl-L-alanine amidase. *Mol Microbiol* **15**: 553-559.

Janssen, G. R. & M. J. Bibb, (1993) Derivatives of pUC18 that have *Bgl*II sites flanking a modified multiple cloning site and that retain the ability to identify recombinant clones by visual screening of *Escherichia coli* colonies. *Gene* **124**: 133-134.

Jochl, C., M. Rederstorff, J. Hertel, P. F. Stadler, I. L. Hofacker, M. Schrettl, H. Haas & A. Huttenhofer, (2008) Small ncRNA transcriptome analysis from *Aspergillus fumigatus* suggests a novel mechanism for regulation of protein synthesis. *Nucleic Acids Research* **36**: 2677-2689.

Jones, G. & P. Dyson, (2006) Evolution of transmembrane protein kinases implicated in coordinating remodeling of gram-positive peptidoglycan: inside versus outside. *J Bacteriol* **188**: 7470-7476.

Jones, L. J., R. Carballido-Lopez & J. Errington, (2001) Control of cell shape in bacteria: helical, actin-like filaments in *Bacillus subtilis*. *Cell* **104**: 913-922.

Jonker, H. R., S. Ilin, S. K. Grimm, J. Wohnert & H. Schwalbe, (2007) L11 domain rearrangement upon binding to RNA and thiostrepton studied by NMR spectroscopy. *Nucleic Acids Res* **35**: 441-454.

Kaiser, D., (2004) Signaling in myxobacteria. *Annu Rev Microbiol* **58**: 75-98.

Kana, B. D., B. G. Gordhan, K. J. Downing, N. Sung, G. Vostroktunova, E. E. Machowski, L. Tsenova, M. Young, A. Kaprelyants, G. Kaplan & V. Mizrahi, (2008) The resuscitation-promoting factors of *Mycobacterium tuberculosis* are required for virulence and resuscitation from dormancy but are collectively dispensable for growth *in vitro*. *Mol Microbiol* **67**: 672-684.

Kawaji, H., M. Nakamura, Y. Takahashi, A. Sandelin, S. Katayama, S. Fukuda, C. O. Daub, C. Kai, J. Kawai, J. Yasuda, P. Carninci & Y. Hayashizaki, (2008) Hidden layers of human small RNAs. *BMC Genomics* **9**: 157.

Kawano, M., A. A. Reynolds, J. Miranda-Rios & G. Storz, (2005) Detection of 5'- and 3'-UTR-derived small RNAs and cis-encoded antisense RNAs in *Escherichia coli*. *Nucleic Acids Res* **33**: 1040-1050.

Keep, N. H., J. M. Ward, M. Cohen-Gonsaud & B. Henderson, (2006) Wake up! Peptidoglycan lysis and bacterial non-growth states. *Trends Microbiol* **14**: 271-276.

Kelemen, G. H. & M. J. Buttner, (1998) Initiation of aerial mycelium formation in *Streptomyces*. *Curr Opin Microbiol* **1**: 656-662.

Kell, D. B., A. S. Kaprelyants, D. H. Weichart, C. R. Harwood & M. R. Barer, (1998) Viability and activity in readily culturable bacteria: a review and discussion of the practical issues. *Antonie Van Leeuwenhoek* **73**: 169-187.

Kieser, T., M. J. Bibb, M. J. Buttner, K. F. Chater & D. A. Hopwood, (2000) *Practical Streptomyces Genetics*, p. 1-616. John Innes Foundation, Norwich, England.

Kleinschnitz, E.-M., A. Heichlinger, K. Schirner, J. Winkler, A. Latus, I. Maldener, W. Wohlleben & G. Muth, (2011) Proteins encoded by the *mre* gene cluster in *Streptomyces coelicolor* A3(2) cooperate in spore wall synthesis. *Mol Microbiol* **79**: 1367-1379.

Korat, B., H. Mottl & W. Keck, (1991) Penicillin-binding protein 4 of *Escherichia coli*: molecular cloning of the *dacB* gene, controlled overexpression, and alterations in murein composition. *Mol Microbiol* **5**: 675-684.

Korgaonkar, A. K. & M. Whiteley, (2011) *Pseudomonas aeruginosa* enhances production of an antimicrobial in response to *N*-acetylglucosamine and peptidoglycan. *J Bacteriol* **193**: 909-917.

Kuroda, A. & J. Sekiguchi, (1990) Cloning, sequencing and genetic mapping of a *Bacillus subtilis* cell wall hydrolase gene. *J Gen Microbiol* **136**: 2209-2216.

Laemmli, U. K., (1970) Cleavage of structural proteins during the assembly of the head of bacteriophage T4. *Nature* **227**: 680-685.

Lam, H., D.-C. Oh, F. Cava, C. N. Takacs, J. Clardy, M. A. De Pedro & M. K. Waldor, (2009) D-Amino acids govern stationary phase cell wall remodeling in bacteria. *Science* **325**: 1552-1555.

Lau, N. C., L. P. Lim, E. G. Weinstein & D. P. Bartel, (2001) An abundant class of tiny RNAs with probable regulatory roles in *Caenorhabditis elegans*. *Science* **294**: 858-862.

Lawlor, E. J., H. A. Baylis & K. F. Chater, (1987) Pleiotropic morphological and antibiotic deficiencies result from mutations in a gene encoding a tRNA-like product in *Streptomyces coelicolor* A3(2). *Genes Dev* **1**: 1305-1310.

Leclerc, D. & A. Asselin, (1989) Detection of bacterial cell wall hydrolases after denaturing polyacrylamide gel electrophoresis. *Can J Microbiol* **35**: 749-753.

Lee, S. R. & K. Collins, (2005) Starvation-induced cleavage of the tRNA anticodon loop in *Tetrahymena thermophila*. *J Biol Chem* **280**: 42744-42749.

Leskiw, B. K., M. J. Bibb & K. F. Chater, (1991) The use of a rare codon specifically during development? *Mol Microbiol* **5**: 2861-2867.

Levitz, R., D. Chapman, M. Amitsur, R. Green, L. Snyder & G. Kaufmann, (1990) The optional *E. coli prr* locus encodes a latent form of phage T4-induced anticodon nuclease. *EMBO J* **9**: 1383-1389.

Li, Y., J. Luo, H. Zhou, J. Liao & L. Ma, (2008) Stress-induced tRNA-derived RNAs: a novel class of small RNAs in the primitive eukaryote *Giardia lamblia*. *Nucleic Acids Res* **36**: 6048-6055.

Li, Z., S. Reimers, S. Pandit & M. P. Deutscher, (2002) RNA quality control: degradation of defective transfer RNA. *EMBO J* **21**: 1132-1138.

Liebeke, M., H. Meyer, S. Donat, K. Ohlsen & M. Lalk, (2010) A metabolomic view of *Staphylococcus aureus* and its Ser/Thr kinase and phosphatase deletion mutants: involvement in cell wall biosynthesis. *Chem Biol* **17**: 820-830.

Litzinger, S., A. Duckworth, K. Nitzsche, V. Risinger, V. Wittmann & C. Mayer, (2010) Muropeptide rescue in *Bacillus subtilis* involves sequential hydrolysis by beta-*N*-acetylglucosaminidase and *N*-acetylmuramyl-L-alanine amidase. *J Bacteriol* **192**: 3132-3143.

Loh, E., O. Dussurget, J. Gripenland, K. Vaitkevicius, T. Tiensuu, P. Mandin, F. Repoila, C. Buchrieser, P. Cossart & J. Johansson, (2009) A trans-acting riboswitch controls expression of the virulence regulator PrfA in *Listeria monocytogenes*. *Cell* **139**: 770-779.

Lowe, J., F. van den Ent & L. A. Amos, (2004) Molecules of the bacterial cytoskeleton. *Annu Rev Biophys Biomol Struct* **33**: 177-198.

MacNeil, D. J., K. M. Gewain, C. L. Ruby, G. Dezeny, P. H. Gibbons & T. MacNeil, (1992) Analysis of *Streptomyces avermitilis* genes required for avermectin biosynthesis utilizing a novel integration vector. *Gene* **111**: 61-68.

Magnusson, L. U., A. Farewell & T. Nystrom, (2005) ppGpp: a global regulator in *Escherichia coli*. *Trends Microbiol* **13**: 236-242.

Majdalani, N., C. K. Vanderpool & S. Gottesman, (2005) Bacterial small RNA regulators. *Crit Rev Biochem Mol Biol* **40**: 93-113.

Mandal, M. & R. R. Breaker, (2004) Adenine riboswitches and gene activation by disruption of a transcription terminator. *Nat Struct Mol Biol* **11**: 29-35.

Manteca, A., U. Mader, B. A. Connolly & J. Sanchez, (2006) A proteomic analysis of *Streptomyces coelicolor* programmed cell death. *Proteomics* **6**: 6008-6022.

Margolin, W., (2009) Sculpting the bacterial cell. *Curr Biol* **19**: R812-822.

Margot, P., M. Wahlen, A. Gholamhoseinian, P. Piggot & D. Karamata, (1998) The *lytE* gene of *Bacillus subtilis* 168 encodes a cell wall hydrolase. *J Bacteriol* **180**: 749-752.

Masaki, H. & T. Ogawa, (2002) The modes of action of colicins E5 and D, and related cytotoxic tRNases. *Biochimie* **84**: 433-438.

Mathy, N., A. Hebert, P. Mervelet, L. Benard, A. Dorleans, I. L. de la Sierra-Gallay, P. Noirot, H. Putzer & C. Condon, (2007) *Bacillus subtilis* ribonucleases J1 and J2 form a complex with altered enzyme behaviour. *Mol Microbiol* **75**: 489-498.

Mauck, J., L. Chan & L. Glaser, (1971) Turnover of the cell wall of Gram-positive bacteria. *J Biol Chem* **246**: 1820-1827.

Mazza, P., E. E. Noens, K. Schirner, N. Grantcharova, A. M. Mommaas, H. K. Koerten, G. Muth, K. Flärdh, G. P. van Wezel & W. Wohlleben, (2006) MreB of *Streptomyces coelicolor* is not essential for vegetative growth but is required for the integrity of aerial hyphae and spores. *Mol Microbiol* **60**: 838-852.

Mei, Y., J. Yong, H. Liu, Y. Shi, J. Meinkoth, G. Dreyfuss & X. Yang, (2010) tRNA binds to cytochrome c and inhibits caspase activation. *Mol Cell* **37**: 668-678.

Merrick, M. J., (1976) A morphological and genetic mapping study of bald colony mutants of *Streptomyces coelicolor*. *J Gen Microbiol* **96**: 299-315.

Molle, V. & L. Kremer, (2010) Division and cell envelope regulation by Ser/Thr phosphorylation: *Mycobacterium* shows the way. *Mol Microbiol* **75**: 1064-1077.

Molle, V., W. J. Palframan, K. C. Findlay & M. J. Buttner, (2000) WhiD and WhiB, homologous proteins required for different stages of sporulation in *Streptomyces coelicolor* A3(2). *J Bacteriol* **182**: 1286-1295.

Morita, T. & H. Aiba, (2011) RNase E action at a distance: degradation of target mRNAs mediated by an Hfq-binding small RNA in bacteria. *Genes Dev* **25**: 294-298.

Morlot, C., T. Uehara, K. A. Marquis, T. G. Bernhardt & D. Z. Rudner, (2010) A highly coordinated cell wall degradation machine governs spore morphogenesis in *Bacillus subtilis*. *Genes Dev* **24**: 411-422.

Mukamolova, G. V., A. S. Kaprelyants, D. I. Young, M. Young & D. B. Kell, (1998) A bacterial cytokine. *Proc Natl Acad Sci U S A* **95**: 8916-8921.

Mukamolova, G. V., A. G. Murzin, E. G. Salina, G. R. Demina, D. B. Kell, A. S. Kaprelyants & M. Young, (2006) Muralytic activity of *Micrococcus luteus* Rpf and its relationship to physiological activity in promoting bacterial growth and resuscitation. *Mol Microbiol* **59**: 84-98.

Mukamolova, G. V., O. A. Turapov, K. Kazarian, M. Telkov, A. S. Kaprelyants, D. B. Kell & M. Young, (2002a) The rpf gene of *Micrococcus luteus* encodes an essential secreted growth factor. *Mol Microbiol* **46**: 611-621.

Mukamolova, G. V., O. A. Turapov, D. I. Young, A. S. Kaprelyants, D. B. Kell & M. Young, (2002b) A family of autocrine growth factors in *Mycobacterium tuberculosis*. *Mol Microbiol* **46**: 623-635.

Nahvi, A., J. E. Barrick & R. R. Breaker, (2004) Coenzyme B12 riboswitches are widespread genetic control elements in prokaryotes. *Nucleic Acids Res* **32**: 143-150.

Nahvi, A., N. Sudarsan, M. S. Ebert, X. Zou, K. L. Brown & R. R. Breaker, (2002) Genetic control by a metabolite binding mRNA. *Chem Biol* **9**: 1043.

Noens, E. E., V. Mersinias, B. A. Traag, C. P. Smith, H. K. Koerten & G. P. van Wezel, (2005) SsgA-like proteins determine the fate of peptidoglycan during sporulation of *Streptomyces coelicolor*. *Mol Microbiol* **58**: 929-944.

Nwagwu, M. & M. Nana, (1980) Ribonucleic acid synthesis in embryonic chick muscle, rates of synthesis and half-lives of transfer and ribosomal RNA species. *J Embryol Exp Morphol* **56**: 253-267.

Ochi, K., (1986) Occurrence of the stringent response in *Streptomyces* sp. and its significance for the initiation of morphological and physiological differentiation. *J Gen Microbiol* **132**: 2621-2631.

Ochi, K., (1987) Metabolic initiation of differentiation and secondary metabolism by *Streptomyces griseus* - significance of the stringent response (ppGpp) and GTP content in relation to A-factor. *J Bacteriol* **169**: 3608-3616.

Oliver, J. D., (2005) The viable but nonculturable state in bacteria. *J Microbiol* **43 Spec No**: 93-100.

Oliver, J. D., (2010) Recent findings on the viable but nonculturable state in pathogenic bacteria. *FEMS Microbiol Rev* **34**: 415-425.

Paget, M. S., L. Chamberlin, A. Atrih, S. J. Foster & M. J. Buttner, (1999a) Evidence that the extracytoplasmic function sigma factor sigmaE is required for normal cell wall structure in *Streptomyces coelicolor* A3(2). *J Bacteriol* **181**: 204-211.

Paget, M. S., E. Leibovitz & M. J. Buttner, (1999b) A putative two-component signal transduction system regulates sigmaE, a sigma factor required for normal cell wall integrity in *Streptomyces coelicolor* A3(2). *Mol Microbiol* **33**: 97-107.

Paidhungat, M. & P. Setlow, (2001) Localization of a germinant receptor protein (GerBA) to the inner membrane of *Bacillus subtilis* spores. *J Bacteriol* **183**: 3982-3990.

Panek, J., J. Bobek, K. Mikulik, M. Basler & J. Vohradsky, (2008) Biocomputational prediction of small non-coding RNAs in *Streptomyces*. *BMC Genomics* **9**: 217.

Park, J. T. & T. Uehara, (2008) How bacteria consume their own exoskeletons (turnover and recycling of cell wall peptidoglycan). *Microbiol Mol Biol Rev* **72**: 211-227.

Park, S. Y., M. J. Cromie, E. J. Lee & E. A. Groisman, (2010) A bacterial mRNA leader that employs different mechanisms to sense disparate intracellular signals. *Cell* **142**: 737-748.

Passalacqua, K. D., A. Varadarajan, B. D. Ondov, D. T. Okou, M. E. Zwick & N. H. Bergman, (2009) Structure and complexity of a bacterial transcriptome. *J Bacteriol* **191**: 3203-3211.

Pei, J. & N. V. Grishin, (2005) COG3926 and COG5526: a tale of two new lysozyme-like protein families. *Protein Sci* **14**: 2574-2581.

Petrickova, K. & M. Petricek, (2003) Eukaryotic-type protein kinases in *Streptomyces coelicolor*: variations on a common theme. *Microbiology* **149**: 1609-1621.

Pfeffer, J. M., H. Strating, J. T. Weadge & A. J. Clarke, (2006) Peptidoglycan *O* acetylation and autolysin profile of *Enterococcus faecalis* in the viable but nonculturable state. *J Bacteriol* **188**: 902-908.

Pfister, P., M. Risch, D. E. Brodersen & E. C. Bottger, (2003) Role of 16S rRNA Helix 44 in Ribosomal Resistance to Hygromycin B. *Antimicrob Agents Chemother* **47**: 1496-1502.

Phizicky, E. M. & A. K. Hopper, (2010) tRNA biology charges to the front. *Genes Dev* **24**: 1832-1860.

Piret, J. M. & K. F. Chater, (1985) Phage-mediated cloning of *bldA*, a region involved in *Streptomyces coelicolor* morphological development, and its analysis by genetic complementation. *J Bacteriol* **163**: 965-972.

Pope, M. K., B. D. Green & J. Westpheling, (1996) The *bld* mutants of *Streptomyces coelicolor* are defective in the regulation of carbon utilization, morphogenesis and cell--cell signalling. *Mol Microbiol* **19**: 747-756.

Popham, D. L., J. Meador-Parton, C. E. Costello & P. Setlow, (1999) Spore peptidoglycan structure in a *cwlD dacB* double mutant of *Bacillus subtilis*. *J Bacteriol* **181**: 6205-6209.

Rahman, O., S. P. Cummings & I. C. Sutcliffe, (2009) Phenotypic variation in *Streptomyces* sp. DSM 40537, a lipoteichoic acid producing actinomycete. *Lett Appl Microbiol* **48**: 226-229.

Ravagnani, A., C. L. Finan & M. Young, (2005) A novel firmicute protein family related to the actinobacterial resuscitation-promoting factors by non-orthologous domain displacement. *BMC Genomics* **6**: 39.

Renberg, I. & M. Nilsson, (1992) Dormant bacteria in lake sediments as palaeoecological indicators. *J Paleolimnol* **7**: 127-135.

Rivas, E. & S. R. Eddy, (2001) Noncoding RNA gene detection using comparative sequence analysis. *BMC Bioinformatics* **2**: 8.

Roth, A. & R. R. Breaker, (2009) The structural and functional diversity of metabolite-binding riboswitches. *Annu Rev Biochem* **78**: 305-334.

Russell-Goldman, E., J. Xu, X. Wang, J. Chan & J. M. Tufariello, (2008) A *Mycobacterium tuberculosis* Rpf double-knockout strain exhibits profound defects in reactivation from chronic tuberculosis and innate immunity phenotypes. *Infect Immun* **76**: 4269-4281.

Sambrook, J. & D. W. Russell, (2001) *Molecular cloning : a laboratory manual.* Cold Spring Harbor Laboratory Press, Cold Spring Harbor, N.Y.

Sauvage, E., F. Kerff, M. Terrak, J. A. Ayala & P. Charlier, (2008) The penicillin-binding proteins: structure and role in peptidoglycan biosynthesis. *FEMS Microbiol Rev* **32**: 234-258.

Scheffers, D. J. & M. G. Pinho, (2005) Bacterial cell wall synthesis: new insights from localization studies. *Microbiol Mol Biol Rev* **69**: 585-607.

Scheurwater, E., C. W. Reid & A. J. Clarke, (2008) Lytic transglycosylases: bacterial space-making autolysins. *Int J Biochem Cell Biol* **40**: 586-591.

Scheurwater, E. M. & L. L. Burrows, (2011) Maintaining network security: how macromolecular structures cross the peptidoglycan layer. *FEMS Microbiol Lett.*

Schleifer, K. H. & O. Kandler, (1972) Peptidoglycan types of bacterial cell walls and their taxonomic implications. *Bacteriol Rev* **36**: 407-477.

Sedlmeier, R., T. Werner, H. M. Kieser, D. A. Hopwood & H. Schmieger, (1994) tRNA genes of *Streptomyces lividans*: new sequences and comparison of structure and organization with those of other bacteria. *J Bacteriol* **176**: 5550-5553.

Seltmann, G. & O. Holst, (2001) *The bacterial cell wall,* p. ix, 280 p. Springer, Berlin ; New York.

Serganov, A. & D. J. Patel, (2007) Ribozymes, riboswitches and beyond: regulation of gene expression without proteins. *Nat Rev Genet* **8**: 776-790.

Setlow, P., (2003) Spore germination. *Curr Opin Microbiol* **6**: 550-556.

Shah, I. M. & J. Dworkin, (2010) Induction and regulation of a secreted peptidoglycan hydrolase by a membrane Ser/Thr kinase that detects muropeptides. *Mol Microbiol* **75**: 1232-1243.

Shah, I. M., M. H. Laaberki, D. L. Popham & J. Dworkin, (2008) A eukaryotic-like Ser/Thr kinase signals bacteria to exit dormancy in response to peptidoglycan fragments. *Cell* **135**: 486-496.

Sharma, C. M., S. Hoffmann, F. Darfeuille, J. Reignier, S. Findeiss, A. Sittka, S. Chabas, K. Reiche, J. Hackermuller, R. Reinhardt, P. F. Stadler & J. Vogel, (2010) The primary transcriptome of the major human pathogen *Helicobacter pylori*. *Nature* **464**: 250-255.

Shimkets, L. J. & D. Kaiser, (1982a) Induction of coordinated movement of *Myxococcus xanthus* cells. *J Bacteriol* **152**: 451-461.

Shimkets, L. J. & D. Kaiser, (1982b) Murein components rescue developmental sporulation of *Myxococcus xanthus*. *J Bacteriol* **152**: 462-470.

Shockman, M. & J. V. Holtje, (1994) *Microbial peptidoglycan (murein) hydrolases*. Elsevier Science, Amsterdam.

Signoretto, C., M. M. Lleo & P. Canepari, (2002) Modification of the peptidoglycan of *Escherichia coli* in the viable but nonculturable state. *Curr Microbiol* **44**: 125-131.

Smith, T. J., S. A. Blackman & S. J. Foster, (2000) Autolysins of *Bacillus subtilis*: multiple enzymes with multiple functions. *Microbiology* **146 (Pt 2)**: 249-262.

Sonenshein, A. L., J. A. Hoch & R. Losick, (2002) *Bacillus subtilis and its closest relatives : from genes to cells,* p. xvi, 629 p. ASM Press, Washington, D.C.

Steen, A., G. Buist, N. E. Kramer, R. Jalving, G. F. Benus, G. Venema, O. P. Kuipers & J. Kok, (2008) Reduced lysis upon growth of *Lactococcus lactis* on galactose is a consequence of decreased binding of the autolysin AcmA. *Appl Environ Microbiol* **74**: 4671-4679.

Steen, A., G. Buist, K. J. Leenhouts, M. El Khattabi, F. Grijpstra, A. L. Zomer, G. Venema, O. P. Kuipers & J. Kok, (2003) Cell wall attachment of a widely distributed peptidoglycan binding domain is hindered by cell wall constituents. *J Biol Chem* **278**: 23874-23881.

Susstrunk, U., J. Pidoux, S. Taubert, A. Ullmann & C. J. Thompson, (1998) Pleiotropic effects of cAMP on germination, antibiotic biosynthesis and morphological development in *Streptomyces coelicolor*. *Mol Microbiol* **30**: 33-46.

Swiercz, J. P., Hindra, J. Bobek, J. Bobek, H. J. Haiser, C. Di Berardo, B. Tjaden & M. A. Elliot, (2008) Small non-coding RNAs in *Streptomyces coelicolor*. *Nucleic Acids Res* **36**: 7240-7251.

Takacs, C. N., S. Poggio, G. Charbon, M. Pucheault, W. Vollmer & C. Jacobs-Wagner, (2009) MreB drives de novo rod morphogenesis in *Caulobacter crescentus* via remodeling of the cell wall. *J Bacteriol* **192**: 1671-1684.

Tezuka, T., H. Hara, Y. Ohnishi & S. Horinouchi, (2009) Identification and gene disruption of small noncoding RNAs in *Streptomyces griseus*. *J Bacteriol* **191**: 4896-4904.

Thakur, M. & P. K. Chakraborti, (2008) Ability of PknA, a mycobacterial eukaryotic-type serine/threonine kinase, to transphosphorylate MurD, a ligase involved in the process of peptidoglycan biosynthesis. *Biochem J* **415**: 27-33.

Thompson, D., C. Lu, P. Green & R. Parker, (2008) tRNA cleavage is a conserved response to oxidative stress in eukaryotes. *RNA*.

Thompson, D. & R. Parker, (2009a) Stressing out over tRNA cleavage. *Cell*.

Thompson, D. & R. Parker, (2009b) The RNase Rny1p cleaves tRNAs and promotes cell death during oxidative stress in *Saccharomyces cerevisiae*. *Science's STKE*.

Tosa, T. & L. I. Pizer, (1971) Biochemical bases for the antimetabolite action of L-serine hydroxamate. *J Bacteriol* **106**: 972-982.

Traag, B. A., A. Driks, P. Stragier, W. Bitter, G. Broussard, G. Hatfull, F. Chu, K. N. Adams, L. Ramakrishnan & R. Losick, (2010) Do mycobacteria produce endospores? *Proc Natl Acad Sci U S A* **107**: 878-881.

Traag, B. A. & G. P. van Wezel, (2008) The SsgA-like proteins in actinomycetes: small proteins up to a big task. *Antonie Van Leeuwenhoek* **94**: 85-97.

Tucker, B. J. & R. R. Breaker, (2005) Riboswitches as versatile gene control elements. *Curr Opin Struct Biol* **15**: 342-348.

Tufariello, J. M., W. R. Jacobs, Jr. & J. Chan, (2004) Individual *Mycobacterium tuberculosis* resuscitation-promoting factor homologues are dispensable for growth in vitro and in vivo. *Infect Immun* **72**: 515-526.

Tufariello, J. M., K. Mi, J. Xu, Y. C. Manabe, A. K. Kesavan, J. Drumm, K. Tanaka, W. R. Jacobs, Jr. & J. Chan, (2006) Deletion of the *Mycobacterium tuberculosis* resuscitation-promoting factor *Rv1009* gene results in delayed reactivation from chronic tuberculosis. *Infect Immun* **74**: 2985-2995.

Turnbaugh, P. J., M. Hamady, T. Yatsunenko, B. L. Cantarel, A. Duncan, R. E. Ley, M. L. Sogin, W. J. Jones, B. A. Roe, J. P. Affourtit, M. Egholm, B. Henrissat, A. C. Heath, R. Knight & J. I. Gordon, (2009) A core gut microbiome in obese and lean twins. *Nature* **457**: 480-484.

Uchida, K. & K. Aida, (1979) Taxonomic significance of cell-wall acyl type in *Corynebacterium-Mycobacterium-Nocardia* group by a glycolate test. *J Genl App Microbiol* **25**: 169-183.

Uehara, T. & J. T. Park, (2008) Growth of *Escherichia coli*: significance of peptidoglycan degradation during elongation and septation. *J Bacteriol* **190**: 3914-3922.

Uehara, T., K. R. Parzych, T. Dinh & T. G. Bernhardt, (2010) Daughter cell separation is controlled by cytokinetic ring-activated cell wall hydrolysis. *The EMBO Journal* **29**: 1412-1422.

Uehara, T., K. Suefuji, N. Valbuena, B. Meehan, M. Donegan & J. T. Park, (2005) Recycling of the anhydro-*N*-acetylmuramic acid derived from cell wall murein involves a two-step conversion to *N*-acetylglucosamine-phosphate. *J Bacteriol* **187**: 3643-3649.

van den Ent, F., C. M. Johnson, L. Persons, P. de Boer & J. Lowe, (2010) Bacterial actin MreB assembles in complex with cell shape protein RodZ. *EMBO J* **29**: 1081-1090.

Viala, J., C. Chaput, I. G. Boneca, A. Cardona, S. E. Girardin, A. P. Moran, R. Athman, S. Memet, M. R. Huerre, A. J. Coyle, P. S. DiStefano, P. J. Sansonetti, A. Labigne, J. Bertin, D. J. Philpott & R. L. Ferrero, (2004) Nod1 responds to peptidoglycan delivered by the *Helicobacter pylori cag* pathogenicity island. *Nat Immunol* **5**: 1166-1174.

Vollmer, W., (2008) Structural variation in the glycan strands of bacterial peptidoglycan. *FEMS Microbiology Reviews* **32**: 287-306.

Vollmer, W. & U. Bertsche, (2008) Murein (peptidoglycan) structure, architecture and biosynthesis in *Escherichia coli*. *Biochim Biophys Acta* **1778**: 1714-1734.

Vollmer, W., D. Blanot & M. A. De Pedro, (2008a) Peptidoglycan structure and architecture. *FEMS Microbiology Reviews* **32**: 149-167.

Vollmer, W., B. Joris, P. Charlier & S. Foster, (2008b) Bacterial peptidoglycan (murein) hydrolases. *FEMS Microbiology Reviews* **32**: 259-286.

Waksman, S. A., (1967) *The actinomycetes : a summary of current knowledge,* p. 280 p.,ill. Ronald P., New York.

Waksman, S. A. & H. B. Woodruff, (1940) The soil as a source of microorganisms antagonistic to disease-producing bacteria. *J Bacteriol* **40**: 581-600.

Waldron, C. & F. Lacroute, (1975) Effect of growth rate on the amounts of ribosomal and transfer ribonucleic acids in yeast. *J Bacteriol* **122**: 855-865.

Walsh, C., (2003) Where will new antibiotics come from? *Nat Rev Microbiol* **1**: 65-70.

Wassarman, K. M., F. Repoila, C. Rosenow, G. Storz & S. Gottesman, (2001) Identification of novel small RNAs using comparative genomics and microarrays. *Genes Dev* **15**: 1637-1651.

Waters, L. S. & G. Storz, (2009) Regulatory RNAs in bacteria. *Cell* **136**: 615-628.

Watve, M. G., R. Tickoo, M. M. Jog & B. D. Bhole, (2001) How many antibiotics are produced by the genus *Streptomyces*? *Arch Microbiol* **176**: 386-390.

Weadge, J. T. & A. J. Clarke, (2006) Identification and characterization of *O*-acetylpeptidoglycan esterase: a novel enzyme discovered in *Neisseria gonorrhoeae*. *Biochemistry* **45**: 839-851.

Weadge, J. T. & A. J. Clarke, (2007) *Neisseria gonorrheae O*-acetylpeptidoglycan esterase, a serine esterase with a Ser-His-Asp catalytic triad. *Biochemistry* **46**: 4932-4941.

Weadge, J. T., J. M. Pfeffer & A. J. Clarke, (2005) Identification of a new family of enzymes with potential *O*-acetylpeptidoglycan esterase activity in both Gram-positive and Gram-negative bacteria. *BMC Microbiol* **5**: 49.

Willemse, J., J. W. Borst, E. De Waal, T. Bisseling & G. P. Van Wezel, (2011) Positive control of cell division: FtsZ is recruited by SsgB during sporulation of *Streptomyces*. *Genes & Development* **25**: 89-99.

Willey, J., R. Santamaria, J. Guijarro, M. Geistlich & R. Losick, (1991) Extracellular complementation of a developmental mutation implicates a small sporulation protein in aerial mycelium formation by *S. coelicolor*. *Cell* **65**: 641-650.

Winkler, W. & R. Breaker, (2005) Regulation of bacterial gene expression by riboswitches. *Microbiology* **59**.

Wray, G. M., S. J. Foster, C. J. Hinds & C. Thiemermann, (2001) A cell wall component from pathogenic and non-pathogenic gram-positive bacteria (peptidoglycan) synergises with endotoxin to cause the release of tumour necrosis factor-alpha, nitric oxide production, shock, and multiple organ injury/dysfunction in the rat. *Shock* **15**: 135-142.

Yamasaki, S., P. Ivanov, G. Hu & P. Anderson, (2009) Angiogenin cleaves tRNA and promotes stress-induced translational repression. *Science's STKE.*

Yeats, C., R. D. Finn & A. Bateman, (2002) The PASTA domain: a beta-lactam-binding domain. *Trends Biochem Sci* **27**: 438.

Zhang, S., L. Sun & F. Kragler, (2009) The phloem-delivered RNA pool contains small noncoding RNAs and interferes with translation. *Plant Physiol* **150**: 378-387.